UNIVERSITAT POLITÈCNICA DE CATALUNYA BARCELONATECH

# *Remaining Useful Life and Fault Detection Models for High Voltage Electrical Connectors Focused on Predictive Maintenance*

**Jimmy Arturo Martínez Reyes**

UNIVERSITAT POLITÈCNICA DE CATALUNYA
BARCELONATECH

PhD program in Electrical Engineering

# Remaining Useful Life and Fault Detection Models for High Voltage Electrical Connectors Focused on Predictive Maintenance


**Author:**

Jimmy Arturo Martínez Reyes

**Thesis advisor:**

Dr. Jordi-Roger Riba Ruiz

Dr. Manuel Moreno Eguílaz


Thesis submitted to obtain the title of Doctor

Terrassa, March 2022

*Dedicated to,*

*My beloved parents* ***Jimmy Martínez*** *and* ***Susy Reyes*** *and*

*My dear siblings* ***Rodri, Tita*** *and* ***Santi,***

*without whom this success would have been impossible.*

*“Knowledge is of no value unless you put in into practice”*

- *Anton Chekhov*

# ABSTRACT

In recent years, industries have chosen to invest in technology with the aim of making their processes more efficient and thus offering market products of higher quality. Nowadays it is very common for companies to use special systems to predict failures and avoid unexpected delays, reduction of costs, etc. SBI Connectors, along with the Universitat Politècnica de Catalunya, have been collaborating to develop research projects for more than 10 years. As a result of the collaboration with the university, patents and international publications have been generated, which have helped to situate and reinforce SBI Connectors leadership in the international market while offering an image of scientific-technical credibility. This research is carried out, with the collaboration of SBI connectors and Universitat Politècnica de Catalunya, in order to develop the *Smartconnector* project (within the Retos de Colaboración Spanish research frame). The thesis proposed by the author is dedicated to develop and validate *RUL* (*Remaining Useful Life*) and fault detection approaches for electrical substation connectors. The RUL approach proposed in this work is based on a simple and accurate model of the degradation with time of the electrical resistance of the connector (main health indicator), which has two parameters, whose values are identified from on-line acquired data. Next, the fault detection chapter is divided into two parts. The first part presents an on-line condition monitoring method to predict early failures in power connectors from on-line acquired data in conjunction with another parametric degradation model of the resistance of the connector, whose parameters are identified by means of the Markov chain Monte Carlo stochastic method. The second part presents, analyzes and compares the performance of three simple and effective methods for online determination of the State of Health (SoH) of power connectors with low computational requirements. The proposed approaches are based on monitoring the evolution of the connectors' electrical resistance, which determines the degradation trajectory. Furthermore, this work includes an in-depth study of the temperature dependence of the electrical contact resistance (ECR). To analyze and validate results presented in this work, data is acquired in real time, including main parameters such as the electrical current and voltage drop across the terminals of the connector, conductor and connector temperature, thus estimating the phase shift between voltage drop and electrical current waveforms and the contact resistance by means of accelerated aging tests (ADT).

# SUMARIO

En los últimos años, la industria ha optado por invertir en tecnología con el objetivo de hacer más eficientes sus procesos y así ofrecer al mercado productos de mayor calidad. Hoy en día es muy habitual que las empresas utilicen sistemas especiales para predecir fallos y evitar retrasos inesperados, reducción de costes, etc. SBI Connectors, junto con la Universitat Politècnica de Catalunya, colaboran para desarrollar proyectos de investigación desde hace más de 10 años. Fruto de la colaboración con la universidad se han generado patentes y publicaciones internacionales, que han ayudado a situar y reforzar el liderazgo de SBI Connectors en el mercado internacional, al tiempo que ofrece una imagen de credibilidad científico-técnica. Esta tesis doctoral se realiza con la colaboración de SBI connectors y la Universitat Politècnica de Catalunya, para desarrollar el proyecto Smartconnector (dentro del marco de investigación Retos de Colaboración). La tesis propuesta por el autor está dedicada a desarrollar y validar modelos de RUL (Remaining Useful Life) y detección de fallos para conectores de subestaciones eléctricas enfocador al mantemiento predictive. El enfoque RUL propuesto en este trabajo se basa en un modelo simple y preciso de la degradación de la resistencia eléctrica del conector respecto al tiempo (indicador principal de salud), el cual tiene dos parámetros cuyos valores se identifican a partir de datos adquiridos en línea. A continuación, el capítulo de detección de fallos se divide en dos partes. En la primera parte se presenta un método de monitoreo en línea de condición para predecir fallos tempranos en conectores de potencia a partir de datos adquiridos en línea en conjunto con otro modelo paramétrico de degradación de la resistencia del conector, cuyos parámetros son identificados por medio del algoritmo de Markov Chain Monte Carlo. La segunda parte presenta, analiza y compara las prestaciones de tres métodos simples y efectivos para la determinación en línea del Estado de Salud (SoH) de conectores de potencia con bajos requerimientos computacionales. Los enfoques propuestos se basan en el seguimiento de la evolución de la resistencia eléctrica de los conectores, que determina la trayectoria de degradación. Además, este trabajo incluye un estudio en profundidad de la dependencia de la temperatura de la resistencia eléctrica de contacto (ECR). Para analizar y validar todo el trabajo presentado, se adquieren datos en tiempo real, incluyendo parámetros principales como la corriente eléctrica y la caída de tensión en los terminales del conector, la temperatura del conductor y del conector, estimando así el desfase entre la caída de tensión y la tensión eléctrica, forma de onda de corriente y la resistencia de contacto por medio de ensayos de envejecimiento acelerado (ADT).

# ACKNOWLEDGMENTS

First, I would like to start by saying “Thank you so much” to my thesis advisors Jordi Riba and Manuel Moreno from “Universitat Politècnica de Catalunya” for offering and trusting me the opportunity to work and study on such an interesting and motivating research project in Amber Laboratory besides their continuous supervision and patience during the whole project. Manolo, thanks for being the person you are. I have learned a lot of both technical and personal stuff from you. Please keep being so with the other students. Jordi, I really appreciate all the experiences and teachings you gave me. I am pretty sure I will not forget these three years working in Amber because this place has made me to see the life in a different way. I am really grateful with you. This achievement would have been impossible without both of you.

Afterward, I like to express all my gratefulness to my treasured family. My parents Jimmy Martínez and Susy Reyes and my siblings Rodri, Tita and Santi, without whom this success would have been impossible. Despite the long distance and the jetlag between us, we are always connected, and that is what encourages me to keep walking forward. This thesis is made of your love. Also, I like to thank to my love Carla, for supporting me during the ups and downs of the last stage of this process. Thanks for encourage me to keep standing up.

Next, I wish to express my gratitude towards to David Gonzalez for his technical knowledge, proficiency, friendship and support, which helps me too much throughout this project. Thank you so much David, I always saw you as older brother during these years. In addition, I would also like to thank Carlos Abomailek and Francesca Capelli for the advices and helps you gave me in some part of this thesis either by speaking with you or by reading your outstanding works.

Then, special thanks to Akash, Carlos, Gabriel. For all the good times in Amber. Guys, you know the special you were for me all this time. Thanks a lot and I wish you the best in your future. Also, I take this opportunity to thank all the past members of Amber as Ivan, Marc and specially Alvaro, who I respect to so much. Thanks for your advices and the help you gave me. Liu and Pau, you are next ones. Keep working as both of you have done so far.

Finally, I like to finish by saying thanks to my friends: Mikel, Aqua, Irune, Pablo, Geovanny, Canario, Santi, Adrian, Papu, Akash again, Xanti, Borja and Liam for having been like my family all these years.

# CONTENTS

# LIST OF FIGURES

# LIST OF TABLES

# INTRODUCTION

# 1. INTRODUCTION

Electric power connectors are devices that join electrical conductors each other in low-, medium-, and high-voltage power systems, thus becoming critical components. Despite the electrical connectors are simple components, they play a critical role in power systems as any failure can lead to severe power outages with costly and disastrous consequences [1]. Therefore, it is necessary to apply predictive maintenance strategies, which are able to report the remaining useful life (*RUL*) or potential failures in the connectors thus anticipating possible faults. However, since the substation connectors are subjected to voltages of tens or hundreds of kV and high electric currents, in the order of some kA, it is very challenging to acquire real-time data of the main variables such as current, temperature, contact resistance, etc., to estimate the operational condition of the connector or the RUL. Currently, the maintenance of the substation connectors is of corrective type, which means they are replaced when there is a major failure that usually causes major incidents due to their key role in substations. Particularly, the work presented in this thesis proposes RUL and fault detection models for high-voltage power connectors focused on predictive maintenance, which are validated by means of experimental data.

This document is divided into five chapters. The first chapter presents the topics, justifications and the objectives of this thesis, as well as the resulting scientific publications. Consequently, this chapter explains both the structure and the impact of the research work. Afterward, the second chapter characterizes the temperature dependence of the contact resistance in substation connectors by carrying out a deep study from experimental data. Next, the third chapter proposes a method for determining the Remaining Useful Life (*RUL*) based on the on-line monitoring of the electrical resistance evolution with time by acquiring the voltage drop, electrical current and temperature of the connector with the purpose of determining the parameters of the degradation model of the electrical resistance. It also allows estimating the remaining time in order to anticipate a possible failure, by analyzing when the electrical resistance exceeds a defined threshold value. Next, chapter four presents two novel fault detection models for

substations connectors. The first model proposes a simple approach for on-line diagnosis of the health status of power connectors based on continuously monitoring their electrical resistance in conjunction with a parametric degradation model of the connector resistance, which is combined with the application of the *Markov Chain Monte Carlo* (*MCMC*) method. The second model proposes to forecast the State of Health (*SoH*) of power connectors by taking in account the degradation trajectory of the electrical resistance. Finally, the conclusions of this work are presented in chapter five.

## 1.1 Topics and justification

This section describes the topics and justification covered in this thesis.

### 1.1.1 Background

This thesis has been developed within the frame of the *SmartConnector* research project, which was funded under the "Retos de colaboración", program of the Ministerio de Ciencia e Innovación de España, and it has also been supported by the Generalitat de Catalunya. This project is carried out with the collaboration of SBI Connectors SAU, a national manufacturer of power connectors, in conjunction with the MCIA research group from the Universitat Politècnica de Catalunya.

The *SmartConnector* project appears due to the need of manufacturing and commercializing highly reliable substation connectors, which are well-suited for HVAC and HVDC substations, with the aim of simplifying the predictive maintenance of both the connector and the installation, thus leading to a safety electrical substation. However, it is very difficult to evaluate the performance of a predictive maintenance plan by using current substation connectors, since currently they do not incorporate sensors. Therefore, it is not possible to acquire on-line data related of their operating conditions throughout their operational lifetime. Therefore, the *SmartConnector* aims to develop, validate and commercialize a new family of smart substation connectors with the capacity to transmit and receive information in real time, incorporating a sensor system, an energy harvesting or self-feeding, in order to monitor the behavior of the connector itself and make a diagnosis of its health condition, thus simplifying predictive maintenance tasks and also ensuring its correct installation.

It is important to mention that this thesis is focused on the methodologies to validate several proposed algorithms or mathematical models to estimate the Remaining Useful life (RUL) and to detect premature failures in substation connectors, which will be useful to develop predictive maintenance plans from the data acquired by the *SmartConnector*. This strategy, in turn, can imply a significant reduction of the sudden faults and an increase of the useful life of both the connector and the substation, thus avoiding downtimes or delays and the associated economic costs.

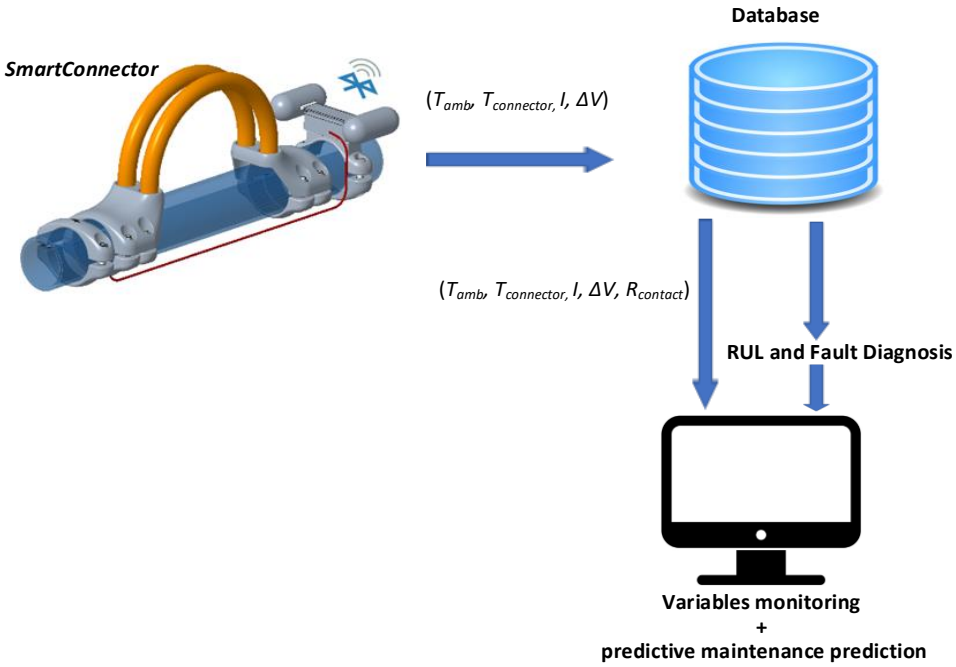


**Figure 1.1.** *SmartConnector* project.

### 1.1.2 Substation connectors

Electrical connectors are devices that join mechanically and electrically two or more electrical conductors, offering a continuous electrical path [2]. On the other hand, substation connectors are electrical connectors found in electrical substations, which are used to connect two or more conductors, bus bars or transformer terminals either with conductors or bus bars.

**Figure 1.2**. Some of the substation connectors from the SBI Connectors catalogue [3].

Substation connectors are simple elements, but at the same time, they are critical components of the electrical system, as a failure in any one of them can lead to disconnection of one part of the substation.

### 1.1.3 Accelerated Aging Tests (AAG)

Accelerated aging is based on tests of moderate or long duration that use stress or worse conditions such as electric current, temperature or mechanical vibration, in order to accelerate the normal aging processes of some product or component. These tests are used to determine in much shorter time that the useful life of the product, the long-term effects of the expected levels of stress under normal operating conditions of the product or component. Tests are generally carried out in a laboratory using standard controlled test methods.

Accelerated aging is applicable to estimate the useful life of a product or its useful life when there is not data history available during the past life. This normally occurs with new products from which there is insufficient data history, or with products whose life is very long and these data are not available. In **aging tests**, the product is subjected to controlled laboratory tests, by applying representative levels of stress to the product for long periods of time, unusually high levels of stress used to accelerate the effects of natural aging, or in another words, stress levels that intentionally cause very high temperatures. In the case of **accelerated aging tests**, the aim is to accelerate the natural aging process of the product by applying higher stress levels than those found under normal operating conditions. In the case of substation connectors, the stress levels to be applied refer to values of **electric current**, **temperature** and **vibration** above normal operating values, and applying **accelerated heating and cooling cycles** to simulate the day-night cycling effect.

This part covers different types of Accelerated Aging Tests (AAG). Each type of test is described and a comparison is carried out at the end of section. Afterward, the temperature of accelerated aging tests used in this thesis are briefly described.

*1.1.3.1 Accelerated Life Test (ALT)*

In order to obtain aging data in a reasonable time, in a time frame compatible with the normal development of a product, the degradation processes must be accelerated [4]. Some industries have chosen Accelerated Life Tests (ALT) [5], [6].

ALTs are widely used to obtain degradation data of the products in a shorter time. In an ALT, a set of sample are subjected to an elevated stress level thus producing shorter lives [7]. However, the problem with this type of test is the number of samples required for obtaining reliable results. In the case of substation connectors, this test may not be possible without applying suitable strategies to accelerate the aging process [8].

*1.1.3.2 Accelerated Degradation Tests (ADT)*

For the reasons mentioned above, products such as substation connectors are usually tested using a methodology that does not only use information about the aging time of the product, but also uses information of the degradation process.

Accelerated Degradation Tests (ADT) take degradation data at higher stress levels to be able to predict the useful life of the product, by adjusting the data into a mathematical expression, which is based on the behavior of the product [8]–[10]. Although ADTs are efficient due to they avoid that the test reaches the end of life of the product, they are often costly due to required testing time and materials needed.

*1.1.3.3 Step-Stress Accelerated Degradation Test (SSADT)*

Due to these disadvantages, Tseng [11] proposed a new test to limit this problem, the **SSADT test (Step-Stress Accelerated Degradation Test).** By using an appropriate mathematical model, the lifetime of the product can be quickly predicted, allowing the samples to be tested without reaching the failure, thus saving time and energy costs, while significantly reducing the cost of the degradation test.

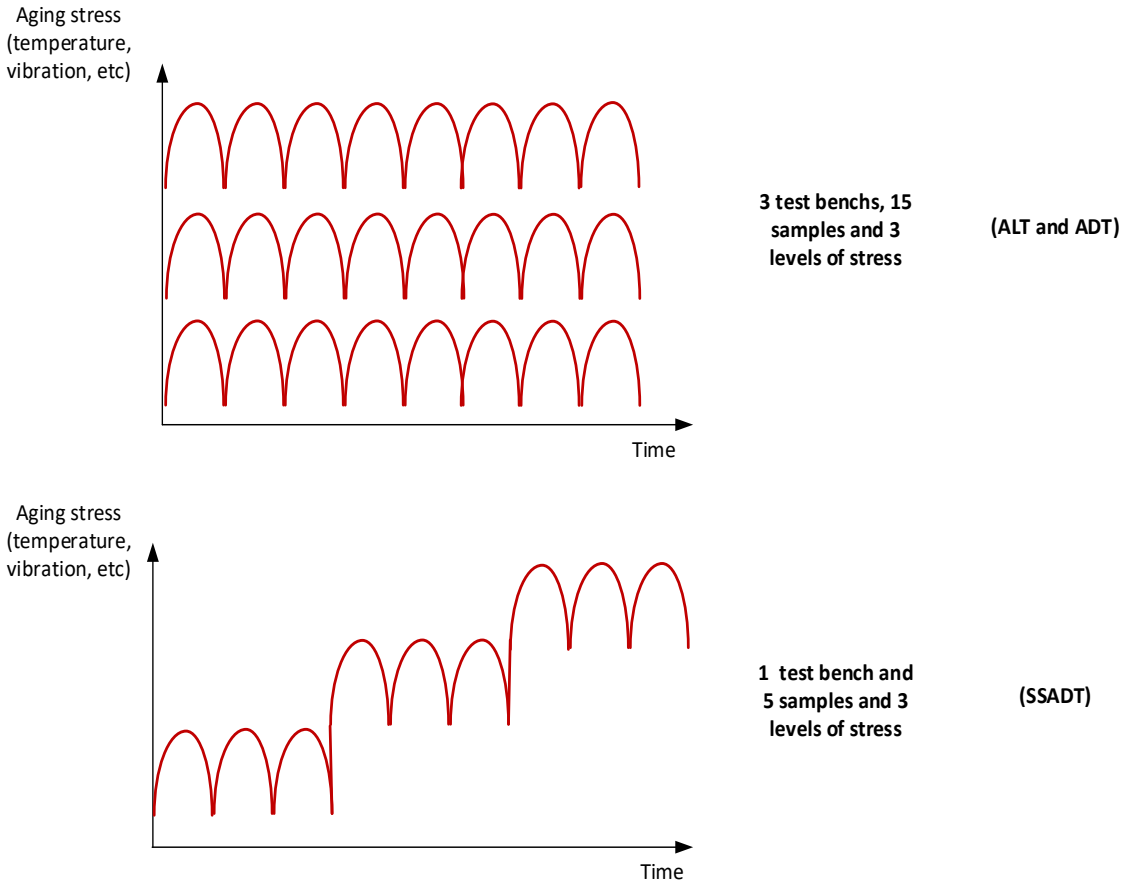


**Figure 1.3.** Types of accelerated aging test [8].

The main differences between an ADT and an SSADT are shown in Figure 1.3. The necessary number of samples to be tested in a SSADT decreases, while the same number of units are used in the different "Stress-Steps" (stress steps). Degradation or aging data obtained from the SSADT depend on the stress level. This means that to concatenate the data of the different temperature or stress levels applied to obtain a parametric model, it is necessary to extrapolate the data from previous cycles.

*1.1.3.4 Comparison of the AAGs*

In order to select the most appropriate accelerated aging test for this research a Table 1.1 compares the advantages and disadvantages of the different types of accelerated aging tests.

**Table 1.1.** Comparison of the types of accelerated aging tests.

| | Advantages | Disadvantages |
|---|---|---|
| **ALT** | • It is used to perform accelerated service life tests | • It is not useful for samples that have a very long operation life or require a long time to degrade.<br>• An aging model is not performed. |
| **ADT** | • The degradation of the connector from its installation is analyzed for each tested stress level, without the need to make estimates of the previous cycles as it happens with SSADTs.<br>• The sample does not need to reach failure to complete the test. | • For each stress level to be tested, a new test needs to be done. For instance, if three temperature levels are applied, three different tests are performed.<br>• The number of samples required increases with the number of stress levels to be tested. For example, if three temperature levels are applied, the number of samples required for the test is multiplied by three. |
| **SSADT** | • Fewer samples are required to perform the test than an ALT or ADT.<br>• Less time is required to obtain results compared to ALTs or ADTs.<br>• The sample does not need to reach failure. | • For each step or stress level, it is required to estimate the evolution of the degradation for previous cycles to the current moment. |

In this research, it is proposed to perform an ADT applied to the analyzed connectors, where the variable that produces stress is the temperature.

*1.1.3.5 Temperature testing standards*

In order to carry out temperature aging tests, international standards should be applied to conduct the experiments and to evaluate the performance of the electrical connectors.

The main reference standard for substation connector is the American National Standards Institute (ANSI) / National Electrical Manufacturers Association (NEMA) CC1 standard. The American ANSI / NEMA standard CC1-2009 [12] establishes a temperature test procedure for electrical power connectors, called TRT (Temperature Rise Tests). This test can be carried out either indoors or outdoors. The TRT test must be carried out at 100%,

125% and 150% of the rated electric current, and the equilibrium temperature must be reached at each level. The equilibrium temperature is defined as a constant temperature (+/- 2ºC) between three successive measurements taken every 5 minutes. Measurements should be made at the end of the first 30 minutes and at one-hour intervals thereafter. In addition, the TRT test is useful for determining the thermal behavior of substation connectors under both transient and steady state conditions, in order to assess whether their design and installation procedure are compatible with the electro-thermal stress to which it is subjected [13]. The rated electric current must be in accordance with the tabulated values established in the standard, depending on the size of the conductor.

Another good option to thermally age electrical connectors is by y applying electrical current cycle tests, which are defined in the ANSI C119.0-2015 standard [14]. There are two options, the current cycle test (CCT) where the connectors are air-cooled, and the current cycle submersion test (CCST) of shorter duration since it requires cooling the connectors in cold water at the end of each cycle. The standard specifies which tests are suitable for each product.

The IEC-61238-1-3:2018 [15] is another standard used to evaluate the thermal behavior of the medium-voltage compression connectors when subjected to thermal heating and cooling cycles for a long period of time, i.e., aging.

From the mentioned standards above, the ANSI / NEMA standard CC1-2009 and the studied IEC-61238-1-3:2018 are used for all the experiments carried out in this thesis.

### 1.1.4 The contact resistance as a condition indicator

The contact resistance is directly affected by the tightening torque applied to the bolting elements of the connector [16]. In addition, the connectors are subjected to daily thermal cycles during all the day besides electrical cycles, which are determined by the change in the electricity demand, thus producing mechanical contractions and expansion cycles, which in conjunction with the vibrations generated by the wind, affect the tightening torque applied on the screws, thus affecting the contact resistance. Consequently, both the thermal behavior of the connector and its useful life are influenced by the changes of

the contact resistance. In addition, the effects of the thermal stresses during the life of the connectors are cumulative, thus favoring their deterioration.

The contact resistance of the connector is a fundamental parameter to know the health condition or state of the connector, being its value very low, typically in the order of a few micro-Ohms. Furthermore, mechanical stresses also influence the condition of the connector. Due to the increased temperature, the contact resistance increases much faster, thus accelerating failure occurrence. Hence, the main parameter that indicates the level of degradation of an electrical connector and therefore, its useful life and state of health, is the contact resistance.

It is worth mentioning that in spite that temperature can indicate possible failure modes in the connector, other variables including the electric current flowing through the connector, vibrations [17], the ambient temperature or different meteorological variables such as wind speed, rain or ice, may produce appreciable changes in the temperature. In addition, the temperature is a key feature, which affects the thermal loss of life [18]. Hence, to use the temperature to indicate the health status, a complete thermal model of the connector is usually required. Although this process can be developed, it is much more complex than a resistance approach (as the proposed in this thesis), due to the characteristic complexity of the thermal models, the need to be experimentally validated under different meteorological conditions (wind speed and direction, fog, rain, ice, etc.) and the fact that the thermal model must be adjusted to each type of connector. Therefore, in this work the contact resistance will be used as a reliable condition indicator.

### 1.1.5 Remaining Useful Life

The reliability of electrical connectors has a critical impact on electrical systems. For this reason, reliability models must be able to estimate or predict their useful life. Reliability analysis has often been applied for predicting the failure rate [19]. Medium- and high-voltage power connectors are designed to work during a long period. The expected useful life of substation connectors is above 30 years [20]. However, early failures can appear long time before.

**Remaining useful life (RUL)** is the expected useful operating time before a device needs to be repaired or replaced. By taking RUL into consideration, predictive maintenance plans can be applied, optimizing the operational efficiency of the substation and avoiding unplanned outages or incidents. The core of predictive maintenance of an electrical connector is to predict the RUL, since by means of this prediction it is possible to identify which electrical connectors should be replaced in the short term, thus avoiding their failure. Therefore, RUL estimation is a priority in predictive maintenance programs.

*1.1.5.1 RUL Prediction Methodology*

Models for estimating the RUL depend on the type of available operating data. According to [21]–[23], different methodologies for RUL prediction are possible, as shown in Figure 1.4. Hence, this research work will focus on a model-based/computational intelligence for RUL prediction (and also for fault detection), since this methodology does not require to have data of the entire life of the component, but only a part of it, thus being applicable to components with extended useful life, when there is only available partial data, as in the case of substation connectors.

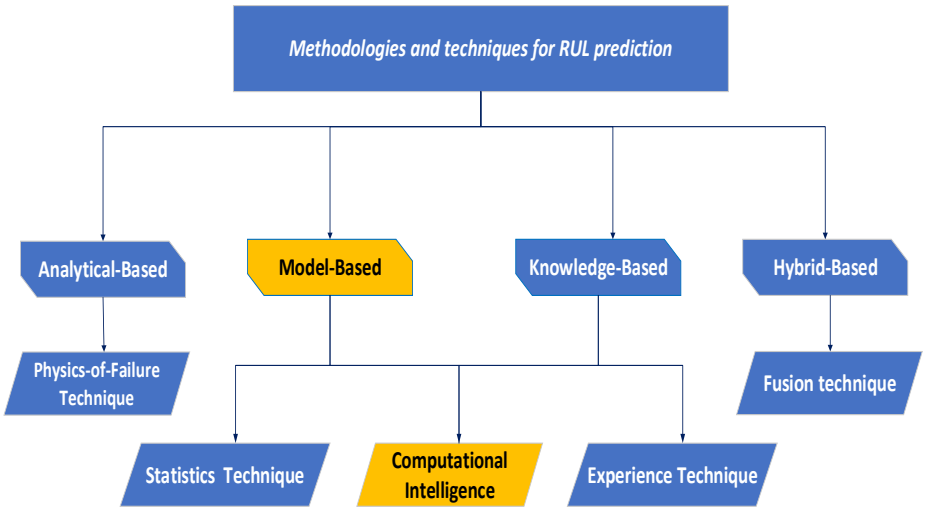


**Figure 1.4.** Methodologies and techniques for RUL prediction [21].

**Model-Based or Degradation Models Methodology** is derived from usage and historical data of a component, being appropriate for maintenance decision making. Basically, in this method, past behavior data is used to predict the future conditions.

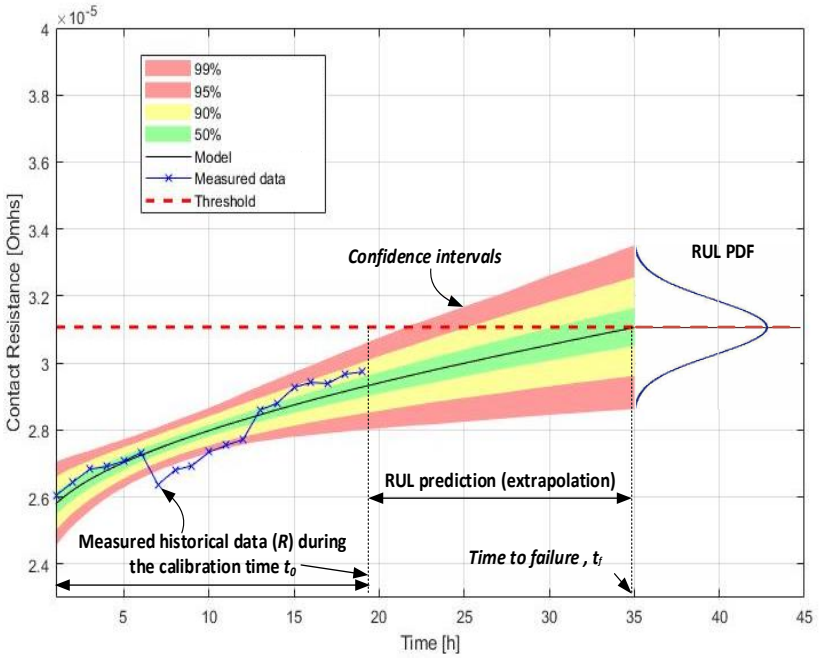


**Figure 1.5.** RUL prediction example of an electrical connector showing the mean value and the 50%, 90%, 95% and 99% confidence intervals (representing the predictive probability limits due to parameter uncertainty) plotted as area bands.

Furthermore, this methodology is not complicated to apply. By using this degradation model, three steps are required. These steps are:

(1) Fitting available historical data before prediction time to the degradation model of the condition indicator (contact resistance).
(2) The degradation model of the electrical connector is used to statistically compute the remaining time until the indicator reaches certain threshold.
(3) Finally, by using historical data about the state of a set of similar electrical connectors, the model can be applied.

*1.1.5.2 Threshold and condition indicator*

When a connector degradation database it is not available, the RUL can be predicted by setting a **threshold value**. The threshold can be defined from specific standards or previous studies based on historical data. For instance, each electrical conductor has a nominal operating electric current. If the operating current exceeds this nominal value, the conductor will work under unsuitable conditions, reaching high temperatures.

Therefore, due to the increased temperature, the **contact resistance** increases much faster, accelerating failure occurrence. Hence, the main parameter that indicates the level of degradation of an electrical connector and therefore, its useful life, is the contact resistance. Therefore, as mentioned above, the **condition indicator** used for predicting the RUL will be the **contact resistance**. According to [24], if the initial contact resistance changes about 20%, it can be assumed that the connector has failed. However, another threshold value for RUL prediction will be proposed in this work.

### 1.1.6 Fault detection

Nowadays, fault diagnosis systems are applied to perform predictive maintenance tasks. Predictive maintenance is a method of industrial maintenance management, used to predict the failure time of some components, so that they can be replaced before failure [20]. Thus, in order to diagnose or determine the state of the operational condition of the connectors, some parameters that demonstrate a predictable relationship with the life cycle of the component must be measured [25], [26]. In the case of an electrical connector, this parameter will be the contact resistance. According to [15], the electrical connector lifespan is divided into three stages:

1) Formation
2) Relative stability
3) Accelerated aging

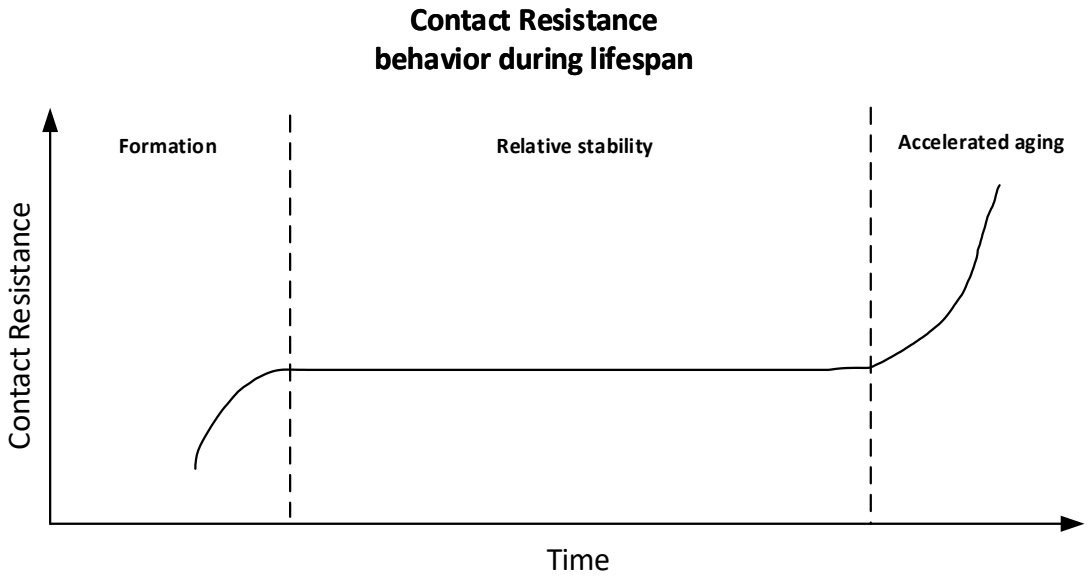


**Figure 1.6** Contact resistance evolution during lifespan. Adapted from IEC 61238-1. Compression and mechanical connectors for power cables for rated voltages up to 30 kV (Um = 36 kV) - Part 1: Test methods and requirements [15].

As shown in Figure 1.6, in the first phase, the stable constriction area is developed, thus generating an outstanding increase of the contact resistance at the beginning of the life. During the relative stability phase or useful life phase, the contact resistance barely increases. Finally, in the accelerated aging phase, since the temperature of the connector notably increases, there is a sharp increase of the contact resistance.

## 1.2 Objectives

This work is a part of the *SmartConnector* project, supported by the Ministerio de Ciencia e Innovación de España and the Generalitat de Catalunya under the framework of Retos de Colaboración (contract number RTC-2017-6297-3).

This thesis is focused on the data processing part of the *SmartConnector*, which aims to facilitate the application of predictive maintenance strategies and also to guarantee the correct operation of the connector throughout its useful life by means of the mathematical models that estimate the remaining useful life of the substation connectors and as well as to detect potential failure by applying fault detection models.

Therefore, the objectives of the thesis are the following:

- ✓ **Analyze in depth the temperature dependence of the contact resistance in order to have a better understanding of the best indicator of health of the substation connectors.**
- ✓ **Research and develop a mathematical model of remaining useful life for substation connectors based on-line data supplied by an accelerated electrical-thermal tests.**
- ✓ **Research and develop a fault detection models for diagnosing the condition of the connector based on-line data supplied by an accelerated electrical-thermal tests.**
- ✓ **Propose and validate ageing tests methodologies for substations connector as well as propose new methods to determine the reliability of the substation connectors.**

## 1.3 Thesis publications

In order to support this thesis, several works have been published during throughoutas a result of the development made in this research. This section summarizes these publications.

### 1.3.1 Conferences

- Kadechkar, J. A. Martinez, J. Riba, M. Moreno-Eguilaz and G. Rojas-Dueñas, "Experimental Study of the Effect of Aeolian Vibrations on the Contact Resistance of Substation Connectors." 2020 IEEE International Conference on Industrial Technology (ICIT), Buenos Aires, Argentina, 2020, pp. 613-618. DOI: 10.1109/ICIT45562.2020.9067145 [27]. **Published**

### 1.3.2 Journals

- Riba, J.-R.; Martínez, J.; Moreno-Eguilaz, M.; Capelli, F. "Characterizing the temperature dependence of the contact resistance in substation connectors." Sens. Actuators A Phys. 2021, 327, 112732. DOI: 10.1016/j.sna.2021.112732 [28]. **Published**

- Martinez, J.; Gomez-Pau, A.; Riba, J.-R.; Moreno-Eguilaz, M. "On-Line Health Condition Monitoring of Power Connectors Focused on Predictive Maintenance." IEEE Trans. Power Delivery. 2020, 36 (6), 3611-3618. DOI: 10.1109/TPWRD.2020.3045289 [29]. **Published**

- Martínez, J.; Riba, J.-R.; Moreno-Eguilaz, M." State of Health Prediction of Power Connectors by Analyzing the Degradation Trajectory of the Electrical Resistance. Electronics 2021, 10, 1409. DOI: 10.3390/electronics10121409 [30]. **Published**

- Riba, J.-R.; Gómez-Pau, Á.; Martínez, J.; Moreno-Eguilaz, M. "On-Line Remaining Useful Life Estimation of Power Connectors Focused on Predictive Maintenance." Sensors 2021, 21, 3739. DOI: 10.3390/s21217079 [31]. **Published**

# CONTACT RESISTANCE

# 2. CONTACT RESISTANCE

## 2.1 Introduction

Power connectors have to guarantee stable electrical connections between conductors or bus bars. For this reason, they are critical elements of the power systems. Power system operators work hard to provide a stable, reliable, continuous and safe power delivery to their customers, by making an effort to reduce service outages [32]. Therefore, it is crucial to guarantee their performance and reliable operation, as the failure of such components can lead to power outages, with catastrophic and costly consequences [1].

The electrical resistance is most likely the best indicator of their health condition for power connectors. An increase of resistance over time is an indication of degradation in power connectors. Also, any resistance rise is expressed as a rise of the connector temperature, which in turn rises the electrical resistance, thus deteriorating the operation condition while decreasing the expected life of the connector [16].

The total resistance of the connector has two components, i.e., the intrinsic or bulk resistance and the contact resistance [33]. On the one hand, the bulk resistance term is defined as the part of the resistance that results only from the shape and dimensions of the connector and also its electrical conductivity. On the other hand, the contact resistance of a connector is the part of the total resistance of the connector that is attributed to the contact interfaces.

The contact resistance is divided into two terms, i.e., the constriction and film resistances and depends on the nominal contact area [16] and the distribution and morphology of the conducting spots existing across the contact interfaces [34]. Factors such as surface roughness, applied pressure [35], the presence of dirt, debris or oxides formed at the contact interfaces have a deep impact on the contact resistance [16].

The development of fault diagnosis methods reduces maintenance costs and enhances the service life of the connectors [36]. Hence, in order to design reliable power connectors with an improved electrical and thermal behavior, and to develop functional condition monitoring and remaining useful life (RUL) strategies to reduce the number of unscheduled downtimes and maintenance costs during the useful life [37], a deep understanding of the behavior of the electrical resistance, and in particular, of the contact resistance, is necessary.

This chapter characterizes the temperature dependence of the contact resistance in substation connectors by performing a deep analysis from experimental tests. To this end, two types of substation connectors are analyzed, i.e., substation connectors designed to join tubular aluminum bus bars and substation connectors designed to join stranded aluminum conductors. These two types of connectors are analyzed due to the specific characteristics of tubular bus bars and stranded conductors where, in both types of conductors, the contact resistance contributes differently to the total resistance. It is worth noting that the knowledge developed in this work can be applied to design substation connectors besides similar devices with improved electrical and thermal features.

## 2.2 Background

Owing to the key role that power connectors play in power systems, the developments made in this chapter can be extremely valuable. In [38], the temperature dependence of the contact resistance of carbon nanotubes was reported. In [39], the pressure and temperature dependences of the contact resistance of different metals was analyzed in order to develop process models for resistance spot welding. In [40], the effect of heat cycles on the electrical resistance of bolted aluminum connectors of high ampacity was studied by applying accelerated heat cycles. In [13], the temperature dependence of the contact resistance between a substation connector and a stranded conductor is studied. However, none of the above mentioned works analyzes the temperature dependence of the film and constriction resistance components of the electrical resistance.

In spite of the important role that contact resistance performs in power systems, there are practically no studies focused on the analysis of the temperature evolution of contact resistance and their main components, the constriction and film resistances, and there are even less works applied to substation connectors. The temperature of the connectors is not constant due to the daily and seasonal load patterns, thus undergoing significant changes, which affect the electrical resistance and its components. Therefore, as the electrical resistance mainly determines the electrical and thermal behavior of the connectors, a good understanding of the temperature evolution of the contact resistance and its contribution to the total electrical resistance is of vital importance.

## 2.2 The analyzed connectors and installation methods

This section describes the analyzed connectors in this work and the methods or techniques to reduce the film resistance, which is necessary for a correct installation between connector and conductor.

### 2.2.1 The connectors

The connectors analyzed in this work are bolted substation connectors, which are made of A356 cast aluminum alloy with T6 thermal treatment. These connectors are designed to ensure stable and reliable connections between two bus bars, thus minimizing the electrical resistance and voltage drop among their terminal points and the associated power losses [41], [42]. Bolted connections enable compact and reliable contacts [43]. When increasing the torque applied to the bolting elements, the contact area tends to increase [44] while the contact resistance tends to decrease. Therefore, in bolted connectors, the applied torque is a key factor to ensure a suitable electrical resistance, which is specified by the manufacturer [20]. During the installation of the connectors, the torque applied to the bolting elements was measured by means of a calibrated dynamometric wrench (TAWM12340 from Bahco, Sweden). The bolting elements consist of M10 stainless steel bolts and nuts.

This work analyzes three models of substation connectors, i.e., two models intended to join two tubular aluminum bus bars of outer and inner diameters of 50 and 40 mm, respectively (straight-type S5SNS and T-type S5TNS models) and one connector intended to join two stranded aluminum conductors of 32 mm diameter (straight-type S330SLS), which are shown in Figure 2.1. It is noted that this work deals with two samples of each connector, so that 6 samples are analyzed for each installation method.

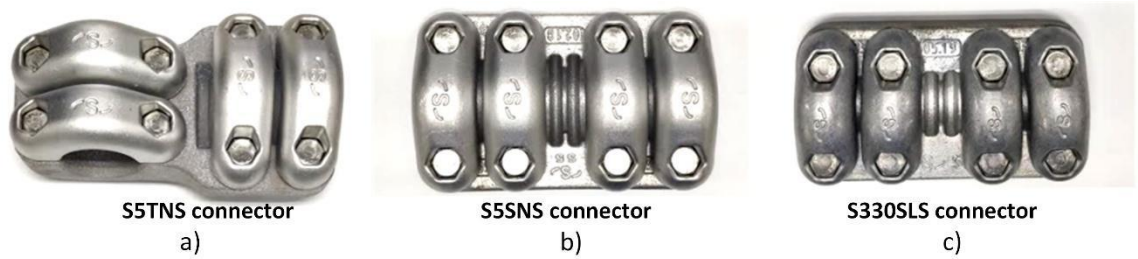


**Figure 2.1.** Substation connectors dealt with in this work from SBI Connectors catalogue. a) S5TNS T-type connector for tubular bus bars. b) S5SNS straight connector for tubular bus bars. c) S330SLS straight connector for stranded conductors [28].

**Table 2.1.** Analyzed connectors.

| Connector model | Connector designation | Connector type | Connector material | Associated conductor |
|---|---|---|---|---|
| **S5SNS** | C1, C2 | Straight | A356 | Bus bar |
| **S5TNS** | C3, C4 | T-type | A356 | Bus bar |
| **S330SLS** | C5, C6 | Straight | A356 | Stranded |

### 2.2.2 Wire brushing and chemical cleaning method

As previously explained, the contact resistance has two terms, named constriction and film resistance. The constriction resistance is directly related to the number and the real area of the contact points established at the contact interface, greatly determining the long term performance of substation connectors, since the current is restricted to flow through these few contact points. In the case of bolted connectors, this term can be minimized by applying a suitable torque and by ensuring proper condition and cleanliness of the interface. The film resistance term is mainly attributed to the alumina (Al2O3) layer formed naturally at the interface. Aluminum tends to react quickly with atmospheric oxygen, thus generating a very thin alumina layer. Since alumina is a very good electrical insulator, it obstructs the flow of current across the interface. In the case of aluminum contacts, the alumina film must be removed to ensure a good electrical contact [45].

There are two known techniques used to reduce the effect of the film resistance. The first method is the conventional **wire brushing method**, which consists of brushing the inner surface of the connector and the outer surface of the conductors or bus bars with a wire

brush, to mechanically remove much of the alumina film. Once the matting surfaces have been brushed, they are covered with a conductive grease (PenetroxTM A electrical joint compound from Burndy), which inhibits the development of the alumina layer [46], while ensuring a good contact and improving the electrical performance of the joint [47]. Since this procedure does not completely remove the alumina layer, a more innovative procedure is required. The second method used in this work is the **chemical cleaning method,** which is applied due to its improved results [45]. It involves applying a chemical solution at the matting surfaces for 20 minutes to completely remove the alumina layer and next, the components are assembled as in the conventional procedure.

## 2.3 The proposed mathematical approach

As the purpose of this chapter is focused on determining the temperature evolution of the electrical contact resistance (ECR) of the connector, $R_{ECR}$, its value must be measured. The total electrical resistance is determined from direct measurements, as shown in (2.1).

$$R_{total,AC,T} = R_{bulk,AC,T} + R_{ECR,T} \tag{2.1}$$

$R_{bulk,AC,T}$ being the intrinsic or bulk resistance term, which mainly depends on the physical dimensions and shape of the connector and its electrical conductivity and the eddy currents effect. However, the bulk resistance is also influenced by the part of the conductor introduced into the connector. Despite the ECR is considerably smaller compared with the total resistance of the connector, the changes in the contact resistance can cause significant alterations of the connector behavior because such changes are attributed to alterations of the contact area. According to [12], [47], [48], the electrical contact resistance of a joint consists of the constriction resistance ($R_{constriction}$) and the resistance of the film layer ($R_{film}$),

$$R_{ECR,T} = R_{constriction,T} + R_{film,T} \tag{2.2}$$

On the other hand, the constriction resistance depends on the mechanical and electrical properties of the connector [49], the resistance of the film is influenced by the conducting and real contact areas. However, when applying a chemical cleaning (see section 2.2.2), the $R_{film}$ term is almost completely removed, so that,

$$R_{ECR,T} \simeq R_{constriction,T} \tag{2.3}$$

Hence, the bulk resistance term can be obtained with the help of Finite Element Method (FEM) simulations, as this term is not possible to measure. Figure 2.2c summarizes the resistances of the conductor-connector assembly, where $R_{ECR}$ is the contact resistance, $R_{conductor,A\text{-}0}$ and $R_{conductor,0\text{-}1}$ are the resistance contributions of the conductor between

points *A-0* and *0-1*, respectively, and $R_{connector}$ is the resistance of one half of the connector. It is a known fact that suitable physical and mathematical descriptions of the system under analysis allow to determine the relation between unknown and measurable parameters [50], [51].

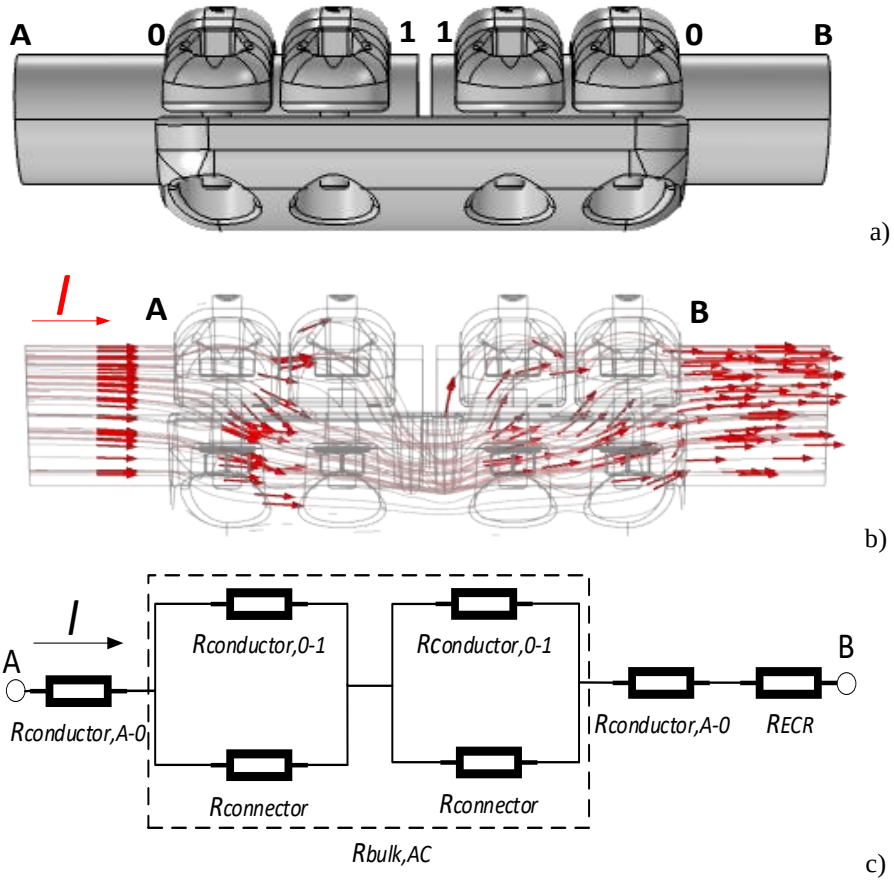


**Figure 2.2**. a) Connector and bus bar assembly. b) FEM simulation of the electrical current passing through the connector. c) Equivalent electrical resistance of the conductor-connector assembly [28].

From Figure 2.2c, it is deduced that the total resistance between points *A* and *B*, $R_{total,A\text{-}B}$ and $R_{ECR}$ are related as,

$$R_{ECR} = R_{total,A-B,T} - 2R_{conductor,A-0,T} - R_{bulk,AC,T} =$$
$$= R_{total,A-B,T} - 2R_{conductor,A-0,T} - \underbrace{2\left[\frac{R_{connector,T} \cdot R_{conductor,0-1,T}}{R_{connector,T} + R_{conductor,0-1,T}}\right]}_{R_{bulk,AC}} \quad (2.4)$$

where $T$ in (2.4) is the temperature at which the resistances have been measured. The values of $R_{total,A-B,T,}$ $R_{conductor,A-0,T}$ and $R_{conductor,0-1,T}$ are directly measurable or calculable, whereas the values of $R_{ECR,T}$ and $R_{connector,T}$ are unknown, so that they must be calculated. $R_{connector,T}$ can be determined from FEM simulations if the electrical resistivity of the A356-T6 alloy is known, whereas $R_{ECR,T}$ is obtained by solving (2.4) once $R_{connector,T}$ is known.

The resistivity of the conductor was previously obtained by measuring the electrical resistance at 20 ºC as,

$$R_{conductor,20ºC} = \rho_{conductor,20ºC} \cdot \frac{L}{S} \quad (2.5)$$

where $\rho_{conductor,20ºC}$ is the electrical resistivity of the conductor measured at 20 ºC, $L$ is its length and $S$ is the cross sectional area. As,

$$R_{total,A-B,T} = R_{total,A-B,20°C} \cdot [1 + \alpha_{total} \cdot (T - 20)] \quad (2.6)$$

by measuring the temperature evolution of $R_{total,A-B}$, the temperature coefficient $\alpha_{total}$ can be determined. As it is not possible to measure directly the resistance of the connector $R_{connector}$, in this work it is calculated by applying multiphysics FEM simulations using the COMSOL® software. The temperature evolution of this resistance with temperature under AC supply can be expressed as,

$$R_{connector,T} = R_{connector,20°C} \cdot [1 + \alpha_{connector} \cdot (T - 20)] \quad (2.7)$$

To determine the temperature coefficient of the conductors (tubular bus bar and stranded conductor), a sample of the tubular bus bar with a length of 0.64 m and a sample of the stranded conductor with a length of 0.73 m were heated and their resistances were measured at different temperatures. In both cases, the temperature coefficient of the conductor $\alpha_{conductor}$ can be obtained from,

$$R_{conductor,T} = R_{conductor,20^{o}C} \cdot [1 + \alpha_{conductor} \cdot (T - 20)] \quad (2.8)$$

Therefore, the flowchart in Figure 2.3 sums up the mathematical approach proposed in this work to characterize the ECR dependence with temperature. This process was repeated twice. Firstly, it was carried out by using the installed connectors by means of the standard procedure (brushing and applying conductive grease) so that the film and constriction terms are included in the $R_{ECR}$ and $\alpha_{ECR}$. Afterward, the same procedure was then applied to the connectors which were installed by applying a chemical cleaning followed by the application of conductive grease, so in this case only the constriction term is included in $R_{ECR}$ and $\alpha_{ECR}$, since the chemical cleaning removes almost completely the film resistance, as explained in section 2.2.2.

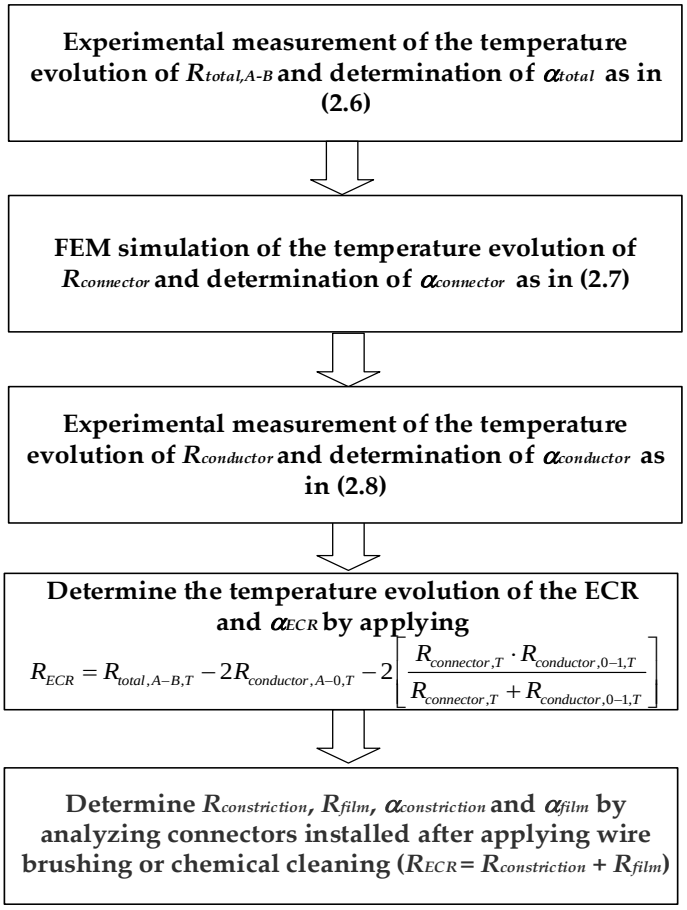


**Figure 2.3.** Flowchart summarizing the proposed mathematical approach [28].

## 2.4 Experimental setup

This sections describes the experimental setup of this test. First, the temperature rise test that was carried out in this work is described. Next, all the equipment and instrumentation used are detailed. Finally, it is explained how the connector resistance is measured during the experiment.

### 2.4.1 The temperature rise test

To evaluate the evolution of the electrical resistance with temperature, experimental temperature rise tests were carried out in two independent electrical loops, which were installed in the AMBER high-current laboratory of the Universitat Politècnica de Catalunya. The first and second loops included, respectively, two S5TNS T-type connectors and two S5SNS straight connectors, joined by means of tubular aluminum bus bar conductors (50 mm outer diameter, 5 mm thickness, 6063-T5 Al alloy). The third electrical loop was composed of four S330SLS straight connectors joined by Hawthorn AAC stranded conductors of 32 mm diameter. During the temperature rise tests, the rated current of the bus bar or stranded conductor was applied to the loop in order to rise the temperature of the connectors.

To run the temperature rise tests, the connectors were fitted on the tubular bus bars or on the stranded aluminum conductors following the procedure detailed in the ANSI/NEMA CC1-2009 standard [12]. Since the electrical resistance between the terminal points of the connectors was measured during the tests, as well as the temperature of the connector, wire equalizers were used and placed on the external surface of the bus bar or conductor side very close to the connector for ensuring an equipotential point to measure the voltage drop. The test consists of a heating phase by applying the rated current of the stranded conductor or the bus bar, thus heating up the connectors and conductor. The test finishes when reaching the thermal equilibrium. To this end, a current of 1015 $A_{RMS}$ (stranded conductor rated current) or 1050 $A_{RMS}$ (tubular bus bar rated current) was applied up to reaching the thermal equilibrium, and then the electrical loop was disconnected from the output of transformer supplying the high-current to the loop. During the heating phase, the temperature, current and voltage drop across the connectors were acquired every 45

seconds, and these values were used to determine the evolution of the electrical resistance with the temperature.

### 2.4.2 Equipment and instrumentation

A high-current transformer (variable input voltage 0 - 400 $V_{RMS}$, output voltage 0 - 10 $V_{RMS}$, output current 0 - 10 $kA_{RMS}$) was used to generate the high current levels required during the experiments. The output current of the transformer, i.e., the current circulating in the electrical loop for heating the connectors was measured using a wide-bandwidth calibrated Rogowski probe (CWT500LFxB 0.06 mV/A from PEM, Nottingham, UK). The temperature of the connectors, bus bars and stranded conductors, was measured using T-type thermocouples, which were associated with an 8-channel thermocouple data logger (USB TC-08, Omega, Egham, Surrey, UK), obtaining an accuracy superior to 1 °C. The voltage drop across the connectors was measured by means of an 8-channel data acquisition device providing an absolute resolution of 88 µV (NI USB-6210, National Instruments, Austin, Texas, USA). The Rogowski coil was also connected to one of the inputs of the NI USB-6210 data acquisition device, so that the voltage drop and current waveforms were acquired synchronously and sampled at 50 kSamples/s for 0.2 seconds (10 electrical periods). This setup allows measuring the electrical resistance of the connectors with an accuracy better than 0.2 micro-Ohm. Figure 2.4 shows the electrical loops analyzed in this work. Finally, Figure 2.5 shows the connector-conductor joint.

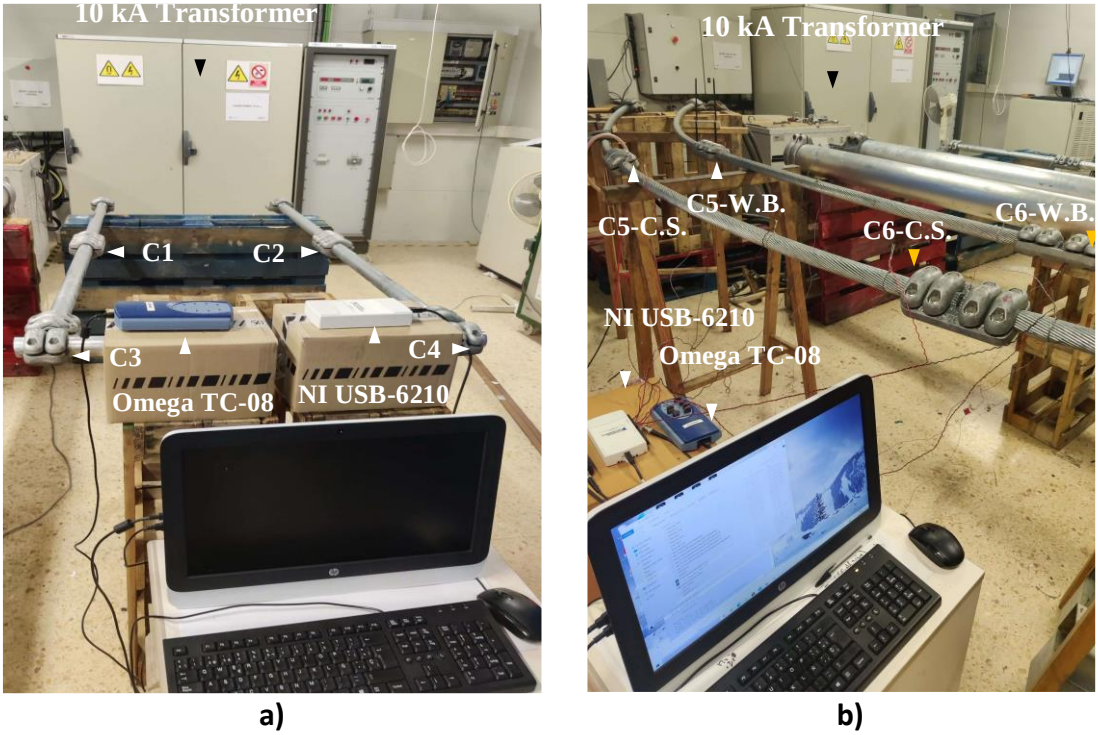


**Figure 2.4.** Electrical loops under test. a) Loops #1 and #2. b) Loop #3. (W.B. and C.S. stand for wire brushing and chemical solution, respectively) [28].


**Figure 2.5.** The connector-conductor joint [28].

The electrical resistivity and temperature coefficient of the A356-T6 connector material were measured using a programmable electric muffle (Digitheat-TFT, 200 ºC, from JP SELECTA, Abrera, Barcelona, Spain) and an A356-T6 test specimen (4 mm x 4 mm square cross section, 150 mm length). To this end a precision DC power supply (BK Precision 9205, 0.1%+10 mA, Yorba Linda, California, USA) was used to generate 5 Amps, jointly with a digital multimeter (4461A Keysight Technologies, ± 0.01% accuracy, Santa Rosa, California, USA) that was applied to measure the voltage drop.

### 2.4.3 Measurement of the resistance

Substation connectors offer a very low resistance to the flow of an electric current, this resistance being in the order of several micro-Ohms. Due to this low value, an on-line measurement is a challenging task. In this work, because it is recognized that under alternating current supply the resistance is the real part of the impedance [52], the on-line measurement of the total electrical resistance of the connector under power frequency supply was done by acquiring the voltage drop waveform $\Delta V$ across the connector between point A and B (see Figure 2.2a), the current waveform $I$ flowing through the connector, and the phase shift $\varphi$ between both waveforms. Then, from the instantaneous values of $\Delta V$, $I$ and $\varphi$, the total resistance of the connector $R_{Total,A\text{-}B,\,,T}$ measured at an arbitrary temperature $T$ is obtained as [53],

$$R_{total,A-B,T} = \frac{\Delta V}{I} \cdot \cos\varphi \tag{2.9}$$

As the resistance depends on the resistivity of the material of the connector/conductor and the resistivity in turns depends on the temperature, the AC resistance will also depend on the temperature. Under AC supply, the skin effect alters the value of the resistance and its temperature dependence, because the resistivity of the connector/conductor material increases with temperature, thus decreasing the impact of the skin effect. Due to the impact of the temperature in the value of the electrical resistance, it is a common practice to refer the resistance to 20 ºC [1] [54], by applying (2.10),

$$R_{total,A-B,20°C} = \frac{R_{total,A-B,T}}{1+\alpha_{total,A-B}(T-20)} \tag{2.10}$$

$\alpha_{total,A\text{-}B}$ being the temperature coefficient expressed in $^{o}C^{-1}$, which accounts for both the temperature and skin effects. It is noted that whereas any temperature increase tends to raise the effective resistivity and thus the electrical resistance, the intensity of the skin effect tends to decrease when the temperature increases, thus reducing the increase of the electrical resistance. Due to the relatively low impact of the skin effect on the AC

resistance of the connector, the resistance increase with temperature due to the rise of the electrical resistivity has more impact than the reduction of the intensity of the skin effect with temperature.

## 2.5 Results

This section presents the results attained in this work.

### 2.5.1 Simulation results to determine the temperature evolution of the connector resistance.

This section describes the results attained to determine the temperature evolution of $R_{connector,T}$. As explained in Section 2.3, $R_{connector,T}$ is calculated from FEM simulations assuming that the conductivity of the A356-T6 alloy is known. FEM simulations also allow determining $\alpha_{connector}$ under AC supply by applying (2.7), as it is not directly measurable. It is worth mentioning that FEM simulations performed under AC supply already consider the skin effect generated by the eddy currents.

Figure 2.6 shows, respectively, FEM simulation meshes of the connectors S5SNS, S5TNS and S330SLS carried out under power frequency AC supply. These simulations are used to determine the resistance of the connector by applying a 50 Hz electric current of 100 $A_{RMS}$ while determining the voltage drop across the terminal points of the connector. To determine only the resistance due to the connector, i.e., to neglect the resistance of the conductors, simulations assume that the conductors have infinite conductivity.

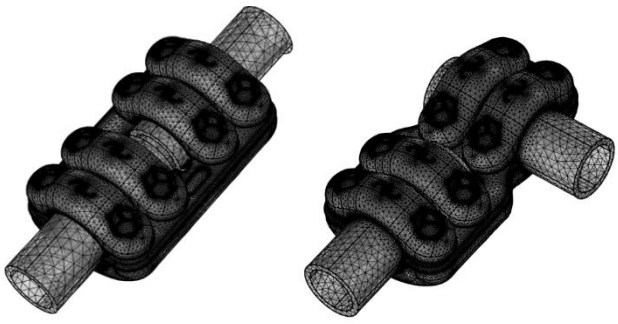

a) b)

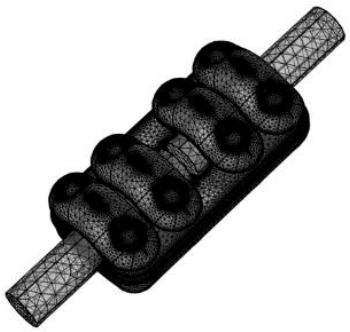

c)

**Figure 2.6.** Voltage drop obtained by means of FEM simulations to determine the connector resistance and the temperature coefficient under AC supply when applying a current of 100 A. Simulations assume infinite conductivity of the conductor material in order to only determine the resistance due to the connector. a) S5SNS connector. b) S5TSNS connector. c) S330SLS connector [28].

**Table 2.2.** Connector resistance obtained at 20ºC obtained from FEM simulations.

| **Connector model** | **Connector designation** | **Connector resistance $R_{connector,20ºC}$ [micro-Ohm]** |
|---|---|---|
| **S5SNS** | C1, C2 | 1.95 |
| **S5TNS** | C3, C4 | 1.80 |
| **S330SLS** | C5, C6 | 2.60 |

**Table 2.3.** Connector temperature coefficient obtained from FEM simulations.

| **Connector model** | $\alpha_{connector}$ [°C$^{-1}$] | $R^2$ |
|---|---|---|
| **S5SNS** | 0.0012 | 0.999 |
| **S5SNS** | 0.0014 | 0.999 |
| **S330SLS** | 0.0013 | 0.999 |

Tables 2.2 and 2.3 show, respectively, the values of the connectors resistance and temperature coefficient obtained from FEM simulations, $R_{connector\,,20ºC}$ and $\alpha_{connector}$. FEM simulations assume an initial electrical resistivity of the aluminum alloy of $\rho_{A356\text{-}T6,DC,20ºC}$= 5.26·10$^{-8}$ Ωm and a temperature coefficient of $\alpha_{A356\text{-}T6,DC}$= 0.0025°C$^{-1}$. Both values were measured as explained in Section 2.4.2. In the simulations carried out under power frequency supply, the temperature was changed, so that both the connector resistance and the temperature coefficient were altered due to the skin effect. In addition, the coefficient of determination $R^2$ is calculated in Table 2.3, which measures the

proximity between the experimental data and the fitted regression line. As shown in Table 2.3, due to the skin effect, the effective temperature coefficient of the connector under power frequency supply, $\alpha_{connector}$, is lower than the temperature coefficient of its material, the A356-T6 alloy, measured under DC supply. This is due to the resistivity of the A356-T6 alloy increases with the temperature, thus reducing the intensity of the skin effect.

### 2.5.2 Results attained to determine the total resistance, stranded conductor and tubular bus bar resistance temperature dependences

This section describes the experimental results carried out to determine the temperature evolution of the total resistance $R_{total,A\text{-}B,T}$, of all the connector/conductor assemblies, the stranded conductor resistance $R_{stranded\_conductor,T}$ and the tubular bus bar conductor resistance $R_{bus\_bar,conductor,T}$. To this end, the experimental results of twelve substation connectors, a sample of a stranded conductor and a sample of a tubular bus bar collected by performing temperature rise tests are presented.

As explained in section 2.4.1, the conductors and substation connectors were put together in three electrical loops. First, loop #1 is composed by a tubular bus bar conductor circuit, which was assembled with two S5SNS connectors and two S5TNS connectors after applying chemical cleaning. Next, loop #2 was assembled by joining tubular bus bar conductors with two S5SNS connectors and two S5TNS connectors by applying wire brushing. Finally, loop #3 was installed by using stranded conductors, which were assembled with two S330SLS connectors after applying the chemical cleaning, and also with two S330SLS connectors after applying wire brushing.

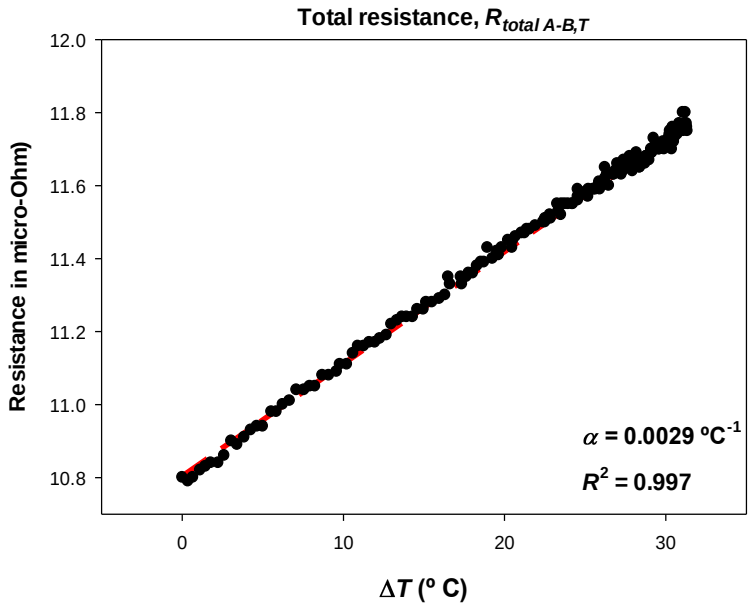
Total resistance, $R_{total\ A\text{-}B,T}$
Resistance in micro-Ohm)
12.0
11.8
11.6
11.4
11.2
11.0
10.8
0
10
20
30
$\Delta T$ (º C)
$\alpha$ = 0.0029 ºC$^{-1}$
$R^2$ = 0.997

a)

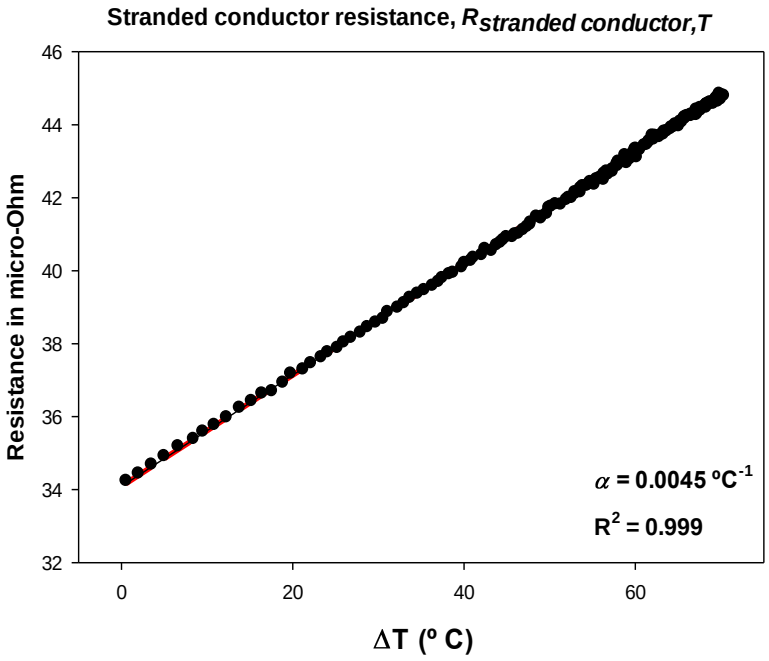
Stranded conductor resistance, $R_{Stranded\ conductor,T}$
Resistance in micro-Ohm
46
44
42
40
38
36
34
32
0
20
40
60
ΔT (º C)
$\alpha$ = 0.0045 ºC$^{-1}$
R$^2$ = 0.999

b)

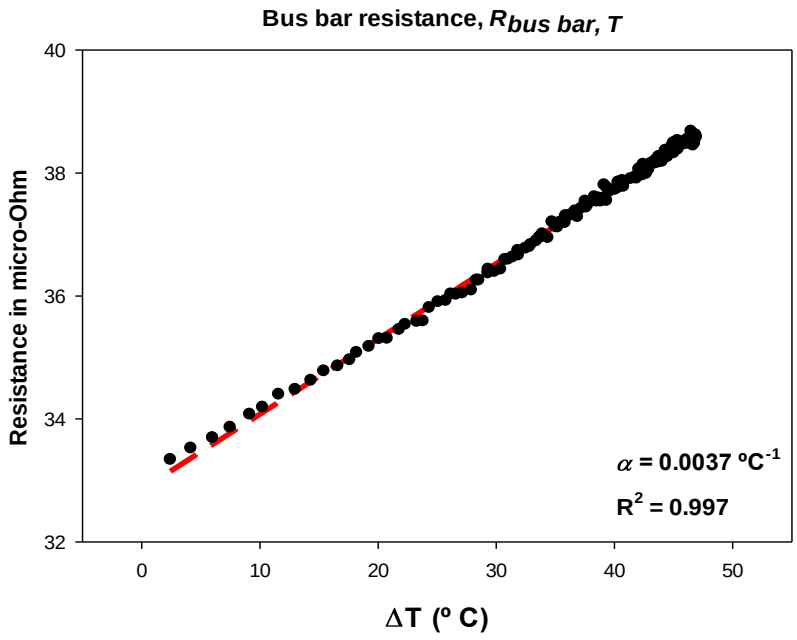


c)

**Figure 2.7.** Measured values of $R_{total,A\text{-}B,T}$, $R_{stranded\ conductor,T}$ and $R_{bus\_bar\ conductor,T}$ against $\Delta T = T - 20$ °C. a) $R_{total,A\text{-}B,T}$ of connector C1 after applying a chemical cleaning. b) $R_{stranded\ conductor,T}$ d) $R_{bus\_bar\ conductor,T}$ [28].

Figure 2.7 shows the temperature evolution of the total resistance of connector #1, the resistances of the stranded conductor and the tubular bus bar, respectively. In order to heat the connectors, temperature rise tests were performed until reaching the thermal equilibrium. In order to determine the ECR contribution to the total resistance and its temperature evolution, the temperature coefficients of all connector-conductor sets were estimated by measuring the total resistance $R_{total,A\text{-}B}$ and the temperature of the components on real time under AC supply. The temperature coefficients presented in Figure 2.7 were calculated by applying (2.6) and (2.8).

**Table 2.4.** Bus bar and stranded conductor resistances measured at 20°C.

| Conductor type | $R_{A\text{-}0,20°C}$ [micro-Ohm] | $R_{0\text{-}1,20°C}$ [micro-Ohm] |
|---|---|---|
| **Tubular bus bar** | 2.3 | 4.1 |
| **Stranded conductor** | 2.7 | 4.8 |

Table 2.4 shows that the total resistance at 20°C of all connectors-conductor sets after applying the chemical cleaning treatment are below the values of the total resistance of the connectors treated with wire brushing. This is because the chemical solution cleans the alumina film formed at the interface, thus reducing the film resistance and consequently the ECR. It is worth mentioning that the values presented in Table 2.4 are derived from the results shown in Figure 2.7, which are required in (2.4) to determine the resistance of the ECR term.

**Table 2.5.** Total resistance measured at 20°C when applying wire brushing or chemical cleaning.

| **Connector model** | **Connector designation** | **Wire brushing** | **Chemical cleaning** |
|---|---|---|---|
| | | $R_{total,A\text{-}B,20°C}$ **[micro-Ohm]** | $R_{total,A\text{-}B,20°C}$ **[micro-Ohm]** |
| **S5SNS*** | C1 | 11.9 | 10.8 |
| | C2 | 11.7 | 10.4 |
| **S5TNS*** | C3 | 12.7 | 12.2 |
| | C4 | 13.0 | 12.4 |
| **S330SLS**** | C5 | 18.6 | 16.3 |
| | C6 | 19.2 | 16.4 |

*Associated with bus bars **Associated with stranded conductors

Table 2.5 shows that the connectors associated with stranded conductors exhibit larger values of the total resistance than the connectors assembled with tubular bus bars. This is because tubular bus bars offer a much smoother and uniform contact surface with the connectors than that offered by stranded conductors, thus maximizing the contact area and minimizing the constriction resistance term. In addition, a smoother and more uniform contact surface offered by the tubular bus bars allow reducing the interstitial air voids, thus minimizing the formation of the alumina layer, and the film resistance term.

**Table 2.6.** Total temperature coefficient calculated when applying chemical cleaning or wire brushing.

| Connector model | Connector designation | Wire brushing | | Chemical cleaning | |
|---|---|---|---|---|---|
| | | $\alpha_{total,A-B}$ [°C$^{-1}$] | $R^2$ | $\alpha_{total,A-B}$ [°C$^{-1}$] | $R^2$ |
| S5SNS* | C1 | 0.0030 | 0.998 | 0.0029 | 0.997 |
| | C2 | 0.0029 | 0.998 | 0.0028 | 0.999 |
| S5TNS* | C3 | 0.0030 | 0.995 | 0.0029 | 0.999 |
| | C4 | 0.0030 | 0.997 | 0.0029 | 0.999 |
| S330SLS** | C5 | 0.0042 | 0.996 | 0.0039 | 0.996 |
| | C6 | 0.0040 | 0.990 | 0.0038 | 0.992 |

*Associated with bus bars **Associated with stranded conductors

Finally, Table 2.6 shows that the temperature coefficient $\alpha_{total,A-B}$ of connector S330SLS is higher than those of the other connectors. This is because connector S330SLS is associated with stranded conductors, which have temperature coefficients higher than those of the bus bars, to which the S5SNS and S5TNS connectors are associated. Results presented in Table 2.6 also shows high values of the coefficients of determination $R^2$, thus proving the suitability of the equations dealt with in this work.

### 2.5.3 Determination of the temperature evolution and temperature coefficients of the ECR

This section describes the results carried out to determine the temperature evolution of the ECR, i.e., $R_{ERC,T.}$ and its components, the constriction $R_{constriction,T}$ and film resistance $R_{film,T}$.

The experimental results presented in sections 2.5.1 and 2.5.2 in conjunction with (2.4) were used to determine the temperature evolution of the ECR. This is because $R_{total,A-B,T}$, $R_{conductor,0-1,T}$ and $R_{conductor,A-0,T}$ are measured values, whereas $R_{connector,T}$ was obtained from FEM simulations. Since when applying a chemical cleaning the oxide film is almost completely removed, in this case the value of the ECR is mostly attributed to the constriction resistance term $R_{constriction,T}$. However, when applying wire brushing, the value of the ECR is due to both the film and constriction resistance terms. In this case,

the film resistance can be calculated by subtracting the constriction resistance term from the ECR, as easily deduced from (2.2), i.e., by applying $R_{film,T} = R_{ECR,T} - R_{constriction,T}$.

**Table 2.7.** Contact, constriction and film resistances of the substation connectors.

| Connector type | Connector designation | $R_{ECR,20°C}$ | $R_{constriction,20°C}$ [micro-Ohm] | $R_{film,20°C}$ |
|---|---|---|---|---|
| **S5SNS** | C1 | 4.6 | 3.5 | 1.1 |
| | C2 | 4.5 | 3.2 | 1.3 |
| **S5TNS** | C3 | 5.6 | 5.1 | 0.5 |
| | C4 | 5.9 | 5.3 | 0.6 |
| **S330SLS** | C5 | 9.7 | 7.5 | 2.2 |
| | C6 | 10.2 | 7.4 | 2.6 |

Table 2.7 shows the ECR $(R_{ECR,20°C})$, constriction $(R_{constriction,20°C})$ and film resistance $(R_{film,20°C})$ values at 20 °C of all connectors/conductor sets. It can be observed that the ECR values of the S3330SLS connectors are greater than those of connectors S5SNS and S5TNS because connector S3330SLS is associated with a stranded conductor instead of being associated with tubular bus bars, being this the case of connectors S5SNS and S5TNS. The air gaps between the strands produce a poorer contact between the conductor and connector compared to the contact between the bus bar and connector, increasing the risk of oxide film build-up.

**Table 2.8.** Contact, constriction and film temperature coefficients of the substation connectors.

| Connector | $\alpha_{ECR}$ [°C$^{-1}$] | $R^2$ | $\alpha_{constriction}$ [°C$^{-1}$] | $R^2$ | $\alpha_{film}$ [°C$^{-1}$] | $R^2$ |
|---|---|---|---|---|---|---|
| **C1** | 0.0045 | 0.992 | 0.0045 | 0.986 | 0.0044 | 0.821 |
| **C2** | 0.0045 | 0.992 | 0.0045 | 0.996 | 0.0046 | 0.924 |
| **C3** | 0.0041 | 0.998 | 0.0041 | 0.998 | 0.0044 | 0.899 |
| **C4** | 0.0041 | 0.998 | 0.0040 | 0.998 | 0.0044 | 0.948 |
| **C5** | 0.0049 | 0.987 | 0.0049 | 0.965 | 0.0049 | 0.926 |
| **C6** | 0.0053 | 0.982 | 0.0053 | 0.997 | 0.0052 | 0.900 |

Finally, Table 2.8 shows the temperature coefficients $\alpha_{ECR}$, $\alpha_{constriction}$ and $\alpha_{film}$ of the analyzed substation connectors. In addition, the coefficients of determination $R^2$ of the

obtained temperature dependences are also provided, which prove the accuracy of the fittings made. From results in Table 2.8 it can be observed that the temperature coefficients of ECR ($\alpha_{ECR}$), constriction ($\alpha_{constriction}$) and film ($\alpha_{film}$) of all the analyzed connectors are similar but quite different from those of the $\alpha_{total}$ and $\alpha_{connector}$.

## 2.6 Conclusions

Substation connectors must endure daily and seasonal load cycle profiles, which alter their temperature and thus, their electrical resistance. In this chapter the temperature dependence of the contact resistance of aluminum substation connectors was analyzed in detail.

Electrical loops including several connectors have been installed and analyzed in order to obtain experimental results. The total electrical resistance of the analyzed connectors was measured on-line by monitoring the current flowing in the loops, the voltage drop across the terminal points A and B of the connectors and their temperature. All terms of the total electrical resistance were analyzed, i.e., the bulk or intrinsic resistance and the electrical contact resistance, which is divided into the constriction and film resistance terms. In addition, the influence of resistance of the conductor was also analyzed for both tubular bus bars and stranded conductors. There is a lack of works analyzing in detail the temperature dependence of the contact resistance, and the effect of temperature on the constriction and film resistance terms.

Results presented in this chapter show that all resistance terms increment linearly with temperature, but at a different rate. This means that each term has its own temperature coefficient. Furthermore, results also demonstrate that the contact resistance increases linearly with temperature at a faster rate than the increase of the bulk resistance under AC supply.

The findings of this chapter allow a better understanding of the impact of the contact resistance on the total resistance of power connectors, thus providing valuable data and knowledge to design substation connectors and similar devices with improved electrical and thermal behaviors.

# REMAINING USEFUL LIFE (*RUL*)

# 3. REMAINING USEFUL LIFE (RUL)

## 3.1 Introduction

It is well-known that power connectors are critical components for the suitable operation of power systems. After long-term operation, degradation mechanisms can negatively influence the contact resistance, and consequently, their performance.

Medium voltage connectors are power connectors designed to provide a reliable and stable electrical connection between two conductors or bus bars. The most common materials for medium voltage connectors are copper and aluminum [53] and they are often of compressed type, since compression provides a reduced contact resistance and a reliable electrical connection. These electromechanical devices are designed to transmit electrical power with minimum power losses [41], consequently with minimum voltage drop.

It can be said that two predominant processes rule the rise of the contact resistance, thus the ageing process of electrical connectors. The first process is when the contact resistance increases as a result of a low pressure contact between the connector and the conductor, due to poor installation and/or peak and off-peak daily current cycles, generating contraction and expansion patterns, which tend to lose the contact. The second process is due to the chemical reactions at the contact interfaces, which generate non-conductive compounds, influencing the ageing behavior and affecting negatively the contact resistance [15]. Once the resistance of the connector exceeds a threshold value, it must be substituted to prevent any failure.

Prognostics and health management allow to evaluate the reliability of different elements in their life cycles, while mitigating risks of sudden breakdowns [55]. Nowadays, health management and prognostics is evolving from failure management to degradation management [56]. On the other hand, reliability analysis has been typically based on

predicting the failure rate [19]. Reliability engineering is directly related to predict the remaining useful life of systems by incorporating all available data [57].

The *Remaining Useful Life* (*RUL*) of a power connector is the expected operating time before it needs to be replaced. An accurate RUL prediction of power connectors is of great interest to guarantee satisfactory reliability and safety of power systems, which provides reference data to apply predictive maintenance plans, while allowing to optimize power system operational efficiency, in order to reduce costs due to unscheduled failures and to avoid premature connector faults and major power system failures [47], thus reducing the probability of disaster occurrence [58]. Power connectors are designed for a continuous operation of several years, in the order of 30-40 years for substation connectors, although premature failure modes may happen much before [20]. Therefore, a correct RUL estimation is interesting in order to apply predictive maintenance programs, as it allows determining and planning the connectors that must be replaced in the short or medium term, thus avoiding their failure and the undesirable consequences of these catastrophic faults.

This chapter proposes a RUL approach based on acquiring on-line data (voltage drop across the connector, electric current and temperature) to determine the current level and the evolution of the electrical resistance of the analyzed connector, since it is a reliable indicator of the health status of the connector [59], thus allowing to determine its power efficiency and the expected lifetime [60]. Any increase of the contact resistance leads to a raise of the temperature of the connector, with a consequent increase of the contact resistance, thus deteriorating the behavior of the connector and reducing the RUL [20]. It is also important to mention that the RUL model proposed in this work is based on an oxidation multi spot equation which describes the rise of the electrical contact resistance with time due to the growth of oxide films at the contact interface [61].

Figure 3.1 summarizes the proposed strategy, which is a novel and low-cost method that determines the RUL based on an on-line monitoring of the evolution of the connector electrical resistance with time in order to achieve a reliable on-line estimation of the RUL. To this end, the instantaneous values of the voltage drop, electrical current and temperature are acquired to determine the parameters of the resistance degradation model,

which is detailed in this chapter. This model allows estimating the expected RUL, i.e., the time at which the electrical resistance exceeds a defined threshold value in order to anticipate and planning the replacement of the connector. This strategy allows to improve and simplify predictive maintenance plans.

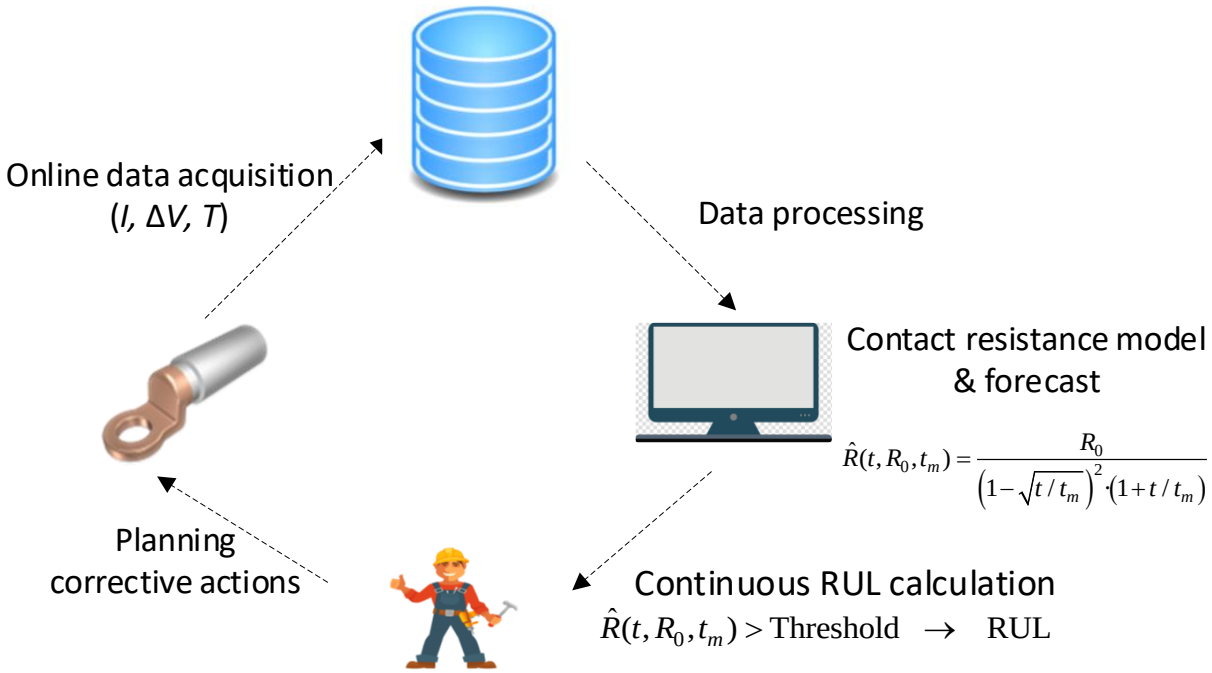


**Figure 3.1.** Proposed approach to predict the RUL of power connectors [31].

## 3.2 Background

Predictive maintenance has a long history. Formerly, methods based on visual inspection were applied for predictive maintenance. Nowadays, predictive maintenance is evolving towards data-driven approaches and physical modeling due to the extensive use of different types of sensors, communication protocols and computational power. Grid reliability can be improved by using online sensing technologies based on low-cost sensors [62]. Despite the progress in predictive maintenance methods, hands-on and time-based maintenance are still widely used [63].

In case of devices whose natural ageing under regular operational conditions involves a long time, accelerated ageing methods are widely applied to analyze their long-term performance [64]. As a result, many works found in the technical literature are based on performing accelerated ageing tests on such devices [64], [65] to study and describe their long-term behavior. However, this strategy is very expensive in terms of consumed energy, human labor, required materials and monetary cost, and the achieved results are specific, thus often lacking of generalization capability. In addition, conventional maintenance approaches are based on failure data of similar devices. Nevertheless, these approaches do not contemplate the specificity of the degradation process of each single device [61]. Therefore, due to the above mentioned issues, it is necessary to use another strategy, which is not complex to apply. Thus, the approach presented in this chapter overcomes this limitation as the predicted RUL is adjusted to each particular connector.

On the other hand, regarding RUL models, there is a lack of literature for power connectors even though they are currently demanded. In [66], the combined effect of vibration and temperature stresses on the value of the contact resistance of automotive connectors was evaluated with the aim to determine the minimum vibration amplitude for fretting-corrosion degradation. In [67], the mechanical behavior and fatigue lifetime of micro electrical connectors were estimated based on the effect of fretting wear. In [19], a RUL method for aviation connectors is presented based on high vibration stress, which combines a vibration-induced physical model, a particle filtering data-driven approach and accelerated degradation testing to evaluate the performance of the proposed approach. In [68], the reliability and failure rate of electrical connectors was predicted under

particulate contamination and temperature stresses by means of accelerated degradation tests to collect degradation data. A similar approach was applied in [69], where in this case the lifetime distribution was described by a two-parameter Weibull distribution, whose parameters were inferred by applying the maximum-likelihood estimation method from degradation test data. RUL estimation of micro switches based on Bayesian updating and expectation maximization combined with strong tracking filtering was presented in [70], the failure threshold being based on the contact voltage drop between contacts once closed, which is directly related to the contact resistance. In [71], failure indicators based on the change of the electrical resistance of small size socket electrical connectors are applied to predict the RUL of such components based on random vibration tests carried out to produce fretting corrosion degradation. Resistance was measured by applying the resistance spectroscopy technique jointly with phase sensitive detection and a Kalman filter was applied for estimating the health status of the socket connector.

This chapter proposes an innovative RUL estimation method and a criterion for power connectors based on an on-line monitoring of the electrical resistance of the connector. This approach is focused to ease predictive maintenance plans, thus contributing in this area due to the scarcity of works in the field of RUL estimation methods for power connectors. The proposed RUL criterion has been experimentally evaluated by using a degradation model based on the contact resistance [72], which shows encouraging results. Furthermore, the proposed strategy brings different novelties, since it is based on the on-line measurement of the electrical resistance using low-cost sensors, and on a simple and fast-to-calculate degradation model of the electrical resistance. Therefore, this process is quite simple, with low mathematical complexity and in consequence, with low computational burden, making it feasible to be embedded in the field via Internet of Things (IoT) devices or wireless sensor networks. In addition, another advantage of this proposal is that it does not require to perform previous accelerated ageing or degradation tests as in [65] which are time-consuming, expensive and require high amounts of energy, besides an accelerated aging test must be performed for each type of connector. The proposed method has the capability to constantly update the model from the recently acquired data. Finally, it is worth mentioning that a similar approach can be applied to many other power devices due to the simplicity of the proposed method.

## 3.3 Degradation model and RUL criterion

### 3.3.1 Degradation model for RUL estimation

This section defines the contact resistance degradation model used to predict the RUL of power connectors, which is a requirement in order to forecast the evolution of the resistance with time.

*3.3.1.1 Degradation model based on the evolution of the contact resistance vs time*

The resistance degradation model analyzed in this chapter is based on the increase of the contact resistance with time. According to [72], the contact lifetime is inversely dependent of the diffusion coefficient of the oxidizing agent at the contact interface. It is known that time increases the growth of oxide films at the contact interface under fretting conditions [72], thus increasing the electrical resistance.

According to [72], the two-parameter ($R_0$,$t_m$) resistance degradation models determining the evolution with time of the contact resistance of the connector, considering the oxidation process for multi-spot contacts can be written as,

$$\hat{R}(t,R_0,t_m)=\frac{R_0}{\left(1-\sqrt{t/t_m}\right)^3\cdot\left(1+2\sqrt{t/t_m}\right)\cdot\left(1+t/t_m\right)} \tag{3.1}$$

Where $R_0$ is the initial resistance of the connector, $t$ the time elapsed from the installation and $t_m$ is the maximal life time, which corresponds to a vertical asymptote of (3.1). Hence, (3.1) applies for multi-spot contacts presenting a beta distribution of the radius of the contact spots [72]. This model has been chosen as it fits well to the experimental data. Figure 3.2 shows the time evolution of the resistance according to (3.1).

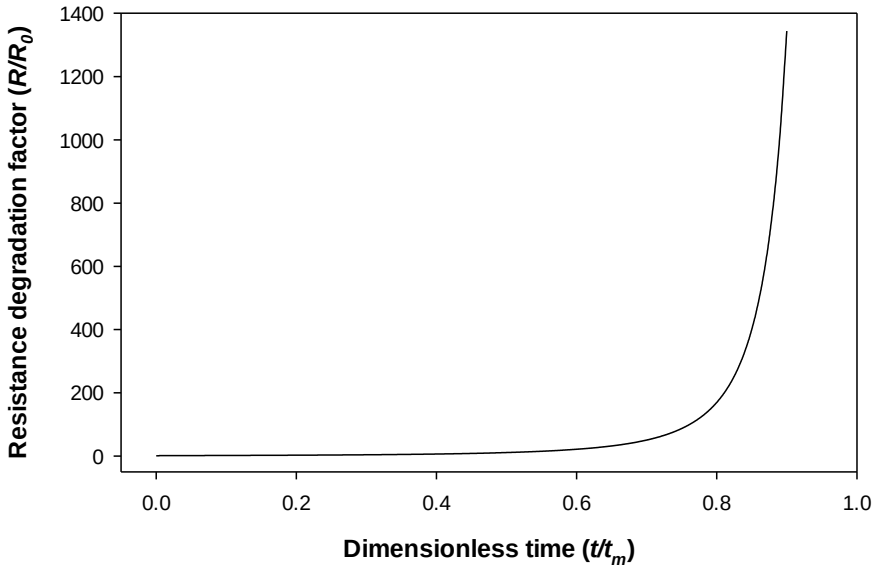


**Figure 3.2.** Plot of the oxidation multi spot contact resistance degradation model. As it can be observed at $t = t_m$, the model predicts a vertical asymptote [31].

*3.3.1.2 Parameter identification*

Once the model (3.1) is established, it is time to identify the parameters $R_0$ and $t_m$ with the Nelder-Mead simplex algorithm. This algorithm is a derivative-free algorithm which is widely used in the field of engineering for parameter estimation [73]–[76]. Moreover, this algorithm is easy to be used due to its simplicity. Therefore, the Nelder-Mead simplex algorithm is applied in this case from previous or past data (temperature, voltage drop and current) of the connectors by using the *Fminsearch* function from Matlab®. Thus, once parameters $R_0$ and $t_m$ are identified, by applying (3.1), which is a simple and fast expression to calculate, it is likely to forecast the future values of the connector resistance, which is the basis of the RUL predictive model proposed in this chapter.

## 3.3.2 RUL criterion

As previously explained, any increase of the resistance of the connector involves more power losses, heat generation and finally degradation of the contact interface. Therefore, it is proposed a RUL criterion based on monitoring the time evolution of the resistance. In order to generate a robust and simple RUL predictive model, a simple end-of-life criterion is required. To this end, it is proposed to determine the inflection point of the resistance degradation curve expressed by using (3.1), being the point at which the resistance transits from convex to concave, i.e., the point wherein the increase of the

electrical resistance accelerates. After equaling the second derivative of (3.1) to zero, the inflection point of (3.1) occurs at $t = 0.0482t_m$, corresponding to $R = 1.395R_0$, i.e., when the connector resistance has increased by at least 39.5% with respect its initial value $R_0$, as shown in Figure 3.3.

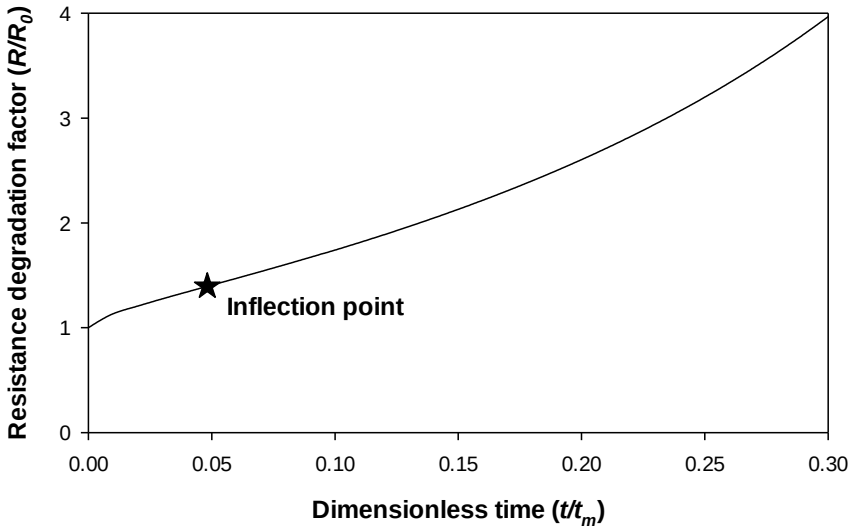


**Figure 3.3.** Detail of Fig. 3.2 up to $t/t_m = 0.3$, together with the proposed RUL criterion, corresponding to the inflection point of (3.1) [31].

The proposed RUL criterion based on the time instant of the inflection point found in model (3.1) makes sense, since it is the point where the derivative of the contact resistance starts to increase. Consequently, above this point, the resistance increases with a higher probability of being degraded quickly.

## 3.4 The proposed RUL approach

This section develops the methodology applied to develop the proposed on-line connector RUL estimation approach from experimental data. Figure 3.4 summarizes the steps required to determine the RUL of the connectors with the proposed approach.

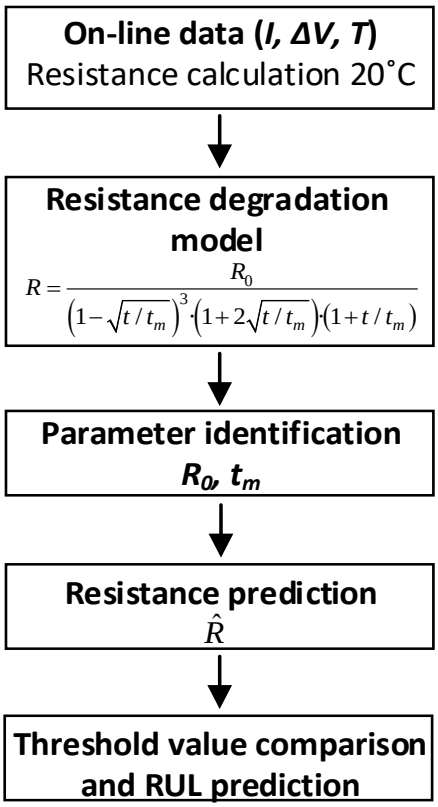


**Figure 3.4.** Steps required to determine the RUL of the connectors [31].

The first step is the acquisition of experimental data when the connector is operating under the conditions which will be further specified. The acquired data includes the current that flows through the connector, the voltage drop across the terminals of the connector, the phase difference between the voltage drop and the current, and finally, the operating temperature of the connector. As previously mentioned, resistance data is fitted to the model (3.1) by using the generalized least squares and Nelder-Mead minimization algorithm. This procedure allows to deduce the model parameters $R_0$ and $t_m$ and finally, predicting the future behavior of connector resistance. Afterward, from such prediction, the RUL criterion can be applied and compared against the threshold value to come up with the actual RUL estimation.

## 3.5 Experimental setup

This sections describes the experimental setup of this test.

### 3.5.1 The electrical connectors

This section describes the bimetallic friction-welded copper-aluminum ICAU120 Al-Cu compression connectors from the catalogue of SBI Connectors, for aluminum conductors size 120 $mm^2$. They are designed for low- and medium-voltage and they are shown in Figure 3.5. The aluminum material is EN AW-1050A aluminum according to the EN 573-3:2014 standard [77], whereas copper material is Cu-ETP according to the EN 13601:2014 standard [78]. In order to reduce the contact resistance between the barrel of the connector and the aluminum conductor, the barrel is compressed by means of a hexagonal crimping tool (69 MPa BURNDI EP-1HP) [79] and the inner surface of the aluminum barrel is covered with contact grease withstanding 140 ºC.

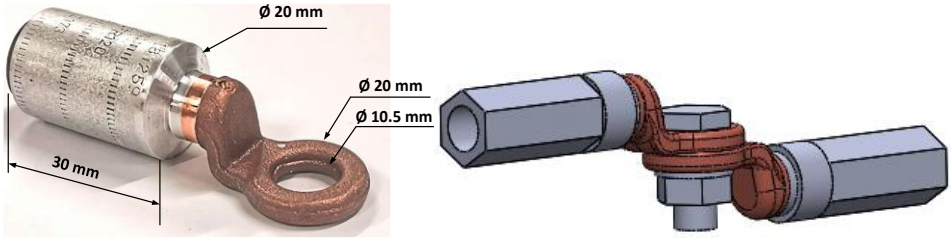


a) b)

**Figure 3.5.** ICAU120 Al-Cu connectors. a) Before compression. b) CAD drawing after compression including the bolting elements.

It is worth mentioning that the results presented in this work are planned to be applied in substation connectors through the *SmartConnector* project (see Section 1.1.1), whose details can be found in [3], [80]. Therefore, the connectors described in this section work are a previous stage to validate the feasibility of the proposed approach to estimate the RUL in a faster and economical way, since due to their geometrical dimensions the required current is lower compared to that required by the substation connectors, thus consuming much less power, whereas the duration of the heat cycle tests is much shorter.

### 3.5.2 The heating cycle test

In order to acquire on-line experimental data of the degradation of the connectors, they were aged by applying heat cycle tests according to the IEC 61238-1-3:2018 international standard [15]. Heat cycle tests are commonly used to characterize the thermal behavior of power connectors and to accelerate the thermal ageing process. These heat cycle tests generate thermal expansion and contraction cycles, because of the heating and cooling effect, thus affecting the contact spots at the interface and tending to increase the contact resistance.

In order to emulate real service life data, an electrical loop including seven ICAU120 Al-Cu connectors and 120 $mm^2$ aluminum alloy conductor was built to apply the heating-cooling cycle test. The heating-cooling experimental test was performed according to the requirements of the IEC-61238-1-3:2018 standard [15] and carried out at the AMBER-UPC laboratory. During the test, a total of about 140 heat cycles were completed, such tests lasting about 92.5 h, while the temperature, electric current and voltage drop in the seven connectors where acquired once each 6 seconds. In order to accelerate the degradation process and to reduce the time required to perform the heat cycle tests, an electrical current between 350 $A_{RMS}$ and 380 $A_{RMS}$ was forced to flow through the loop. Under this current, the conductor reaches the thermal equilibrium at 120 °C and then, the current is disconnected, although the recommended working temperature is below 90 ºC.

It is worth noting that the heat cycles are applied to acquire experimental data for testing the suitability of the RUL approach proposed in this chapter. **In the real field, the *SmartConnector*, which will be installed in a real substation, will provide on-line data, thus the heat cycle test data will not be longer necessary. The data obtained through the heat cycle tests are only used to emulate real service life data.**

### 3.5.3 Equipment and instrumentation

During the heat cycle tests, the electrical loop was supplied by means of a high-current variable transformer (400 $V_{RMS}$/6 $V_{RMS}$ with a rated output current of 2500 $A_{RMS}$), as shown in **Figure 3.6**. Before running the experiment, the initial DC contact resistance (reference value) of all connectors was measured by means of the four wire method, using

a calibrated Micro Centurion II digital micro-ohmmeter from RayTech [81]. This is the reference measurement of the contact resistance, which is used to check that the connector is properly installed before running the degradation heat cycle tests. Next, the heat cycle tests were started. The AC voltage drop waveforms across the terminals of all connectors were acquired by using a NI USB-6210 DAQ instrument, with absolute accuracy 88 μV, [82] (National Instruments, Austin, Texas, USA), which includes 8 differential inputs. The 50 Hz electric current flowing through the loop was measured with a calibrated Rogowski coil (CWT500LFxB from CWT with sensitivity of 0.06 mV/A) connected to the DAQ. The 50 Hz voltage drop and current waveforms were acquired at a rate of 5 kS/s. This setup guarantees a measuring accuracy of the initial electrical resistance better than 1 μΩ. The first differential inputs of the DAQ were used to measure the current, whereas the remaining 7 inputs were used for measuring the voltage drop across the connectors. The sample acquisition frequency used to take the measurements of the voltage drop and the electrical current was one sample every six seconds, thus allowing to calculate the resistance of every connector once each 6 seconds. The temperature of the connectors and reference conductor was also measured by using T-type thermocouples and an USB TC-08 thermocouple data acquisition module from Omega (Omega, Bienne, Switzerland) [83], with an accuracy better than 1 ºC.

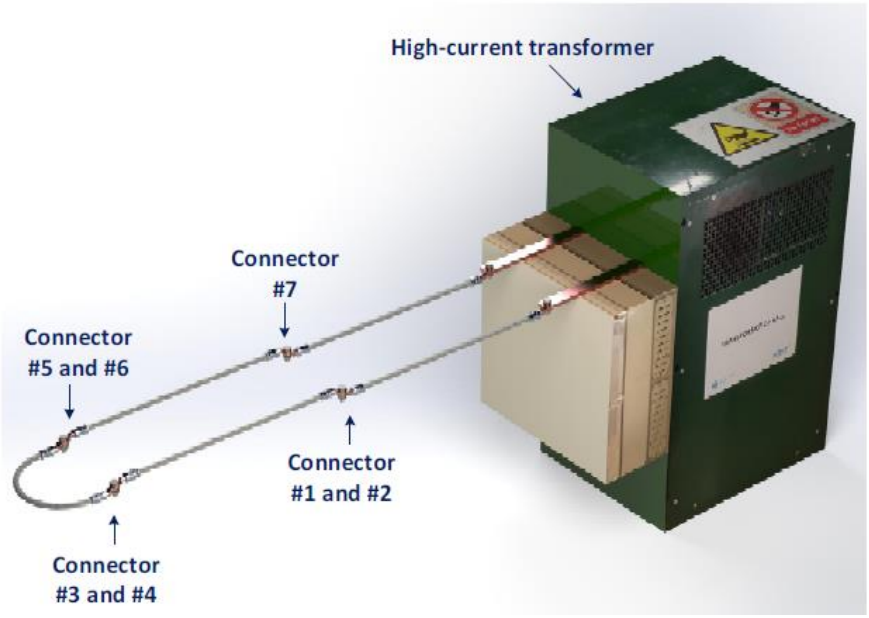


**Figure 3.6.** The electrical loop used in the heat cycle test.

### 3.5.4 Electrical resistance measurement

As explained in section 1.1.4, the electrical resistance is a good indicator of the connector health status, even though its value depends on its instantaneous temperature value. Therefore, measurements of resistances are required to assess the proposed approach. To this end, the measurement of the electrical resistance of the connectors was carried out by acquiring the waveforms of the voltage drop between point A and B, the electrical current that flows through the connector, the phase shift between these waveforms and the temperature of the connector. Afterward, the resistance is calculated by using (2.9) and then referred to 20 ºC with (2.10) as explained in Section 2.4.3. However, the experimental arrangement is not the same. Figure 3.7 shows the arrangement carried out in this test.

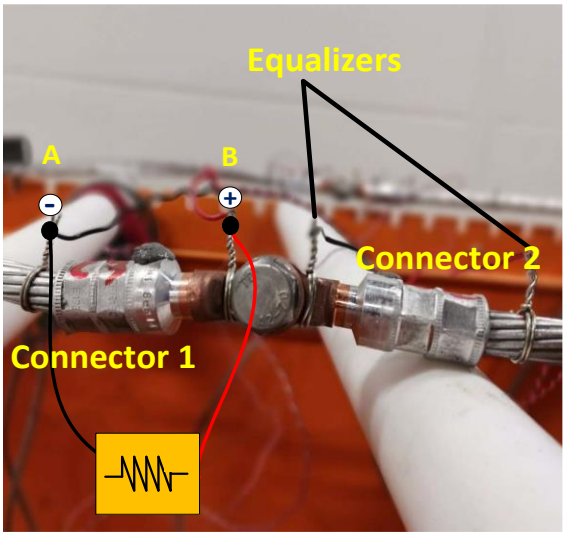


**Figure 3.7.** Experimental arrangement in this experiment [31].

In this case, connector 1 and 2 are joined by means of a screw. In addition, the voltage drop measurement is made from an equalizer in point A to another equalizer set on the copper part of the connector, as shown in Figure 3.7.

## 3.6. Experimental results and evaluation of the RUL model

This section presents the results achieved in this work.

### 3.6.1 Experimental Analysis of the Electrical Resistance Degradation Model (ERDM)

This section analyzes the suitability of the multi-spot resistance degradation model described by (3.1). All experimental data acquired of the electrical resistance of the seven connectors used in this chapter and, obtained from the heat cycle test, are adjusted by means of (3.1). The experimental value of the electrical resistance of the connector is calculated from the instantaneous electric current, voltage drop, phase shift and temperature, as mentioned previously. For instance, **Figure 3.8** displays the experimental evolution of connector's #1 resistance and the fitting values from (3.1), as well as the proposed threshold value to calculate the RUL.

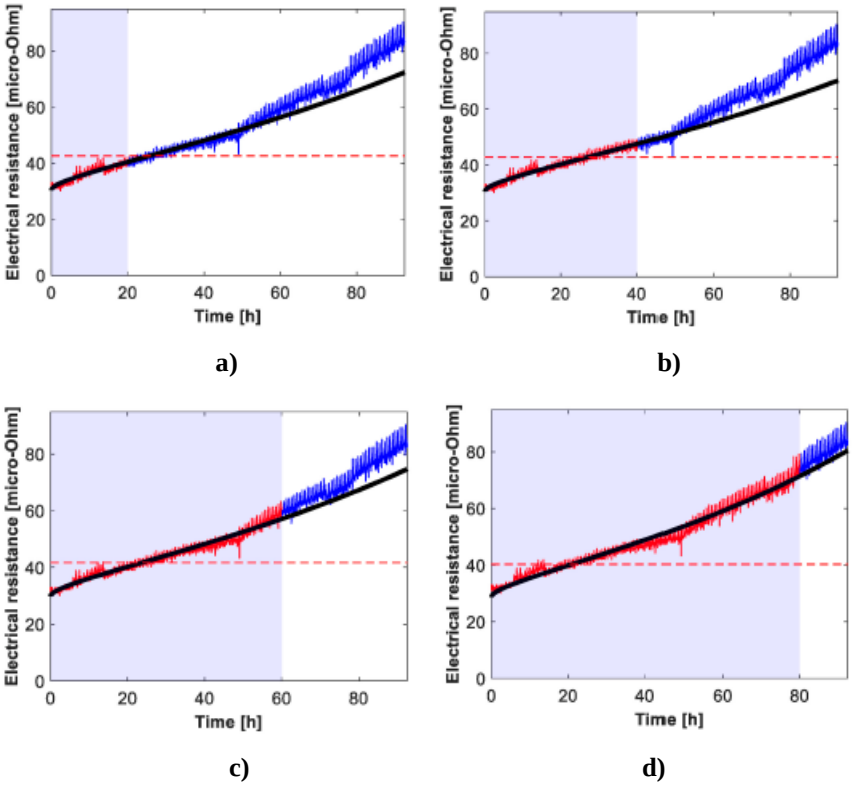


**Figure 3.8.** Detail of the fitting of the multi-spot electrical resistance model during the 92.5 h of the heat cycle test for connector #1. Experimental (red-blue) and fitted (black) values of the electrical resistance versus time and threshold value settled by the inflection point of (3.1). (a) 20–72 model, where 20 refers to the data collected during the first 20 h to fit the model, and 72 refers to the prediction done for the next 72 h ($R^2$ = 0.874). (b) 40–52 model ($R^2$ = 0.967). (c) 60–32 model ($R^2$ = 0.972). (d) 80–12 mode ($R^2$ = 0.981) [31].

Figure 3.8 shows that the heat cycles (heating and cooling cycles) are reproduced in the instantaneous values of the resistance as it contains peaks and valleys corresponding to the heating and cooling phases, thus resulting a non-smooth profile. Furthermore, results in Figure 3.8 shows that even though the profile of the resistance evolution with time is irregular, the degradation model defined by (3.1) is able to produce a good fitting of the experimental data. In addition, in order to determine the accuracy of the multi-spot model of the electrical resistance in predicting the degradation of the connectors, the coefficients of determination $R^2$ obtained by fitting (3.1) to the experimental data are summarized in Table 3.1. Results presented in both Figure 3. 8 and Table 3.1 demonstrate the suitability and accuracy of the multi-spot resistance degradation model.

**Table 3.1.** Fitting results of the experimental evolution of the connector resistance according to (3.1).

| **Connector** | **#1** | **#2** | **#3** | **#4** | **#5** | **#6** | **#7** |
|---|---|---|---|---|---|---|---|
| $R_0$ **(μΩ)** | 28.0 | 25.3 | 32.0 | 34.2 | 24.4 | 24.9 | 43.3 |
| $t_m$ **(h)** | 398.2 | 1281.8 | 1936.3 | 2645.7 | 5582.7 | 471.7 | 1754.4 |
| $R^2$ | 0.988 | 0.895 | 0.882 | 0.918 | 0.893 | 0.967 | 0.913 |

### 3.6.2 On-line RUL prediction based on different prediction horizons

This section describes the experimental results achieved through the heat cycle test and the RUL estimation obtained by applying the methodology summarized in **Figure 3.4.** The experimental data was divided into two groups, i.e., past and future data, aiming to simulate a real situation where the current and past values of the connector variables (temperature, voltage drop and current) are available, from which the RUL must be determined. Therefore, the data acquired during the heat cycle test, and labeled as future data, were used to evaluate the performance and accuracy of the RUL model. Hence, the data acquired during the first 20 test hours were used to predict the evolution of the connectors' resistance during the remaining 70 h (20-72). Next, the first 40 hours were used to predict the remaining 52 h (40-52), the first 60 hours to predict the remaining 32 h (60-32) and finally the first 80 hours to predict the remaining 12. It is important to mention that, in a real case, this estimation could be done in an hourly basis or any appropriate interval. Thus, Figure 3.9 shows the RUL estimation for the 20-72, 40-52, 60-32 and 80-12 prediction horizons for all connectors #1 to #7. As the data is acquired on-line, the RUL estimation evolves with time depending on the resistance profile.

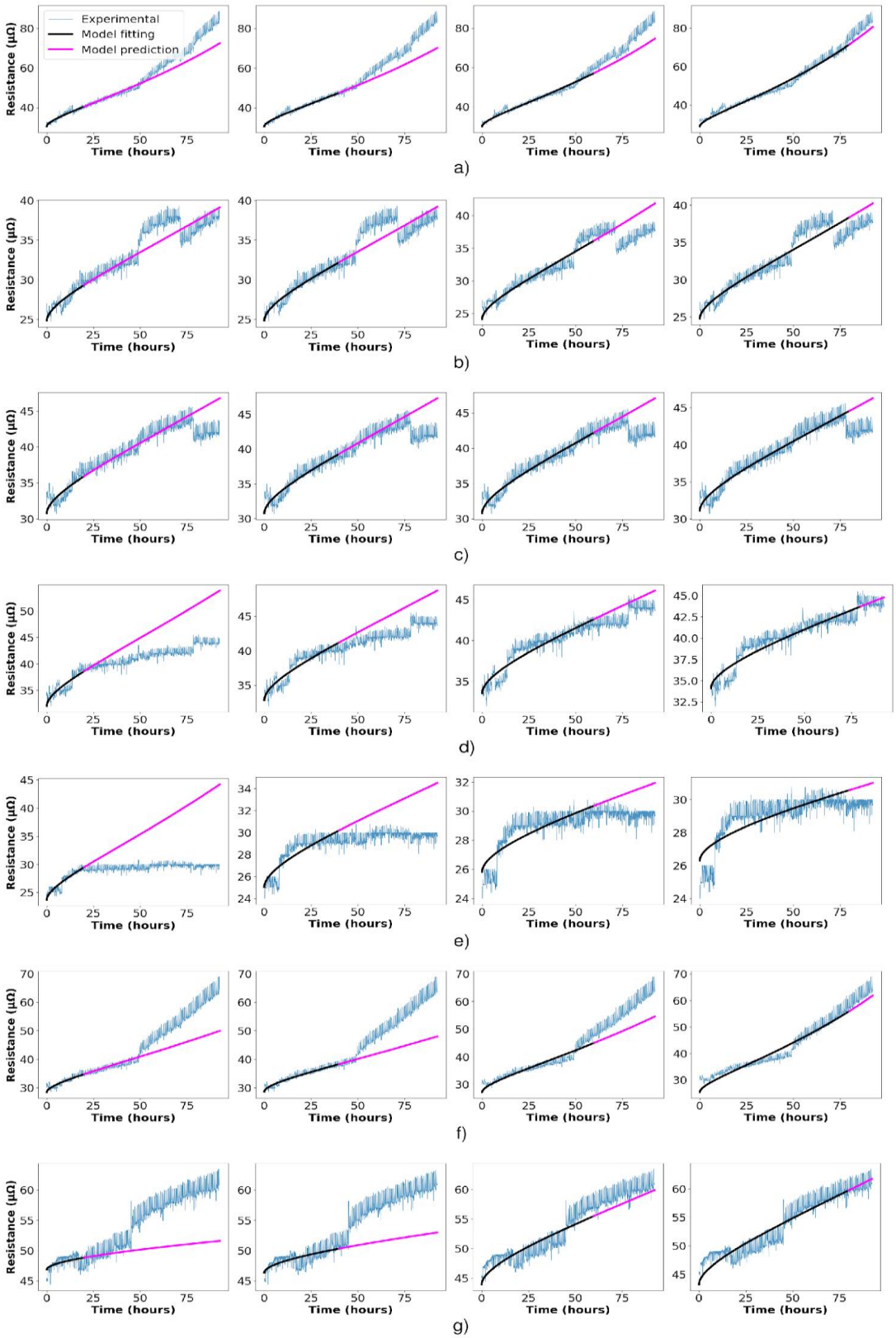


**Figure 3.9.** Fitting of the multi-spot electrical resistance models during the 92.5 h of the heat cycle tests until the conductors reach thermal equilibrium at 120 ºC for the seven connectors (#1 to #7), considering four models (20-72, 40-52, 60-32 and 80-12 models). (**a**) #1. (**b**) #2. (**c**) #3. (**d**) #4. (**e**) #5. (**f**) #6. (**g**) #7 [31].

Results presented in Figure 3.9 prove that in some cases, the contact resistance requires some time before stabilizing. Therefore, it is better to gather a minimum amount of experimental data before predicting the RUL, about 20 h in this case. It is important to mention that the RUL is calculated as the difference between the end-of-life (EOL) and the current time. For instance, the current time for the 20-72 models is 20, for the 40-52 models the current time is 40 and finally, 60 and 80 for the other two models. Results in Figure 3.9 clearly indicate that the predictive capability of the proposed model evolves with time, and therefore, the model provides a different value of the RUL at each time instant. This fact is validated with the results presented in Table 3.2, which summarizes the main parameters of the RUL estimation using the prediction horizons mentioned above, i.e., 20-72, 40-52, 60-32 and 80-12.

**Table 3.2.** Fitting parameters and RUL estimation for different connectors.

| Model | Connector | #1 | #2 | #3 | #4 | #5 | #6 | #7 |
|---|---|---|---|---|---|---|---|---|
| 20-72 | $R_0$ ($\mu\Omega$) | 30.4 | 24.8 | 30.8 | 32.0 | 24.9 | 28.4 | 46.90 |
| | $t_m$ (h) | 519.3 | 1219.8 | 1369.0 | 1010.1 | 11549.6 | 905.7 | 14306.3 |
| | EOL (h) | 25.0 | 58.8 | 66.0 | 48.7 | 557.1 | 43.7 | 690.1 |
| | *RUL (h) | 5.0 | 38.8 | 46.0 | 28.7 | 537.1 | 23.7 | 670.1 |
| 40-52 | $R_0$ ($\mu\Omega$) | **30.6** | 24.9 | 30.8 | 32.9 | 24.8 | 28.6 | 46.4 |
| | $t_m$ (h) | **548.3** | 1218.3 | 1321.1 | 1502.4 | 8933.4 | 1023.7 | 8144.4 |
| | EOL (h) | **26.4** | 58.8 | 63.7 | 72.5 | 430.9 | 49.4 | 392.8 |
| | *RUL (h) | - | 18.8 | 23.7 | 32.5 | 390.9 | 9.4 | 352.8 |
| 60-32 | $R_0$ ($\mu\Omega$) | **29.8** | **24.2** | 30.8 | 33.5 | 24.8 | **27.2** | 43.9 |
| | $t_m$ (h) | **486.0** | **938.9** | 1339.9 | 2056.2 | 9408.6 | **683.9** | 2129.4 |
| | EOL (h) | **23.4** | **45.3** | 64.6 | 99.2 | 453.8 | **33.0** | 102.7 |
| | *RUL (h) | - | - | 4.6 | 39.2 | 393.8 | - | 42.7 |
| 80-12 | $R_0$ ($\mu\Omega$) | **28.7** | **24.8** | **31.1** | 34.1 | 24.5 | **25.4** | 43.2 |
| | $t_m$ (h) | **424.6** | **1117.1** | **1481.1** | 2595.7 | 6451.3 | **505.5** | 1725.6 |
| | EOL (h) | **20.5** | **53.9** | **71.4** | 125.2 | 311.2 | **24.4** | 83.2 |
| | *RUL (h) | - | - | - | 45.2 | 231.2 | - | 3.2 |

**Bold numbers indicate that the connector has reached its EOL**

*RUL= EOL - Current time (20, 40, 60 or 80h)

Results in **Table 3.2** show the time evolution of the RUL for each connector. The results also show that each connector has its own RUL evolution profile as a result of its particular change of the electrical resistance with time. It is important to note that some of the results presented in **Table 3.2 (**marked in bold) would not be calculated in a real life situation since the connector has already reached the end-of-life (EOL), and therefore, the connector would be replaced before. For example, in connector #1, the fitting and RUL estimation, carried out at 20 h, predicts that it will last only up to hour 25, so it should be replaced.

### 3.6.3 Comparison of ERDM vs ARIMA

This section presents the comparison between the RUL results attained with the electrical resistance degradation model (ERDM) proposed in this chapter and the widely used autoregressive integrated moving average model, ARIMA (p,d,q), where p is the AR order, d is the differencing order, and q is the MA order [64], [84].

Table 3.3 only analyzes connectors #1-3 and #6 because they reached end of life (EOL) during the experiments. In addition, the ARIMA (2,1,2) model shows better accuracy than other combinations of the (p,d,q) orders.

**Table 3.3** RUL estimation for different connectors using ARIMA (2,1,2) and ERDM.

| Connector | | #1 | #2 | #3 | #6 | Error [h] |
|---|---|---|---|---|---|---|
| **20-72** | Measured | 32.7 | 53.1 | 72.2 | 50.8 | - |
| | ERDM | 25.0 | 58.8 | 66.0 | 43.7 | 26.7 |
| | ARIMA | 30.8 | 54.6 | 55.6 | 56.8 | 26.0 |
| **40-52** | Measured | 32.7 | 53.1 | 72.2 | 50.8 | - |
| | ERDM | - | 58.8 | 63.7 | 49.4 | 15.6 |
| | ARIMA | - | 82.4 | >92 | 73.1 | >51.6 |
| **60-32** | Measured | - | - | 72.2 | 50.8 | - |
| | ERDM | - | - | 64.6 | - | 7.6 |
| | ARIMA | - | - | 83.6 | - | 11.4 |
| **Total error** | | | | | **ERDM** | 49.9 |
| | | | | | **ARIMA** | >89.0 |

Results presented in **Table 3.3** shows the better accuracy of the RUL predictions made by the ERDM proposed in this chapter, compared with the ARIMA model. It is worth noting that ERDM is appealing because it combines physical knowledge and a data driven approach, whereas ARIMA only relies on a data driven approach. It is noted that data driven approaches usually include three stages, i.e., data acquisition, health index calculation and RUL prediction [85]. In addition, predictions made by ARIMA highly rely on the difficulty in setting a priori the optimal values of the (p,d,q) orders.

## 3.7 Conclusions

Power substations are commonly examined through visual inspections, using thermal infrared cameras, ultraviolet solar blind cameras or drones equipped with different types of camera. However, these inspection methods cannot be applied very often due to the cost and also the difficulty to be carried out under adverse weather conditions [86]. In addition, they do not provide a sufficient amount of numerical data to develop mathematical RUL models, thus this work contributes in this area.

In this chapter a simple approach was developed with a very low computational burden to determine the remaining useful life (RUL) of power connectors. An attractive feature of this approach is that previous degradation tests of the connectors are not required, which are costly, time-consuming and waste high amounts of electrical energy. Its main application is found in predictive maintenance plans, as the proposed on-line strategy allows anticipating and planning when the connector must be replaced, based on determining the evolution of its RUL via the available data. To this end, the voltage drop between the terminal points of the connector, the current flowing across the connector, and the connector temperature, must be acquired on-line and processed to determine the instantaneous value of its electrical resistance. Next, by using a simple but accurate analytical model of the time evolution of the resistance, i.e., the degradation model, the RUL can be easily predicted. This model depends on two parameters, which are identified by fitting the equation describing such a degradation model to the experimental data, by means of a generalized least squares algorithm. The proposed criterion for determining the RUL is based on the inflection point of the equation describing the degradation of the electrical resistance. Finally, in order to validate the proposed approach to estimate the RUL, an experimental test was performed using a loop with seven connectors, thus proving the potential and viability of this method in determining and anticipating when the connector must be replaced before presenting a major failure. It is worth mentioning that a similar approach can be applied to many other power devices.

# FAULT DETECTION

# 4. FAULT DETECTION

## 4.1 Introduction

It is known that the natural ageing process of the connector increases the electrical resistance along its lifetime , thus increasing the operating temperature and tending to overheat the connector [12]. This temperature increment in turn rises the electrical resistance, thus affecting the electrical and thermal behaviors of the connector [16]. Therefore, the increase of the electrical resistance of the connector is a sign of its degradation level, and thus, this parameter can be used as a signature or indicator of its health condition, besides it has been effectively used as an indicator of the SoH of electrical connectors [33], [80]. However, the evolution of the contact resistance in electrical connectors and therefore, the total electrical resistance is a fluctuating nonlinear non-monotonic process. Due to all this complexity, an exhaustive analysis of the time evolution of the contact resistance is difficult to analyze [87].

During the ageing process, the electrical contacts experiment different stages [15], such stages are formation, relative stability and accelerated ageing, which are a consequence of physical changes and chemical reactions occurring at the constriction areas. The formation stage is characterized by the formation of a quite stable constriction area, whereas during the relative stability stage the resistance of the connector experiments a very small increase. Finally, the accelerated ageing stage is characterized by a fast increase of the resistance due to the combined effect of faster chemical processes and higher temperatures.

On the other hand, diagnosis of electrical and electronic systems has received much attention over the last few decades [88]. Power lines and electrical substations are inspected periodically to determine their condition. However, due to the lack of on-line data, at present the most applied inspection systems are based on manual, robot and unmanned aerial vehicle inspection [89]. Condition monitoring is directly related to different methods for identifying changes occurring in a system due to the development of faults or a degradation of its SoH, thus generating an alarm to indicate a possible failure or degradation of the SoH [90]. On-line condition monitoring is an active field of research in power systems [91]–[94]. To apply effective predictive maintenance strategies, to reduce maintenance and unexpected outages and shutdown costs, there is a need to detect

typical or degraded behavior modes in the early stage, when the degraded behavior is still developing. However, detecting abnormal behaviors at the early stage is no easy, as minor changes are often difficult to diagnose, so great care has to be taken to reduce false alarm events [95].

Real-time data acquisition and the associated deployment of distributed sensors is a key point for the expansion of intelligent power systems. Such systems allow a more stable and controllable power delivery since real-time data allow applying different condition monitoring strategies [96]. Therefore, the on-line measurement of the electrical resistance using electronic devices is a key point for a continuous monitoring of the electrical resistance of the connectors in order to develop effective *SoH* prediction tools. Different sensors, including voltage, current and temperature sensors can be used for a nondestructive detection, location and diagnosis of faults in power systems. Traditionally, these sensors have been applied to diagnose the faults after their occurrence. Despite improvements in system robustness, failures cannot be completely eliminated and also they are slightly unpredictable, so maintenance operations are required before operational faults [97].

This chapter presents two innovative fault detection techniques for substations connectors. First, in section 4.1, a simple approach for an on-line diagnosis of the health status of power connectors, based on a continuously monitoring of the electrical resistance by measuring the temperature, voltage drop and the current flowing across the connectors, is presented. Therefore, the current and past values of the electrical resistance are taken as signatures or as an indicator of the health status of the connector. To this end, a parametric degradation model of the connector resistance is combined with the application of the Markov chain Monte Carlo (MCMC) method. MCMC is applied for identifying the most suitable values of the parameters of the resistance degradation model, according to the available experimental data, while providing the confidence intervals of the electrical resistance, thus being possible to confine the expected future values of the resistance within the space defined by the confidence intervals. In the case that the measured value of the resistance falls between these intervals, it can be concluded that the connector operates under healthy conditions. Otherwise, a warning signal should be activated. This strategy allows anticipating severe faults, thus limiting the consequences

of the degradation of the connectors with time, and facilitating the application of predictive maintenance plans.

Section 4.2 proposes a novel method to forecast the State of Health (*SoH*) of power connectors by analyzing the degradation trajectory of the electrical resistance. This section presents and evaluates different simple alternatives that present a reduced computational load. The first method determines the near future values of the contact resistance and thus, the SoH, by projecting the past acquired values of the connector resistance according to a least squares linear regression. The remaining two methods evaluated in this work are based on analyzing the degradation trajectory of the connector resistance and performing a non-linear fitting of the acquired data based on the Braunovic degradation model of the electrical resistance [72]. Whereas the first method directly determines the SoH by projecting the future values of the connector resistance according to a least squares fitting of the Braunovic model, the second one applies the Markov chain Monte Carlo (MCMC) method [29] for this purpose. It is worth mentioning that the three methods compared in this section focus on each specific connector, being adapted to the particular characteristics of each power device, only requiring the past and current values of the electrical resistance to determine its SoH.

It is worth mentioning that the behavior of the analyzed methods is assessed by means of experimental data obtained from an accelerated degradation test (ADTs) (by measuring the voltage drop between the connectors' terminals, the electric current and the operating temperature, as done in Chapter 3) since they are designed to analyze the long-term performance of power connectors by minimizing the testing time [64].

## 4.2 On-line health condition monitoring

### 4.2.1 Background

Condition monitoring involves a set of techniques focused to identify noticeable changes in a system, which indicate that a fault is being developed, so that, a warning of imminent failure must be generated, being the basis for applying fault detection approaches. To this end, reliable measured data is required, from which health indicators can be obtained to assess the condition of the analyzed system [98]. However, the development of reliable condition monitoring approaches for power connectors requires a deep knowledge of the failure mechanisms for an on-line diagnosis of the condition of such devices, so that when the behavior of the connectors drifts from the expected one, an appropriate action can be taken well before breakdown or severe deterioration occurs [99].

It is of vital importance detecting the faults in their early stage, when they are still developing. Incipient fault detection is of paramount importance in power systems, since such faults can lead to catastrophic consequences with huge economic losses. The detection and diagnosis of incipient faults enables to apply predictive maintenance plans in power systems, thus minimizing associate failure risks and ensuring stable and reliable operation with minimum interruptions and outages, so that replacement of the failed component can be scheduled well before fault occurrence. However, incipient fault detection is still a challenging problem, since the subtle changes are difficult to detect and false alarm occurrence must be minimized [95]. Different methods can be applied for this purpose, including model-based approaches constructed from the physical laws governing the behavior of the analyzed systems, or based on probabilistic theories. Another possibility is by means of data-driven approaches, which require large amounts of system data, which are analyzed by means of suitable signal processing methods combined with machine learning algorithms [95].

Accelerated degradation tests (ADTs) have been typically applied for evaluating the reliability and long-term performance of high-reliability and long-life products [64]. Due to their characteristics, it is difficult to have sufficient degradation and failure data in a reasonable time. ADTs are often accompanied of a statistical analysis of the data collected to analyze the degradation process [87]. Many works analyzing the long-term behavior

of different products are based on ADTs. However, this approach often requires testing several products simultaneously, so it can be expensive because of the required time, the associated human labor, the consumed energy, and the required materials. In addition, obtained results are usually specific for the tested products, thus lacking of generalization capability.

As a consequence of the above-mentioned issues, this section presents another fast alternative, being possible to be applied almost in real-time, which can be adapted to many other power devices. In addition, the proposed method does not need performing accelerated ageing/degradation tests, which present many downsides, since they require long testing periods and intensive human labor, require large amounts of energy and thus, they result expensive. Even though the key role of power connectors in power systems, there are few studies focusing on an on-line monitoring of the health status of such components, so this work contributes to this area.

### 4.2.2 The degradation model for the fault detection

In order to predict the future value and the evolution with time of the connector resistance, a suitable model is required. The multi spot resistance degradation parametric model presented in [72] is selected in this chapter due to its simplicity, small number of parameters to identify and satisfactory results. It assumes an increase with time of the contact resistance because of the development under fretting conditions of non-conductive oxide films at the contact interface and a uniform distribution of the contact spots. According to [72], the two-parameter time-dependent resistance degradation model that takes into account the oxidation process for uniformly distributed multi-spot contacts can be written as,

$$\hat{R}(t, R_0, \tau) = \frac{R_0}{\left(1-\sqrt{t/\tau}\right)^2 \cdot (1+t/\tau)} \tag{4.1}$$

where $\hat{R}$ is the electrical resistance estimated by the model, $t$ is the time measured from the installation of the connector, $R_0$ is its initial resistance corrected to 20 ºC, and $\tau$ is the maximum life time, i.e., the time at which the resistance increases abruptly, since it produces a zero-value in the denominator of (4.1). Figure 4.1 displays the evolution with time of the resistance according to (4.1).

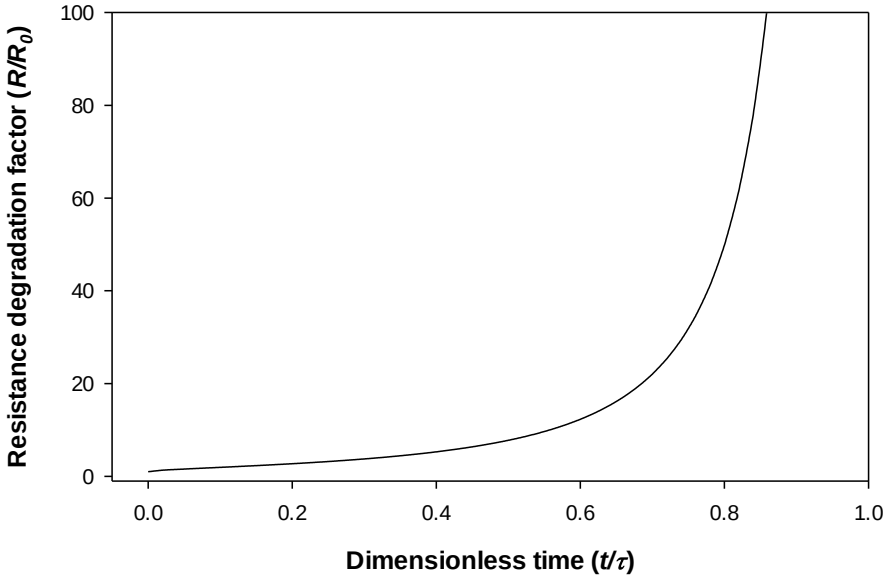


**Figure 4.1.** Oxidation multi spot resistance degradation model [29].

### 4.2.3 Markov Chain Monte Carlo simulations (MCMC)

Markov chain Monte Carlo (MCMC) methods are stochastic parameter estimation methods for complex models, for which standard estimation methods are extremely difficult to apply. In this research, the role of MCMC is to identify the parameters $\theta = (R_0,\tau)$ of the multi-dimensional distribution function corresponding to the contact resistance $\hat{R}(t,R_0,\tau)$ described by (4.1).

The MCMC method iteratively generates random samples to characterize the parameters of the distribution of interest [100]. MCMC methods include different sampling algorithms from a given complex multi-dimensional probability distribution [101]. They build a Markov chain having the chosen multi-dimensional distribution as its equilibrium distribution. Markov chains are stochastic models which define a sequence or collection of random variables moving from one state to another one. The probability to move from one state to the subsequent one only depends on the current state and elapsed time, but it is independent of the sequence of preceding states. By recording states from the chain it is possible to generate a sample of such distribution. When including more steps in the Markov chain, the distribution of the sample tends to match more accurately the actual desired distribution. Markov chains are guided random walks through the space of parameters describing all feasible values of such parameters, although some values have more probability to be generated than others (it depends on the prior information of the experimental data provided by the user). Therefore, Markov chains tend to sample from the more likely sample space regions. Although different algorithms are available to implement the MCMC method, the Metropolis–Hastings (MH) algorithm (see Figure 4.2) is among the most popular [102][103]. MH is a statistical sampling method that generates a Markov chain, thus allowing to generate as many samples as required in the random sequence. The Markov chain is often initialized by sampling from a two-dimensional uniform prior distribution $P(\theta)$ with upper and lower bounds $u_b$ and $l_b$, respectively [104]. It is assumed that when increasing the sample size, the probability density functions built by the Markov chain tend to converge to the actual distribution [103]. Moreover, MCMC is focused to approximate from a sampling of prior distribution $P(\theta)$, the posterior probability density function (PDF) of the model parameters $\theta = (R_0,\tau)$, which is a conditional probability function depending on the measured resistance data $R$, i.e., $P(\theta|R)$. Finally, via Monte Carlo integration, summary statistics are generated from the randomly

generated samples to describe the distribution of the parameters [105].

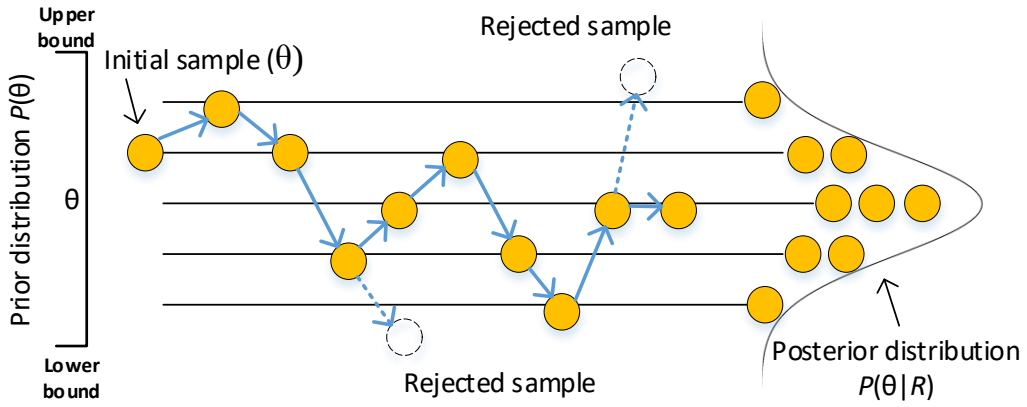


**Figure 4.2.** Construction of the Markov chain by the Metropolis-Hastings algorithm [29], [103].

### 4.2.4 Initial parameter estimation

Parameters $R_0$ and $\tau$ are estimated from measurements of the contact resistance by applying the Markov Chain Monte Carlo (MCMC) method in combination with the *fminsearch* function from Matlab®, which finds the minimum of an unconstrained multivariable function using a derivative-free method [105]. The *fminsearch* function returns the initial estimates or seed values of the parameter estimates $\hat{\theta}_{ini} = (R_0, \tau)_{ini}$ and the sum of squares (*sos*) of the error function, which are required by the MCMC algorithm. The definitive values of the parameters $\hat{\theta}_{def} = (R_0, \tau)_{def}$ are provided by the MCMC algorithm.

MCMC provides many estimated pairs ($R_0$,$\tau$), thus enabling generating confidence intervals for the parameters being estimated. The *fminsearch* function from Matlab® outputs the sum of the squares of the error function as in (4.2), calculated as the squared difference between the measured contact resistance $R$ and the one provided by the model, i.e., $\hat{R}$ as in (4.1). The sum of squares function, *sos*, is expressed as,

$$sos = \sum_{i=1}^{n} [R(t_i) - \hat{R}(t_i)]^2 \tag{4.2}$$

$R(t_i)$ and $\hat{R}(t_i)$ being, respectively, the contact resistance measured at time $t = t_i$, and the contact resistance calculated by means of (4.1), whereas $n$ is the number of acquired data points. MCMC simulations require, as inputs, the initial estimates of the parameters $\hat{\theta}_{ini} = (R_0, \tau)_{ini}$, and the covariance matrix of the parameter estimates $\hat{\theta}$, which is calculated from the initial estimate of the error variance $\hat{\sigma}_\varepsilon^2$, since MCMC requires to know the variance of each parameter. According to [106], $\hat{\sigma}_\varepsilon^2$ can be calculated as,

$$\hat{\sigma}_\varepsilon^2 = sos/(n-p) = \frac{1}{n-p}\sum_{i=1}^{n}[R(t_i) - \hat{R}(t_i)]^2 \tag{4.3}$$

*sos* being the residual sum of squares of the error function and $p$ the number of parameters in the regression model, two in the analyzed case. The covariance matrix of the parameter estimates can be calculated as,

$$\mathrm{cov}(\hat{\theta}) = \hat{\sigma}_\varepsilon^2 (X_i' \cdot X_i)^{-1} \tag{4.4}$$

where $X$ and $X'$ are, respectively, the Jacobian or first-order partial derivatives matrix and its transposed matrix, which from (4.1) results in,

$$X_i = \partial\hat{R}(t_i, \hat{\theta})/\partial\theta = \left[\partial\hat{R}(t_i, \hat{\theta})/\partial R_0 \quad \partial\hat{R}(t_i, \hat{\theta})/\partial\tau\right] \tag{4.5}$$

### 4.2.5 The proposed approach

Figure 4.3 summarizes the different steps of the approach proposed in this work. First, on-line data (temperature, voltage drop and current) are acquired, from which the resistance of the connector is obtained. The past data is fitted using the resistance degradation model given by (4.1), the parameters of the model and the confidence intervals being determined by means of MCMC simulations. Finally, the current measured value of the electrical resistance is compared against the prediction performed by the model, in order to diagnose the health condition of the connector.

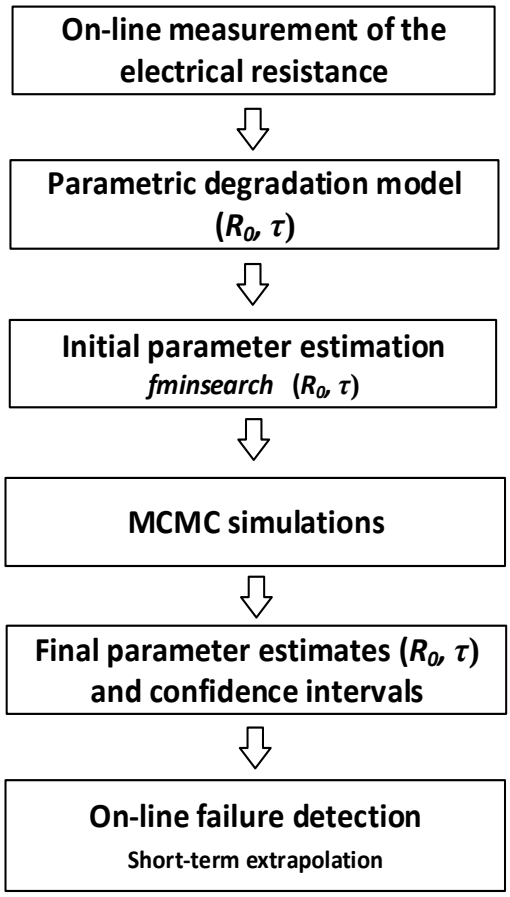


**Figure 4.3.** Proposed on-line health condition monitoring approach [29].

Figure 4.4 explains how the proposed approach works. It shows the evolution of the electrical resistance in one connector (connector #5) and the fitting of the model according to the parameters identified by the MCMC algorithm, along with the calculated confidence intervals. It allows diagnosing the health status of the connector, which is done by comparing the current value of the electrical resistance with the value estimated by the

model. The blue line and "x" symbols in Figure 4.4 are the past measured values of the electrical resistance, the black line represents the fitted model according to (4.1), and the pink line and "x" symbol represents the current measured value of the resistance. When the current measured value of the resistance falls between the confidence intervals, it is assumed that the connector behaves well. Otherwise, an alarm is triggered. In this latter case, if during the consecutive measurements corresponding to a pre-established time interval the resistance falls outside the confidence intervals, a warning, indicating that the connector must be replaced, must be generated.

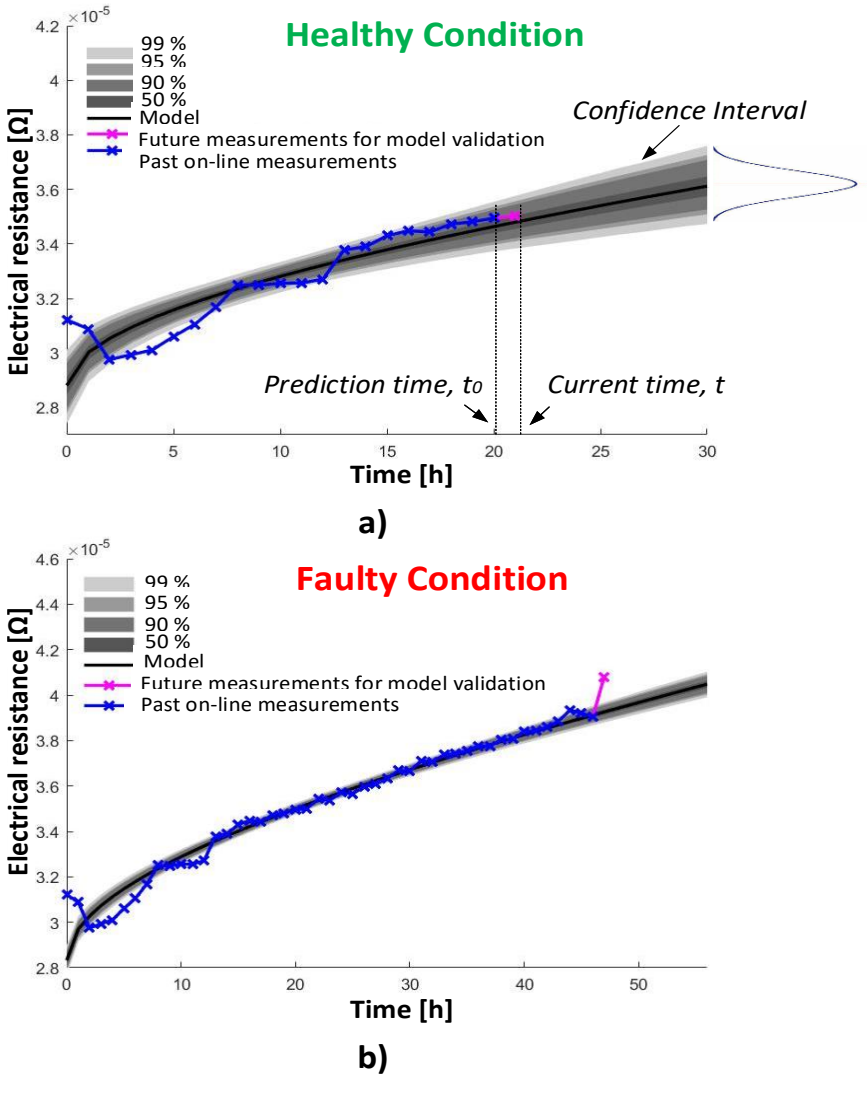


**Figure 4.4.** On-line condition monitoring approach, including the electrical resistance degradation model fitted according to (2), and the 50%, 90%, 95% and 99% confidence intervals plotted as area bands, representing the predictive probability limits due to the uncertainty in the parameters values. a) Healthy condition. b) Fault condition [29].

### 4.2.6 Experimental setup

This sections describes the experimental setup carried out in this test. It is worth to note that the experimental results and the setup used in this section were also used in section 4.3. Therefore, they will only be explained in this section.

#### *4.2.6.1 The analyzed connectors*

Medium voltage connectors are usually made of copper or aluminum. Medium voltage grids typically use compression connectors, because compression is a simple technique producing a relatively low contact resistance and reliable electrical connection.

This work analyzes the behavior of bimetallic copper-aluminum ICAU120 compression connectors from SBI Connectors, which are intended for 120 $mm^2$ aluminum conductors. In these connectors (see Figure 4.5c), aluminum and copper are joined by friction welding. The barrel of the connector is compressed by using a hexagonal crimping machine. To improve the contact between the aluminum conductor and the barrel of the connector, contact grease withstanding 140ºC was applied to the inner barrel surface.

The developments done in this chapter, as well as the presented experimental results, are a means to validate the feasibility to apply this approach in substation connectors by means of the *SmartConnector* project. It includes the substation connector itself, a set of miniature sensors (temperature, voltage drop and current), a thermal energy harvesting unit, and wireless communications.

As previously mentioned, medium voltage connectors instead of substation connectors have been used to experimentally validate the condition monitoring approach proposed in this work since the useful life of the formers is shorter, thus allowing a drastic reduction of testing time, technician hours, power requirements and overall cost.

#### *4.2.6.2 The applied heat cycle tests and equipment*

As explained , ADTs are commonly applied to obtain degradation data defining the behavior of the studied system in a fast manner. To this end, HCTs according to the requirements of the IEC 61238-1-3:2018 standard [15] were performed in the high-current laboratory of the Universitat Politècnica de Catalunya. It is noted that data

acquired from the HCTs are used to simulate the on-line acquired data from a real application. HCTs were performed using an electrical loop consisting of seven ICAU120 bimetallic connectors joined to a 120 $mm^2$ aluminum conductor.

Figure 4.5a shows the experimental loop and the used connectors. In order accelerate the natural ageing of the connectors, around 140 HCTs were run for about 92 h. Heat cycles consists of two phases, namely heating and cooling phases. The consecutive heating and cooling cycles induce thermal expansion and contraction cycles, which affect the contact interface and thus, the contact resistance of the connectors, which in turn alter their electrical and thermal performance. During the heating phase, an alternating electrical current is injected to the loop until the reference aluminum conductor reaches the thermal equilibrium at a temperature of 120 °C, condition attained when injecting an electrical current of about 370 $A_{RMS}$. This temperature is above 90 °C, the temperature recommended by the conductor manufacturer, thus accelerating the thermal degradation process. According to the IEC 61238-1-3:2018 [15], after attaining the thermal equilibrium, this electrical current must be maintained for 15 minutes. After this time the current is switched off, so that it cools down to ambient temperature with the help of forced ventilation using fans, and next a new heat cycle can start.

Heat cycle tests were performed using a high-current 400 V/10 V variable transformer which supplies the electrical loop.The rated output of this transformer is 10 $V_{RMS}$, 10 $kA_{RMS}$. A Rogowski coil with a sensitivity of 0.06 mV/A (500LFxB from PEM, Nottingham, UK) was used to measure the electrical current flowing in the loop. The voltage drops between the external terminals of the connectors were acquired using a USB-6210 DAQ instrument (National Instruments, Austin, Texas, USA), which includes 8 differential inputs. In order to correct the resistance of the connectors to 20 °C, T-type thermocouples were used jointly with a USB TC-08 thermocouple data acquisition module (Omega, Bienne, Switzerland).

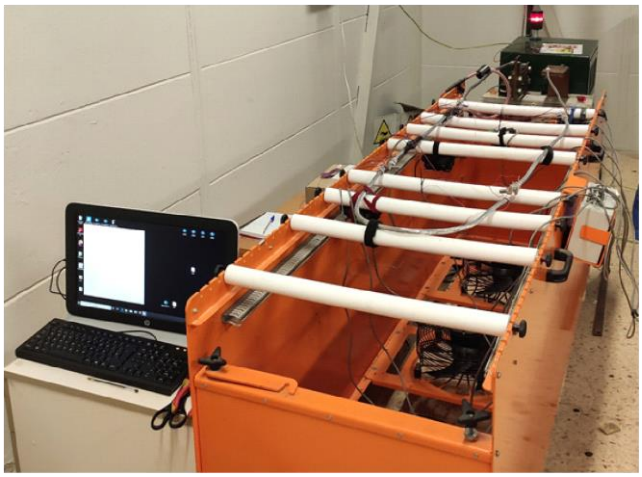

**a)**

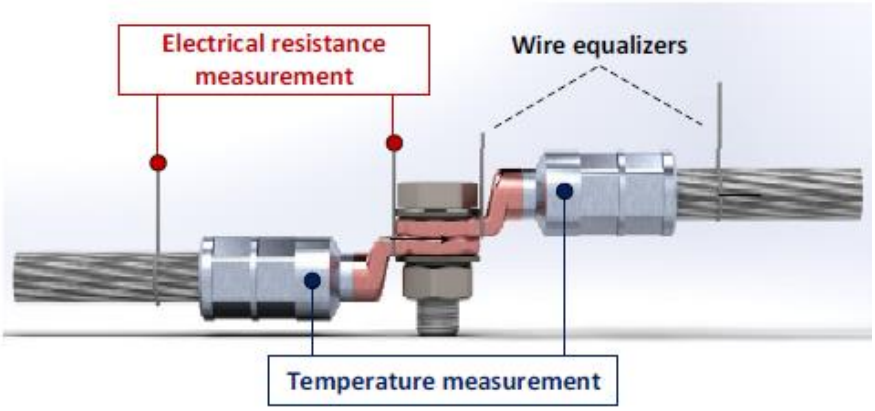


**b)**

**c)**

**Figure 4.5.** a) Electrical loop for the temperature cycle tests. b) Contact resistance measurement by using wire equalizers. c) ICAU120 Al-Cu medium voltage connectors [29],[30].

The measurement of the electrical resistance of the connectors was carried out by acquiring the waveforms of the voltage drop between the points indicated in Figure 4.5b, the electric current that flows through the connector, the phase shift between voltage drop and current waveforms and the temperature of the connector. Afterward, as in section 3.5.4. the resistance is calculated by using (2.9) and then corrected to 20 ºC by applying (2.10).

## 4.2.7 Results

This section presents the results attained in this chapter.

*4.2.8.1 Experimental evaluation of the MCMC-based on-line condition monitoring approach.*

This section evaluates the performance of the proposed condition monitoring approach. To this end, the experimental results of the seven analyzed connectors collected during the accelerated heat cycle tests are presented and compared against the results provided by the MCMC-based degradation model. A total of 5000 MCMC iterations were conducted to obtain suitable results.

Figure 4.6 shows the temporal evolution of the on-line measurements of the contact resistance of connector #5. Results presented in Figure 4.6 indicate that according to the model, the connector #5 behaves well until hour 40, since the new measured resistances (pink line) fall within the confidence intervals. However, according to Figure 4.6.d, from hour 45 on, the new values of the resistance surpasses the confidence intervals, thus indicating an anomalous behavior of the connector.

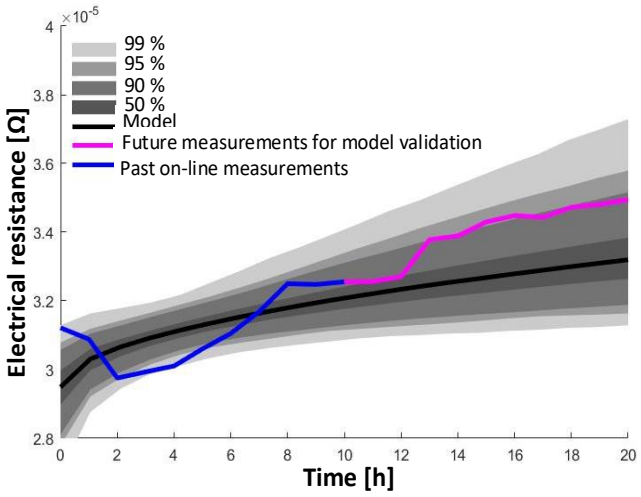


**a)**

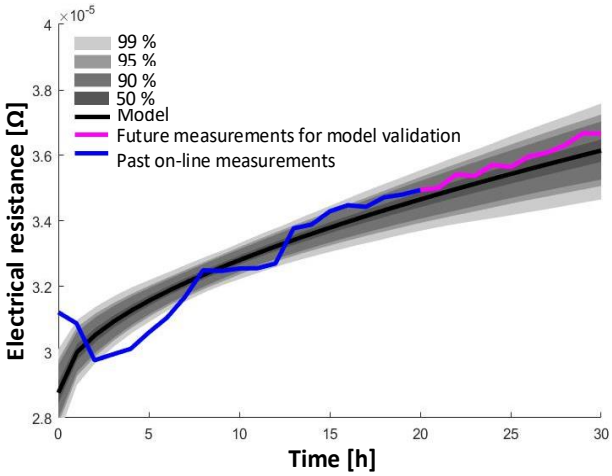


**b)**

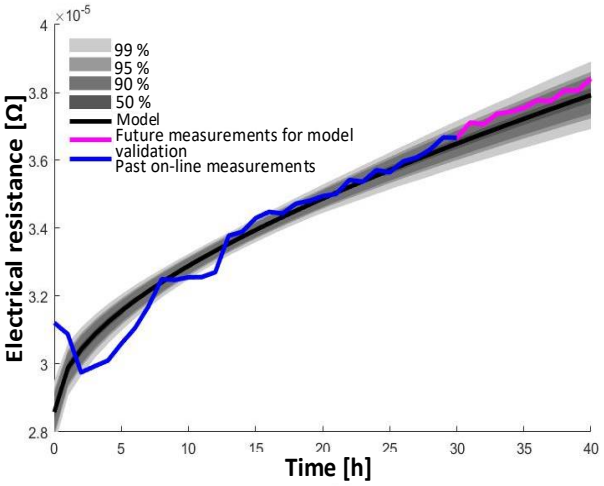


**c)**

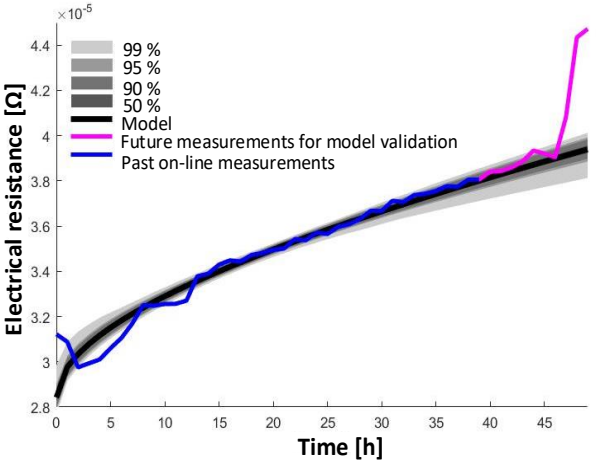


**d)**

**Figure 4.6.** Results of the MCMC-based condition monitoring approach. Predictions made at hours 10, 20, 30 and 40 of the accelerated heat cycle tests for connector #5. Past on-line measurements (blue line), future measurements (pink line) and the predictions made by the fitted model (black line) used for model validation and confidence intervals (99%,95%, 90% and 50%). Prediction made by the model after a) 10 h b) 20 h c) 30 h d) 40h [29].

*4.2.8.2 Results summary*

This section describes the experimental results achieved through the heat cycle test of the analyzed connectors.

Results reported in Figure 4.7 show that the behavior of connectors #1, #5 and #6 starts failing around hour 45, connectors #2, #4 and #7 still do not fail at hour 60, whereas connector #3 starts failing around hour 55. As 5000 MCMC iterations were performed, the MCMC algorithm returns a probability density function of the parameters $R_0$ and $\tau$, so their mean value is calculated, which is shown in Table 4.1 at hour 40 of the heat cycle tests. Table 4.1 also displays the coefficients of determination $R^2$ between the adjusted model and experimental data to prove the accuracy of the model in representing the experimental data. The coefficient of determination of connector #7 is low because this is the only connector that at hour 40 is at the beginning of the relative stability phase or at the end of the formation phase, as shown in Figure 4.7. Therefore, its resistance is stable with no noticeable increment, thus presenting a stable behavior with no symptoms of degradation, as corroborated by the results, which show that the measured value of the resistance is always below the prediction of the model. Results shown in Figure 4.7 and the high determination coefficients presented in Table 4.1 prove the suitability and accuracy of the proposed fault diagnosis method.

**Table 4.1** Model Parameters at Hour 40.

| **Connector** | **#1** | **#2** | **#3** | **#4** | **#5** | **#6** | **#7** |
|---|---|---|---|---|---|---|---|
| $R_0$ **[Ω]** | 2.4E-05 | 3.3E-05 | 3.1E-05 | 2.5E-05 | 2.9E-05 | 3.0E-05 | 2.5E-05 |
| $\tau$ **[h]** | 714285.7 | 3169.3 | 2631.6 | 2325.6 | 1875.4 | 769.2 | 4412.9 |
| $R^2$ | 0.968 | 0.924 | 0.997 | 0.994 | 0.999 | 0.999 | 0.508 |

The procedure presented in this work requires, in average, a computational effort of about 5 seconds using an Inter(R) Xeon(r) CPU E5-2620 0 @ 2.00GHz with 64 Mb RAM memory.

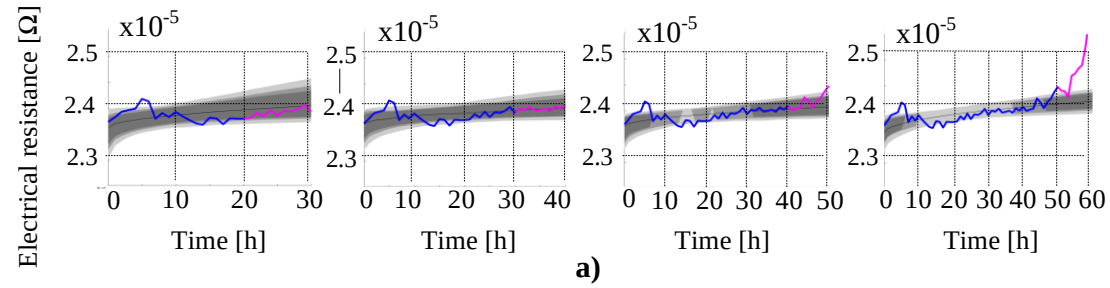
Electrical resistance [Ω]
x10-5
2.5
2.4
2.3
0 10 20 30
0 10 20 30 40
0 10 20 30 40 50
0 10 20 30 40 50 60
Time [h]

a)

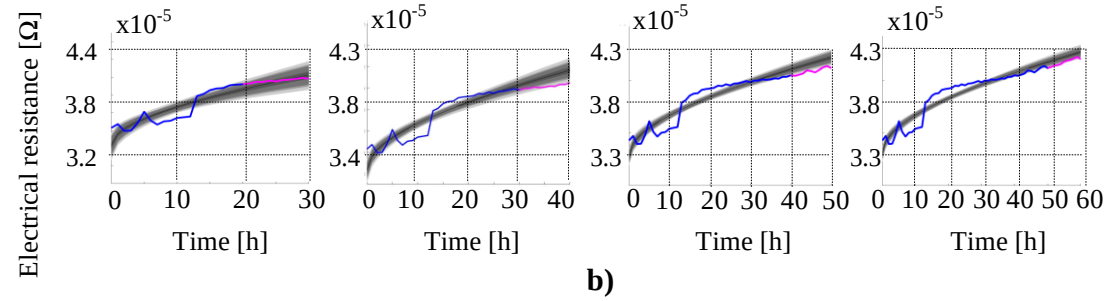
Electrical resistance [Ω]
x10-5
4.4
3.8
3.2
4.3
3.4
3.3
0 10 20 30
0 10 20 30 40
0 10 20 30 40 50
0 10 20 30 40 50 60
Time [h]

b)

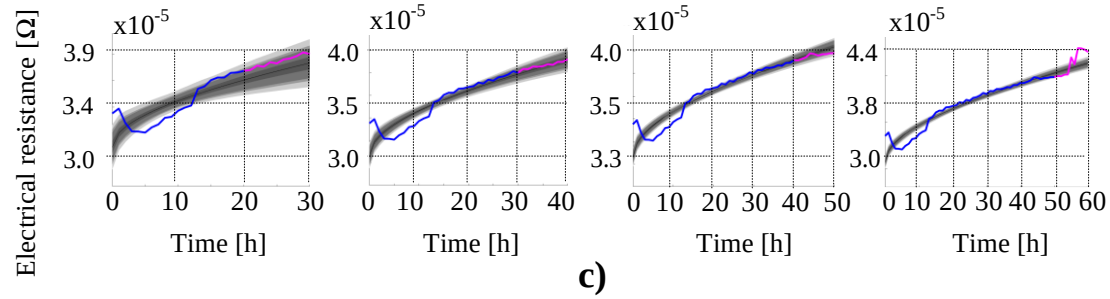
Electrical resistance [Ω]
x10-5
3.9
3.4
3.0
4.0
3.5
4.4
3.8
0 10 20 30
0 10 20 30 40
0 10 20 30 40 50
0 10 20 30 40 50 60
Time [h]

c)

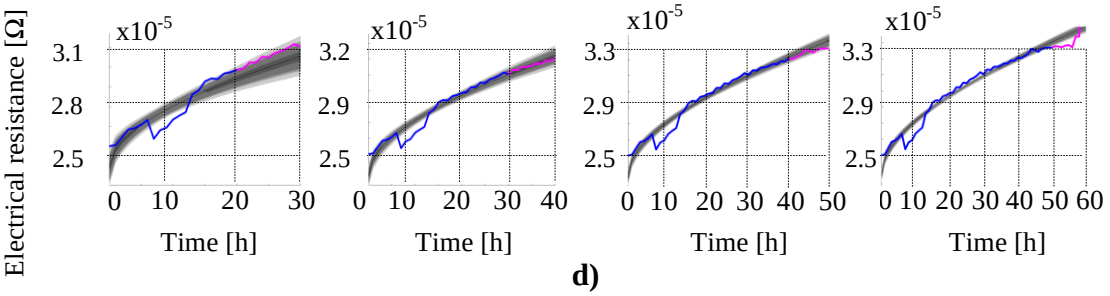
Electrical resistance [Ω]
x10-5
3.1
2.8
2.5
3.2
2.9
3.3
0 10 20 30
0 10 20 30 40
0 10 20 30 40 50
0 10 20 30 40 50 60
Time [h]

d)

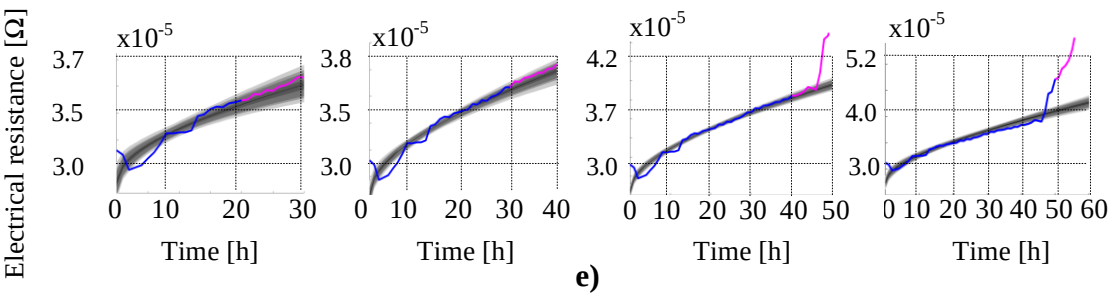
Electrical resistance [Ω]
x10-5
3.7
3.5
3.0
3.8
4.2
5.2
4.0
0 10 20 30
0 10 20 30 40
0 10 20 30 40 50
0 10 20 30 40 50 60
Time [h]

e)

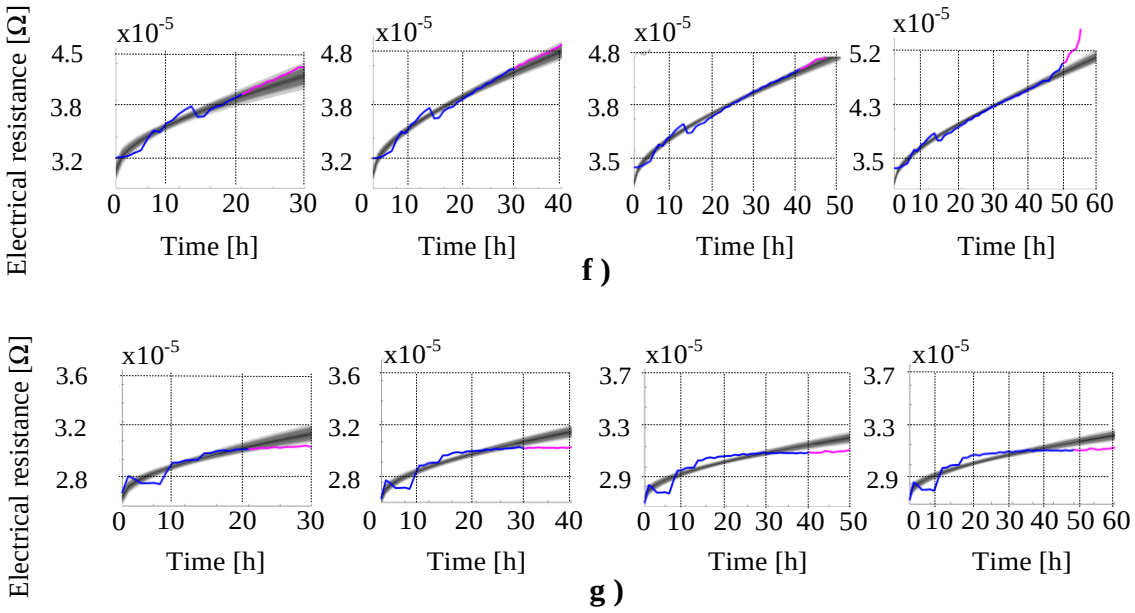


**Figure 4.7.** MCMC-based condition monitoring approach validation during the 100 h of the accelerated heat cycle tests for all connectors (#1 - #7). Model predictions against experimental data during the 100h of the heat cycle tests for all the connector from 20 h to 50 h every 10 hours (#1 - #7). a) Connector #1. b) Connector #2. c) Connector #3. d) Connector #4. e) Connector #5. f) Connector #6. g) Connector #7 [29].

### 4.2.9 Conclusions

This section has presented and verified an on-line condition monitoring method to detect early failures of power connectors. To this end, the electrical resistance of the connector must be continuously monitored, since it is used as a signature of its health condition. It is obtained from on-line measurements of the temperature, voltage drop and current flowing across the connectors. An outstanding benefit of the proposed method is that it allows avoiding to perform previous degradation tests to the connectors, thus simplifying the requirements, and reducing power consumption and operator intervention. The proposed approach is based on a parametric degradation model of the connector resistance, whose parameters are identified by using the Markov chain Monte Carlo (MCMC) method, which also defines the confidence intervals of the electrical resistance. Therefore, when the measured value of the resistance stands within the intervals, it is assumed that the connector behaves well. Otherwise, a warning signal is activated. This approach allows anticipating serious operational faults, thus preventing the connectors and the installation from major failures, while facilitating to apply predictive maintenance plans. Finally, the proposed approach can be applied for on-line condition monitoring of many other elements and devices.

## 4.3 State of health prediction by analyzing the degradation trajectory of the resistance

### 4.3.1 Background

There is a growing demand to develop prognostic methods to predict the faults in advance, i.e., when the system is fully operational, before major faults occurrence. This strategy allows operators to estimate the residual lifetime and to schedule predictive maintenance operations [97]. In addition, suitable real-time analysis algorithms are a key point for this purpose [107]. Although statistical methods have been widely used, they are not the best choice to deal with fault diagnosis problems since statistical methods estimate probability distributions based on a large numbers of training samples [108], which often are not available, thus this strategy is costly and time consuming.

Different strategies can be applied to determine the State of Health (*SoH)*, including approaches based on physical mathematical models, data-driven algorithms or hybrid approaches combining mathematical models and data-driven methods [84] [109], these last methods can perform better since they potentially combine the benefits of the two other approaches [33].

SoH and RUL estimation are currently trending research topics. A review of lithium-ion batteries prognosis methods is presented in [110], where two main groups of models are described, i.e., model-based methods (they establish a degradation model based on a physicochemical description of the problem or on empirical correlations in large amounts of data) and data-driven methods (they do not use a physics model). In [111], a data-driven approach based on machine learning was proposed to predict battery cycle life because it is suitable to predict the dynamic behavior of complex systems. In [112], the finite element method was applied to estimate the fatigue life of a gas turbine blade. Approaches based on the study of the degradation trajectory are under consideration [113]. However, a lot of work remains to be developed dealing with this topic for power connectors. It could be because they are still not instrumented, i.e., there is no electrical data available to monitor the connectors' performance.

Thus, this section proposes predicting the *SoH* of power connectors by studying the degradation trajectory of the electrical resistance that, as mentioned in this thesis, it is a reliable indicator of power connectors' performance and *SoH*. The contributions of this research work are as follows. First, it contributes to develop and test methods with low computational requirements for an on-line *SoH* prediction of electrical connectors from experimental data. This is a field with a clear lack of research works. Second, the methods here analyzed are attractive because of their simplicity and fast response, thus being compatible with low-cost microcontrollers that soon will integrate the new generations of smart connectors. Third, the solution proposed in this work is in line with the development of the smart grids, digital substations and Internet of Things (IoT), where predictive maintenance, prediction of the remaining useful life and the *SoH* are trending topics. However, installed power connectors do not include these developments. Thus, this work makes a clear development in this field. Fourth, the strategy exposed in this work adapts to the particular behavior and evolution of each connector, since it is known that there is a huge variability among connectors. This approach is able to anticipate severe faults, thus allowing to control and limit connectors' degradation process, while enabling to apply predictive maintenance plans. Finally, the methods described in this chapter have reduced computational requirements, being possible to be applied in real-time and they can be easily adapted to determine the *SoH* of many other power devices.

### 4.3.2 The proposed SoH approach

This section describes the approach and the methods which have been applied to determine the SoH of the power connectors. Three methods are compared to determine the SoH of the connector. Such methods are called linear fitting model (LF-SoH), non-linear fitting model (NLF-SoH) and Markov chain Monte Carlo non-linear model (MCMC-NLF-SoH). These methods are described in the following subsections.

#### *4.3.2.1 Methodology*

The three methods predict the next values of the resistance based on measured past values, as shown in Figure 4.8.

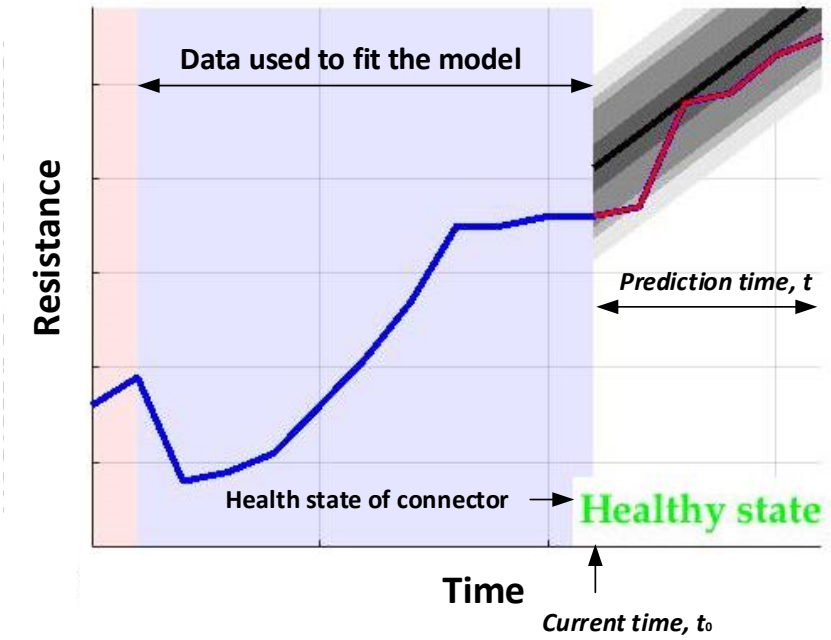


**Figure 4.8** Proposed on-line SoH prediction strategy showing the 50%, 90%, 95% and 99% confidence intervals plotted as area bands [30].

The algorithm takes the past values of the resistance (blue area in Figure 4.8) and fits these points to a given equation, which corresponds to a straight line in the LF-SoH approach or to equation (4.1) in the NLF-SoH and MCMC-NLF-SoH approaches. Next the confidence intervals of the regression coefficients are determined, and the resulting regressions are plotted (gray areas in Figure 4.1). The difference between the NLF-SoH and MCMC-NLF-SoH lies in how the regression coefficients and the confidence intervals of the regression coefficients are determined.

Figure 4.9 summarizes the steps of the proposed approach. The first step consists of determining the current value of the electrical resistance. This is done by measuring on-line the temperature of the connector, the current and the voltage drop and applying (2.10). Next, the best fitting linear degradation model (LF-SoH) or non-linear degradation model according to (4.1) (NLF-SoH and MCMC-NLF-SoH) are found based on the least-squares algorithm (LF-SoH and NLF-SoH) or the Markov Chain Monte Carlo (MCMC) algorithm (MCMC-NLF-SoH), respectively. At this stage the coefficients of the linear and non-linear models as well as their confidence intervals are estimated. Next, a short-term prediction or forecast is made based on the obtained regression curves (see the magenta curve and the gray areas in Figure 4.8). Finally, the last measured values of the resistance and the predicted ones are compared to determine the SoH of the connector, as detailed in the next section.

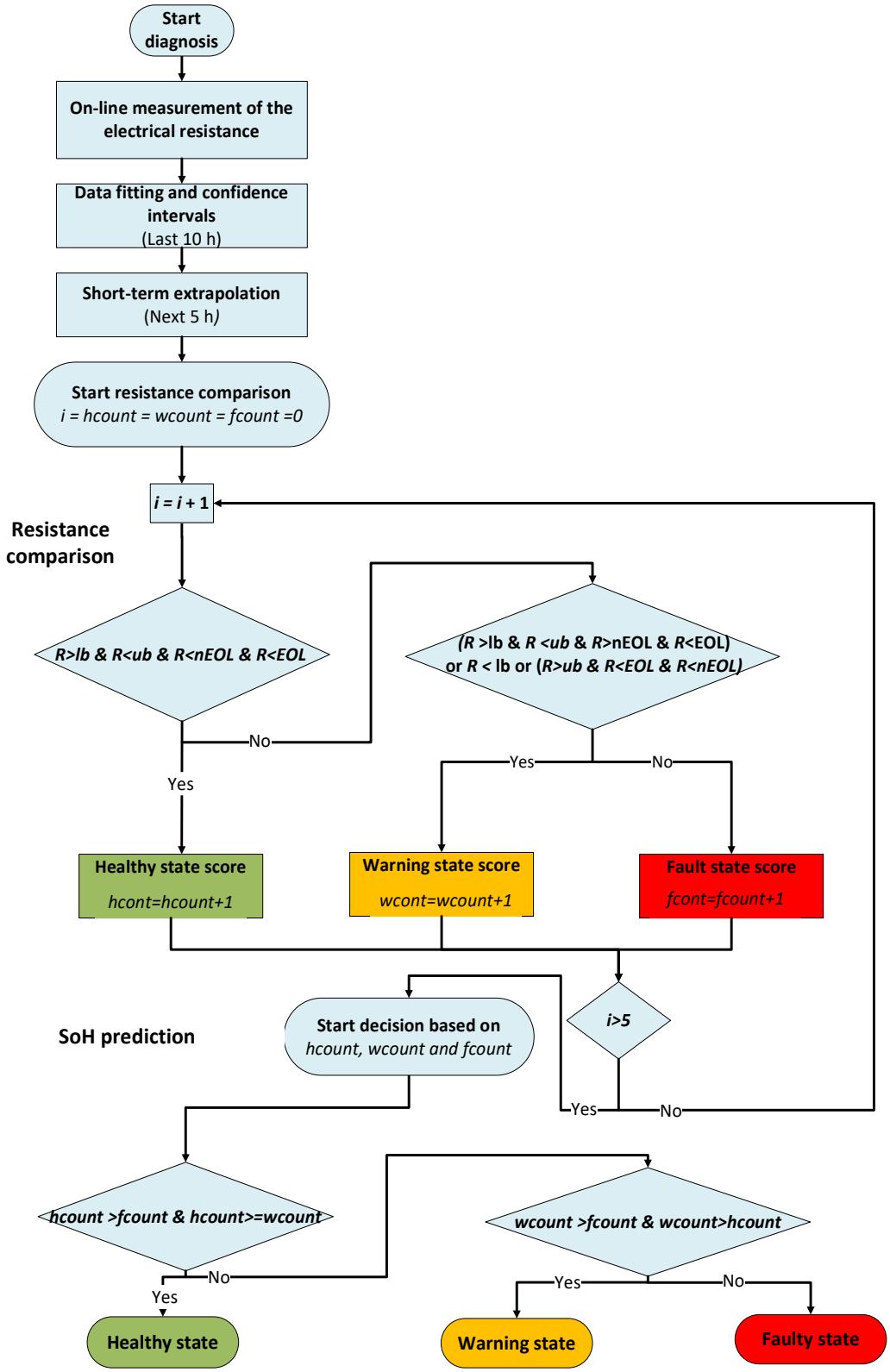


**Figure 4.9.** Proposed SoH prediction approach [30].

*4.3.2.2 Resistance comparison to determine the SoH*

The LF, NLF and MCMC-NF models are fitted using the last ten on-line resistance measurements (10 hours at a rate of 1 measurement/hour) and the mean values of the resistance of the next 5 hours and the lower and upper bounds, *lb* and *ub* respectively, are predicted by the regression models based on the least-squares values of the model coefficients and their confidence intervals.

According to Figure 4.9, the current measured value of the resistance, noted as *R*, is compared to the values of the resistance lower and upper bounds (*lb* and *ub*) and the end-of-life resistance value (EOL) and the near-EOL resistance value (nEOL). It is noted that the EOL is defined as $1.4R_0$ [33], whereas the nEOF is taken as 1.3R0. The nEOL condition is used to define a warning condition before reaching the EOL condition, since at this point the connector must be replaced by a new one to prevent sudden failures and system malfunctioning. This approach allows predicting the SoH of the connectors in three states, namely healthy, warning and faulty condition, thus facilitating the application of predictive maintenance plans and allowing to schedule maintenance actions.

In order to categorize the current state of the connector as healthy, warning or faulty, a score is given to each state (*hcount*, *wcount*, *fcount* are the healthy, warning and faulty state counters that give the final scores, respectively) based on the current value of the measured resistance *R*, as detailed in Figure 4.9, so that the predicted SoH of the connector is attributed to the most scored state (healthy, warning or faulty).

*4.3.2.3 SoH based on the LF-SoH, NLF-SoH and MCMC-NLF-SoH methods*

The LF-SoH method predicts the future values of the resistance by linearly fitting the past measured values to a straight line. It assumes that resistance degradation trajectory follows a straight line. By applying the least squares algorithm both the coefficients of the linear regression and the confidence intervals of such coefficients are found. The confidence intervals allow confining the predicted values of the resistance within the lower and upper boundaries they define.

Similarly, the NLF-SoH method predicts the future values of the resistance by fitting the past measured values to equation (4.1) describing the degradation trajectory of the

resistance according to Braunovic's model. The coefficients of (4.1) and their confidence intervals are also found by applying the least squares algorithm.

The MCMC-NLF-SoH applies the Markov chain Monte Carlo (MCMC) method to find both the values of the coefficients $R_0$ and $\tau$ in (4.1) and their confidence intervals based on the past experimental data. MCMC generates $n$ random samples (3000 samples in this case) of the coefficients $R_0$ and $\tau$ for each simulated time $t$ ($t$ corresponds to time points of the last 10 h) thus obtaining a matrix of resistances with $n$ rows and $t$ columns. Next, each column is sorted from highest to lowest resistance and the 99.5th and 0.5th percentiles are calculated (99% confidence interval). Finally, these values are plotted versus time, as shown in Figure 4.8.

### 4.3.3 Results

This section describes the results attained by means of the three methods analyzed in this research, i.e., the LF-SoH, NLF-SoH and MCMC-NLF-SoH algorithms from the experimental data obtained in the heat cycle tests applied to seven medium-voltage connectors, which was detailed in Section 4.2.7.

#### *4.3.3.1 Results Attained by Applying the LF-SoH Method*

Figure 4.10 summarizes the results attained with the seven connectors by applying the LF-SoH method every 5 h. It is noted that the green color indicates the healthy state, the orange color the warning or pre-fault state and the red color indicates that the connector has reached the faulty state.

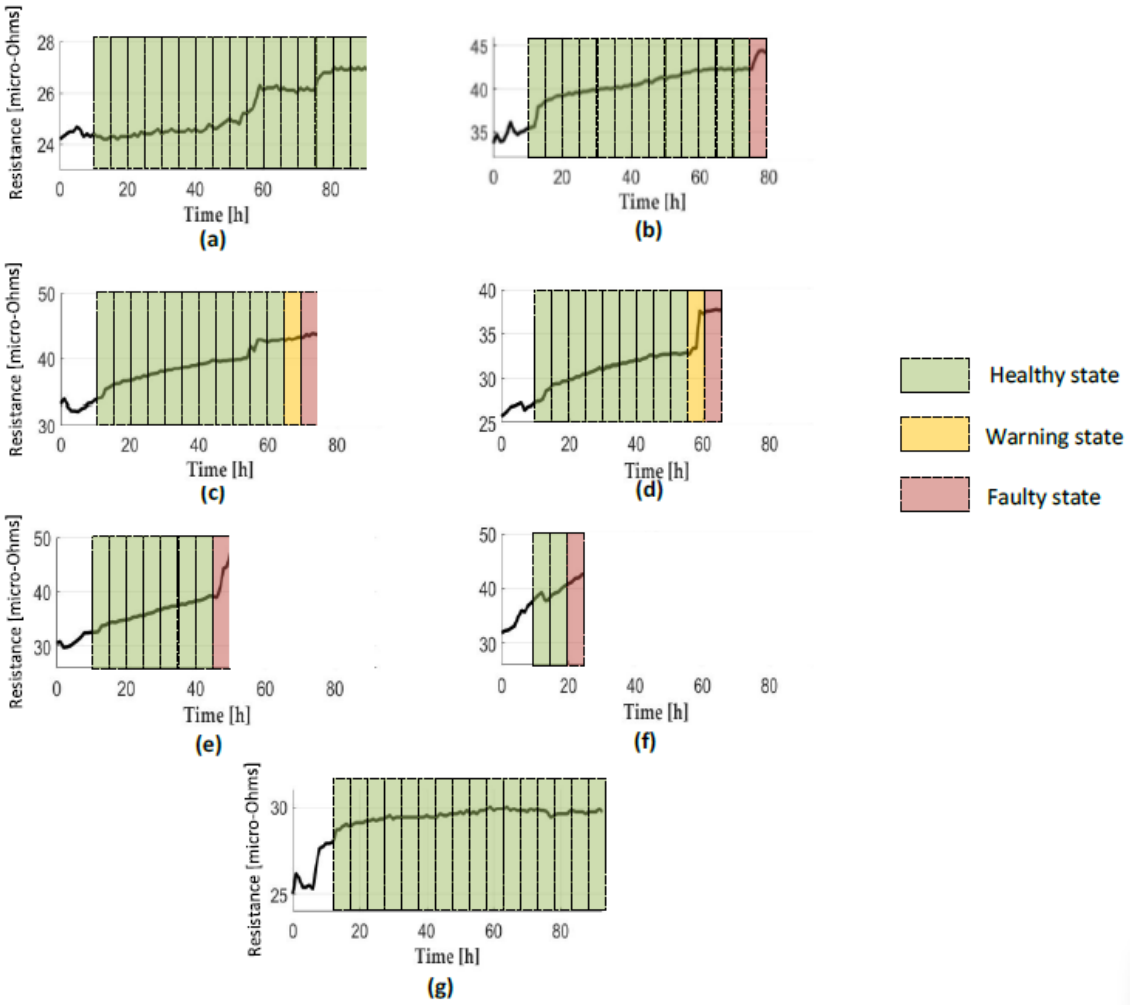


**Figure 4.10.** State of health of the 7 connectors every 5 h by using the LF-SoH method: (a) Connector#1, (b) connector #2, (c) connector #3, (d) connector #4, (e) connector #5, (f) connector #6 and (g) connector #7 [30].

Results presented in Figure 4.10 show that according to the LF algorithm and the rules described in Figure 4.9, connector #2 at hour 80, connector #3 at hour 75, connector #4 at hour 65, connector #5 at hour 50 and connector #6 at hour 25 have reached the fault condition by these time points, so they must be replaced to ensure a safe operation. On the other hand, connectors #1 and #7 still do not reach the faulty state at the end of the tests.

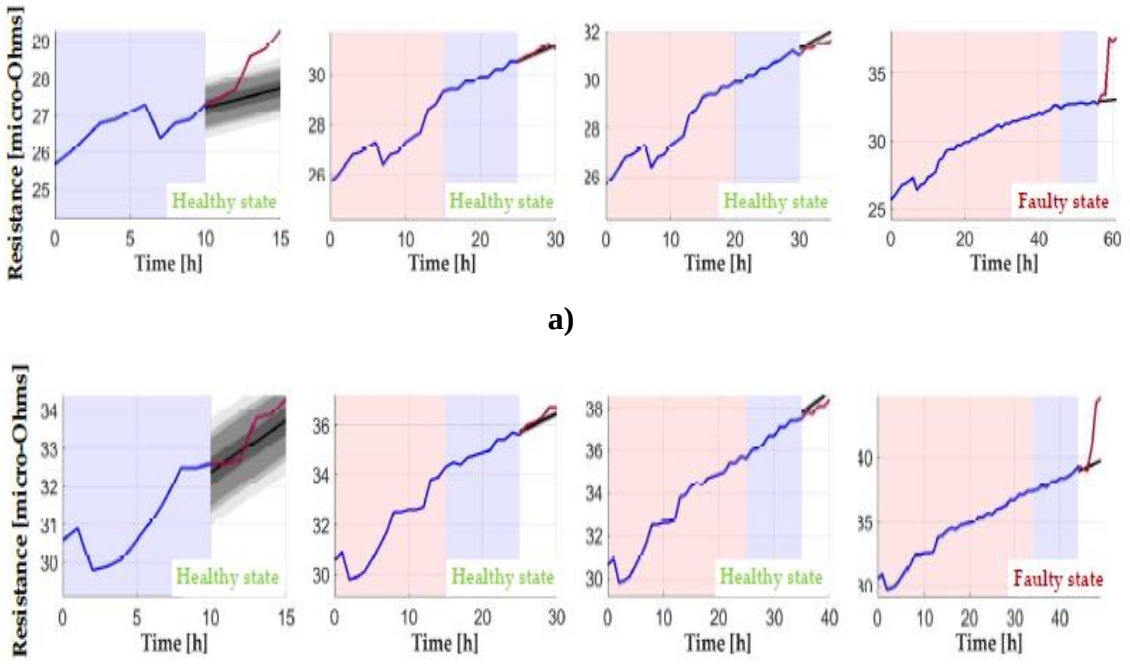


**Figure 4.11.** SoH of connectors #4 and #5 predicted by the LF-SoH method at different times. (a) Connector #4 at present times, $t_0$= 15 h, 30 h, 35 h and 60 h. (b) Connector #5 at $t_0$ = 15 h, 30 h, 40 h an 50h [30].

Figure 4.11 shows the time evolution of the SoH prediction of connectors #4 and #5, respectively. As can be seen, connector #4 operates under healthy condition at the present times $t_0$ = 15 h, $t_0$ = 30 h and $t_0$ = 35 h, whereas connector #5 shows healthy state operation at the present times $t_0$ = 15 h, $t_0$ = 30 h and $t_0$ = 40 h. Finally, both connectors reach the faulty state at $t_0$ = 60 h and $t_0$ = 50 h, respectively, due to the important change of their electrical resistances.

*4.3.3.2 Results Attained by Applying the NLF-SoH Method*

Figure 4.12 shows the results obtained with the seven connectors by applying the NLF-SoH method every 5 h.

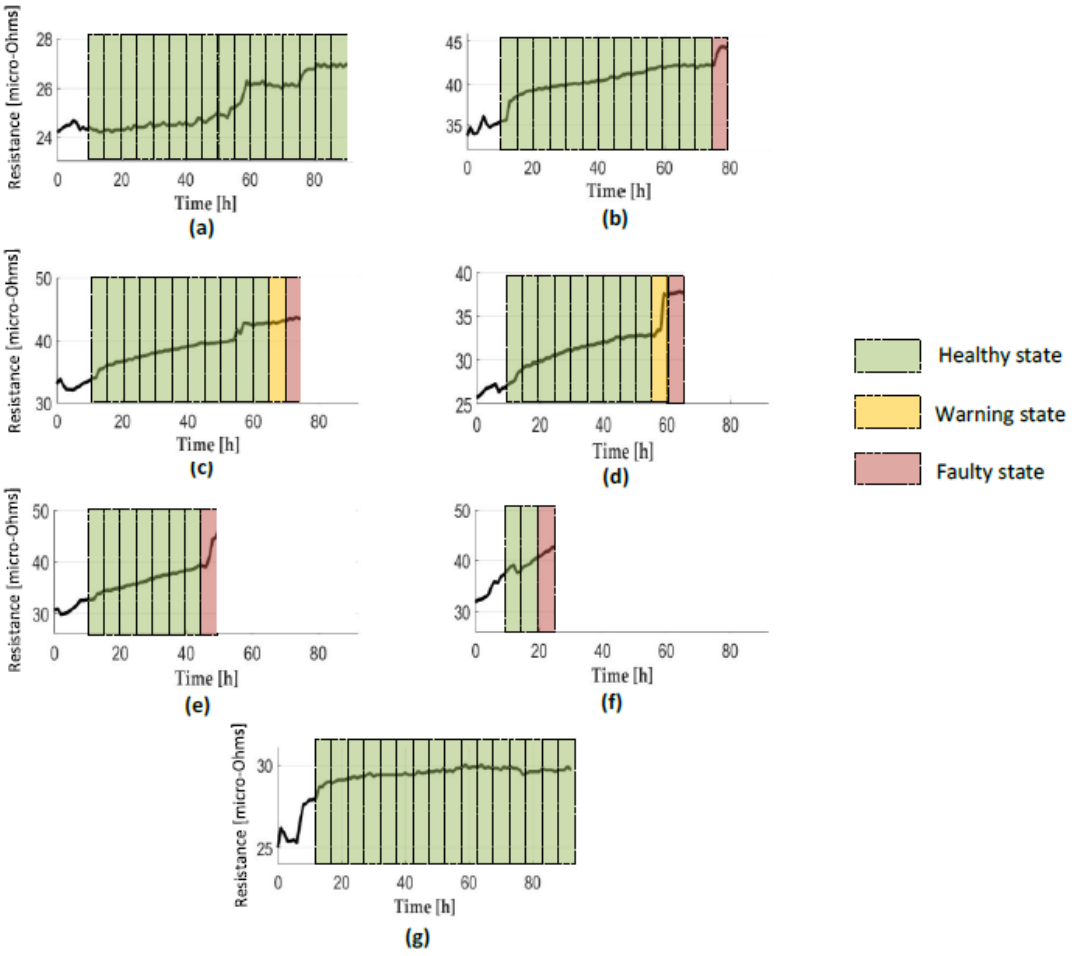


**Figure 4.12.** State of health of the 7 connectors every 5 h by using the NLF-SoH method: (a) Connector #1, (b) connector #2, (c) connector #3, (d) connector #4, (e) connector #5, (f) connector #6 and g) connector 7 [30].

Results presented in Figure 4.12 show that according to the NLF algorithm and the rules described in Figure 4.9, connector #2 at hour 80, connector #3 at hour 70, connector #4 at hour 60, connector #5 at hour 50 and connector #6 at hour 25 have reached the faulty condition by these time points, so they must be replaced. Similar to the predictions of the LF-SoH method, connectors #1 and #7 still do not reach the faulty state at the end of the tests.

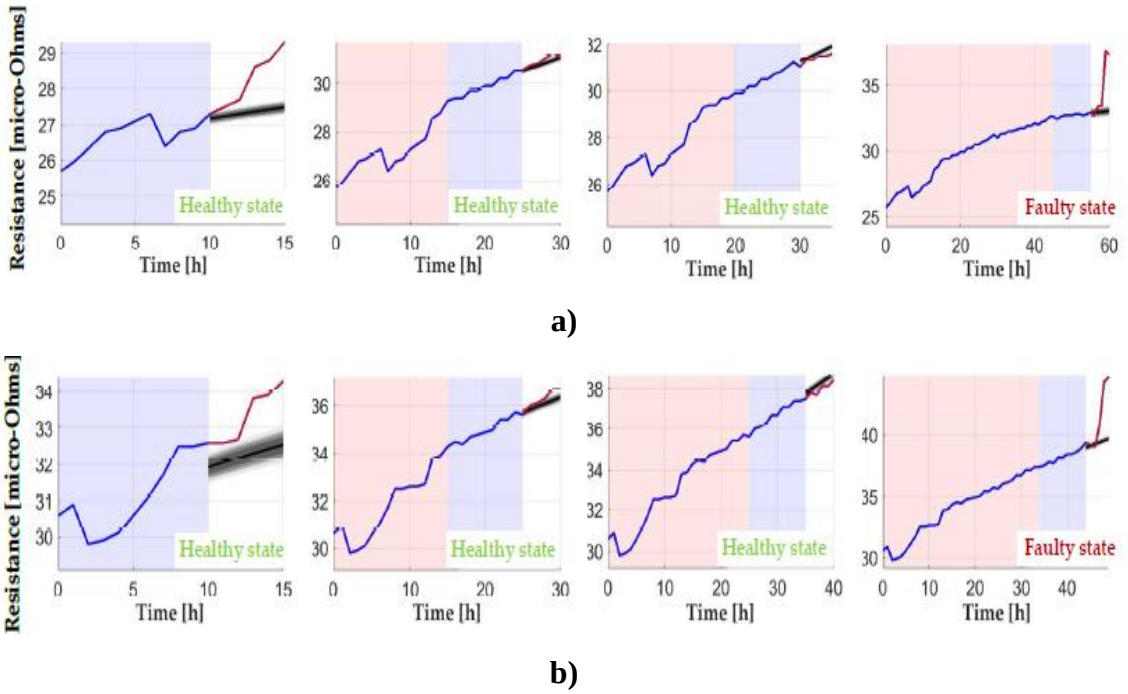


**Figure 4.13.** SoH of connectors #4 and #5 predicted by the NLF-SoH method at different times. (**a**) Connector #4 at present times $t_0$ = 15 h, 30 h, 35 h and 60 h. (**b**) Connector #5 at $t_0$ = 15 h, 30 h, 40 h and 50 h [30].

Figure 4.13a and 4.13b show the time evolution of the SoH prediction of connectors #4 and #5, respectively. These figures also show that both connectors experience a sudden increase of the resistance before $t_0$ = 15 h, which is attributed to the initial or formation phase of the resistance, which is quite common at the first hours, so it is reported as a healthy state. Figure 13a shows that connector #4 reaches the faulty state at $t_0$ = 60 h, whereas connector #5 at $t_0$ = 50 h.

*4.3.3.3 Results Attained by Applying the MCMC-NLF-SoH Method*

Figure 4.14 summarizes the results obtained with the seven connectors by applying the MCMC-NLF-SoH method every 5 h.

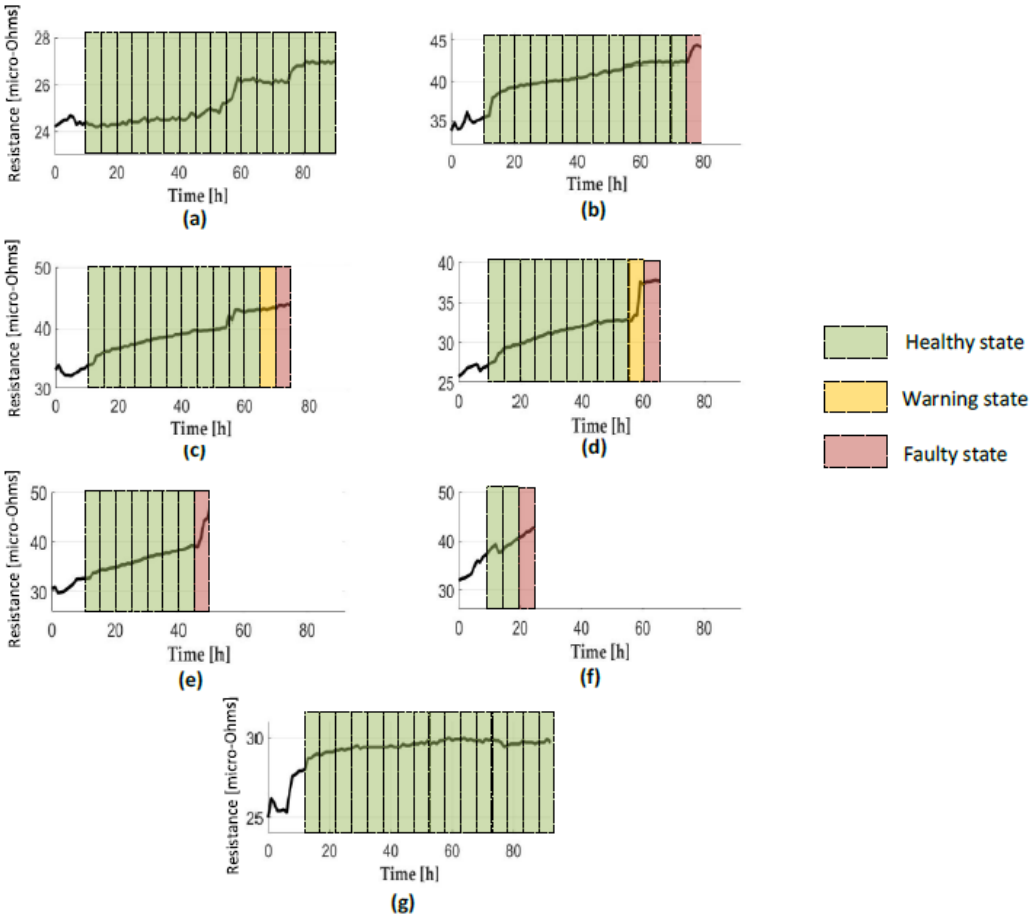


**Figure 4.14.** State of health of the 7 connectors every 5 h by using the MCMC-NLF-SoH method: (a) Connector #1, (b) connector #2, (c) connector #3, (d) connector #4, (e) connector #5, (f) connector #6 and (g) connector #7 [30].

Results presented in Figure 4.14 show that according to this algorithm and the rules described in Figure 4.9, connector #2 at hour 80, connector #3 at hour 70, connector #4 at hour 65, connector #5 at hour 50 and connector #6 at hour 25 have reached the fault condition by these time points. Similar to the predictions of the LF-SoH and NLF-SoH methods, connectors #1 and #7 still do not reach the faulty state at the end of the tests.

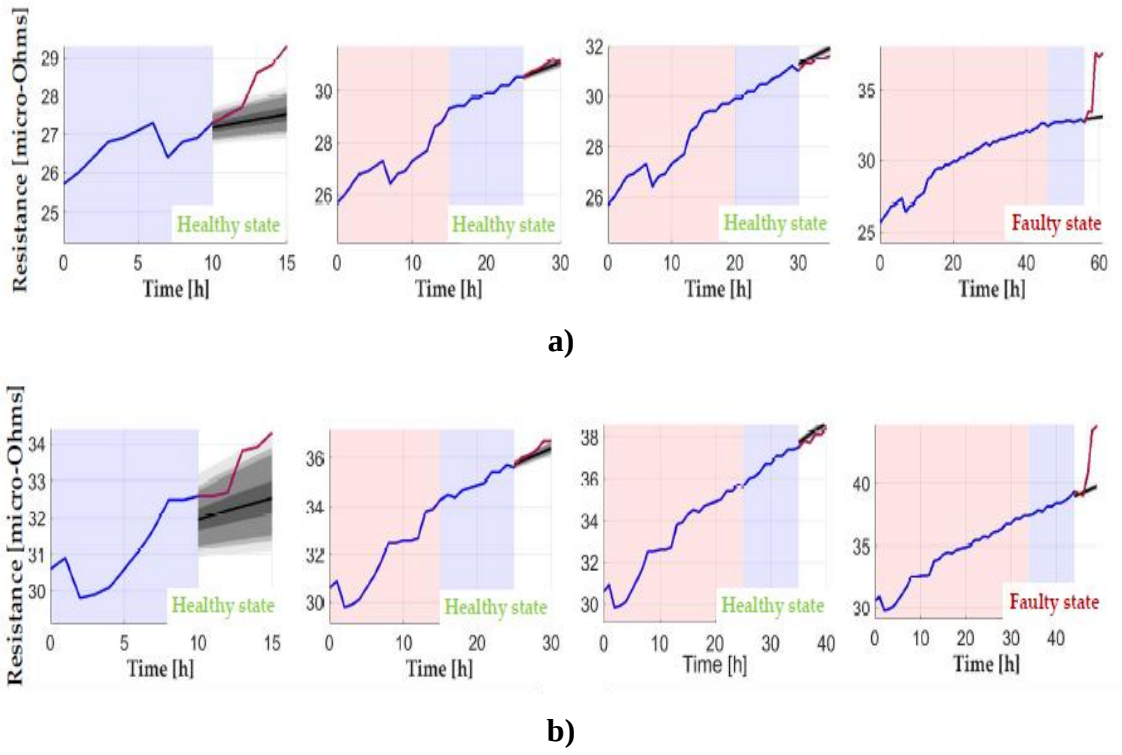


**Figure 4.15.** SoH of connectors #4 and #5 predicted by the MCMC-NLF-SoH method at different times. (**a**) Connector #4 at present times $t_0$ = 15 h, 30 h, 35 h and 60 h. (**b**) Connector #5 at $t_0$ = 15 h, 30 h, 40 h and 50 h 1[30].

Figures 4.15a and 4.15b show the time evolution of the SoH prediction of connectors #4 and #5, respectively. They indicate that connector #4 reaches the faulty state at $t_0$ = 60 h, whereas connector #5 reaches the faulty state at $t_0$= 50 h.

*4.3.3.4 Discussion*

The medium-voltage market is very competitive, so in order to reduce costs, medium-voltage connectors are designed with the minimum material. Thus, their outer diameter being quite similar to that of the conductor at which they are connected. Therefore, medium-voltage connectors are very sensitive to diverse factors, including defects in the conductors or conductors, presence of dirt or oxides, or installation practices, since the crimping process has a great influence. Therefore, the differences among connectors already seen in the previous section are attributed to a combination of these effects, which greatly affect the time to the fault.

The first method (linear fitting SoH or LF-SoH) predicts the SoH of a particular connector by comparing the last measured values of the resistance against the predictions

determined by a least-squares linear regression model. The other two methods (NLF-SoH and MCMC-NLF-SoH) apply a non-linear model of the degradation trajectory of the contact resistance instead of using a linear degradation model. Whereas NLF-SoH determines the SoH by comparing the last measured values of the resistance against the predictions determined by a least-squares fitting of the Braunovic model, MCMC-NLF SoH applies the Markov chain Monte Carlo (MCMC) method for this purpose.

Table 4.2 compares the results attained with the three analyzed SoH prediction methods to better understand their behavior. The results presented in Table 4.2 show a similar performance of the three methods since they predict the healthy, warning and faulty conditions at the same time instants. Finally, Table 4.3 presents the average time required by the three methods to predict the SoH of the connectors.

**Table 4.2.** SoH of the 7 connectors every 5 h according to the LF/NLF/MCMC NLF-SoH methods.

| | **Connector's resistance (micro-Ohms)** | | | | | | |
|---|---|---|---|---|---|---|---|
| **Present time, $t_0$ (h)** | #1 | #2 | #3 | #4 | #5 | #6 | #7 |
| 15 | H/H/H | H/H/H | H/H/H | H/H/H | H/H/H | H/H/H | H/H/H |
| 20 | H/H/H | H/H/H | H/H/H | H/H/H | H/H/H | H/H/H | H/H/H |
| 25 | H/H/H | H/H/H | H/H/H | H/H/H | H/H/H | F/F/F | H/H/H |
| 30 | H/H/H | H/H/H | H/H/H | H/H/H | H/H/H | | H/H/H |
| 35 | H/H/H | H/H/H | H/H/H | H/H/H | H/H/H | | H/H/H |
| 40 | H/H/H | H/H/H | H/H/H | H/H/H | H/H/H | | H/H/H |
| 45 | H/H/H | H/H/H | H/H/H | H/H/H | H/H/H | | H/H/H |
| 50 | H/H/H | H/H/H | H/H/H | H/H/H | F/F/F | | H/H/H |
| 55 | H/H/H | H/H/H | H/H/H | H/H/H | | | H/H/H |
| 60 | H/H/H | H/H/H | H/H/H | W/W/W | | | H/H/H |
| 65 | H/H/H | H/H/H | H/H/H | F/F/F | | | H/H/H |
| 70 | H/H/H | H/H/H | W/W/W | | | | H/H/H |
| 75 | H/H/H | H/H/H | F/F/F | | | | H/H/H |
| 80 | H/H/H | F/F/F | | | | | H/H/H |
| 85 | H/H/H | | | | | | H/H/H |
| 90 | H/H/H | | | | | | H/H/H |

**Table 4.3** The average computation time required by the three methods using an Intel® Core (TM) i7-8750H CPU @2.20 GHz

| Method | Computation time |
|---|---|
| **LF-SoH** | 6 ms |
| **NFL-SoH** | 50 ms |
| **MCMC-NFL-SoH** | 1200 ms |

From the results summarized in Tables 4.2 and 4.3, it can be concluded that the three methods exhibit comparable results. The LF-SoH method, due to its simplicity, is the one requiring lower computational requirements with a similar performance than the NLF-SoH and MCMC-NLF-SoH methods. It is also noted that the MCMC-NLF-SoH algorithm is the one requiring more computational resources.

### 4.3.4 Conclusions

Power connectors are critical elements in power lines and networks, so their fault can lead to important consequences, including power outages, safety-related issues and economic losses. Thus, there is an increasing need to continuously monitor their performance in order to ensure high reliability by anticipating the fault condition before occurrence. With the development of low-cost sensors and wireless communications systems compatible with the Internet of Things, this topic is receiving much attention and interest because these developments facilitate the application of predictive maintenance approaches. Despite the enormous implications of future developments in this area, there is a scarcity of works dealing with this topic applied to power connectors, this research contributing to this field.

This work presented, analyzed and compared the behavior of three methods for an online determination of the SoH of power connectors, namely LF-SoH, NLF-SoH and MCMC-NLF-SoH. These methods were selected based on simplicity, low computational requirements and adaptation to the particular characteristics and behavior of each connector. They rely on monitoring the degradation trajectory of the electrical resistance of the connectors, thus detecting changes that allow anticipating the fault before occurrence, so that predictive maintenance actions can be applied. The resistance is used as an indicator of their SoH because it is known that degradation of the connectors' thermal and electrical behaviors is associated with changes of this magnitude. In order to obtain reliable and realistic data, seven medium voltage connectors were subjected to accelerated heat cycle tests. The electrical resistance of the seven connectors was monitored by measuring the temperature, electrical current and voltage drop across the terminal points of the connectors.

From the experimental validation carried out in this research work, it is concluded that although the three methods show comparable results, the LF-SoH method is the fastest one due to its simplicity, whereas the MCMC-NLF-SoH algorithm is the one requiring more computational resources. Moreover, the results presented show the fast and accurate response and reduced computational load of the three assessed methods and their potential to predict the SoH of power connectors. Furthermore, this approach can also be applied to many other power devices and components.

The results presented in this work, that for the exposed reasons deal with medium voltage connectors, allow assessing the feasibility and potential to apply the proposed method to predict the SoH of substation connectors instead.

# CONCLUSIONS

# 5. CONCLUSIONS

## 5.1 General conclusion

The main objective of this thesis was to develop remaining useful life and fault detection models for high-voltage electrical connectors to simplify the application of predictive maintenance strategies and to guarantee a correct operation of the connector during its useful life. Thus, mathematical models were proposed and validated by means of experimental data. It is worth mentioning that the methodologies and algorithms presented in this thesis can be applied to many other power devices and components with predictive maintenance proposes. Also, the work developed regarding the characterization of the temperature dependence of the contact resistance can be useful to design substation connectors as well as similar devices with better-quality electrical and thermal behavior.

First, the temperature dependence of the contact resistance of aluminum substation connectors was analyzed in detail in Chapter 2. To this end, electrical loops, which included substation connectors and aluminum conductors, were installed and analyzed in order to obtain results from experimental data. The total electrical resistance of the analyzed connectors was measured on-line by acquiring the voltage drop, the electrical current flowing through the loop and the temperature of the connectors. All terms of the total electrical resistance were analyzed. Results prove that all resistance terms increment linearly with temperature, but at a different rate, so that each term has its own temperature coefficient. Furthermore, results also demonstrate that the contact resistance increases linearly with temperature at a faster rate than the increase of the bulk resistance under AC supply.

Next, a simple approach for determining the remaining useful life (RUL) of power connectors, with a very low computational requirements and without the need to perform time-consuming degradation test was proposed in Chapter 3. To this end, an experimental

test was performed on seven connectors, in which the voltage drop, electric current and the connector temperature were acquired on-line and processed to estimate the instantaneous value of electrical resistance of the connectors. Afterward, the two parameters of a simple but effective degradation model were identified by fitting the equation of the degradation model to the experimental data using a generalized least squares algorithm. Finally, the proposed approach to estimate the RUL was validated by comparing the estimates of the algorithms developed with the data acquisitions. It proves the potential and viability of this method in determining and anticipating when the connector must be replaced before presenting a major fault.

Finally, chapter 4 proposed two novel fault detection approaches for substations connectors. The first method is a simple approach for an on-line diagnosis of the health status of power connectors based on continuously monitoring the electrical resistance, which is able to detect premature faults in power connectors. To this end, the value of the resistance was obtained from on-line measurements of the temperature, the voltage drop and the current flowing across the connectors, thus obtaining reliable and realistic data from seven medium voltage connectors, which undergone accelerated heat cycle tests. Afterward, a parametric degradation model of the connector resistance combined with the application of the Markov chain Monte Carlo (MCMC) method was applied for finding the most appropriate values of the parameters of the resistance degradation model. It was applied by using the available experimental data, thus providing the confidence intervals of the electrical resistance and limiting the expected future values of the resistance within the space well-defined by the confidence intervals. Therefore, when the measured value of the resistance falls within the intervals, it is assumed that the connector behaves well. Otherwise, a warning signal is activated. Next, the second approach proposed in Chapter 4 consists of forecasting the State of Health (*SoH*) of power connectors by using the degradation trajectory of the electrical resistance thus detecting changes that allow anticipating the fault condition on time, so that predictive maintenance actions can be applied. To this end, the behavior of three methods for an on-line determination of the SoH of power connectors were analyzed and compared, which are the linear fitting model (LF-SoH), non-linear fitting model (NLF-SoH) and Markov chain Monte Carlo non-linear model (MCMC-NLF-SoH). The resistance was used as an indicator of their SoH because, as mentioned in this thesis, the degradation of the thermal and electrical behavior of the connectors is related to the changes of the resistance. From this research work, it

was concluded that even though the three methods present similar results, the fastest one is the LF-SoH method due to its simplicity, unlike the MCMC-NLF-SoH algorithm, which is the method that requires more computational resources. Also, it was shown the fast and accurate response and reduced computational requirements of the three assessed methods and their potential to predict the SoH of power connectors. In addition, this approach can also be applied to many other power devices and components.

## 5.2 Contributions

This section presents the contributions attained by the development of this thesis. These contributions are:

- ✓ Implementation of novel methods whose strategy allows avoiding to perform previous degradation tests to the connectors, thus simplifying requirements, performing test and monetary costs.

- ✓ Implementation of an in-depth study of the temperature dependence of the electrical contact resistance of substation connectors.

- ✓ Development and validation of the RUL and fault detection models for substation connectors based on on-line data acquisitions. These models are in line with the development of smart grids, digital substations and the Internet of Things (IoT), being compatible with the *SmartConnector* requirements.

- ✓ Development and validation of RUL and fault detection models for electrical connectors with low computational requirements.

## 5.3 Further work

The elaboration of this thesis has provided knowledge related to strategies for the preventive maintenance of high-voltage connectors, as well as a better understanding of the impact of the contact resistance on these devices. However, some gaps related to this topic need to be explored.

First, despite the proposed approaches in this thesis are suitable for predictive maintenance applications on high-voltage connectors, other artificial intelligence approaches could be explored such as neuronal networks (NN), which can be attractive to implement as they today are trending topic in the engineering field. Since with the implementation of IoT technology in the industry, degradation data will be potentially available for manufacturers eventually so that it can be used for predictive maintenance purposes.

Next, a comparison of the RUL and fault detection models between data obtained with laboratory equipment (DAQs) and data obtained directly from the *SmartConnector* might be interesting to perform. Since even though this study is not done, it is the last stage for validating the performance of the *SmartConnector* project.

Also, the RUL and fault detection models presented in this thesis can be applied to develop predictive maintenance strategies for substation conductors (bus bars) in order to reach a wider and fuller monitoring of the substation. Thus, avoiding any contingencies or threats. Moreover, since predictive maintenance is currently a powerful tool used in the industry, these models can be used to develop a research for some different critical devices, such as: bearings, electric motors, batteries, etc., due to their simplicity and calculation speed.

Finally, although this thesis has demonstrated that measuring the resistance is a powerful technique for the predictive maintenance of the substation connectors, has been developed to achieve the *SmartConnector* requirements. It would be interesting to develop a research about other predictive technologies for detecting corona. For instance, to perform an on-line acoustic monitoring and a vibration analysis to predict and detect corona discharges

by using low-cost sensors. This could be a novel method to detect corona discharges in both substation components and other applications.

# BIBLIOGRAPHY


[1] F. Capelli, J. R. Riba, and J. Sanllehí, "Finite element analysis to predict temperature rise tests in high-capacity substation connectors," *IET Gener. Transm. Distrib.*, vol. 11, no. 9, pp. 2283–2291, 2017.

[2] E. Society, *IEEE Guide for Determining the Effects of High-Temperature Operation on*, vol. 2013. 2013.

[3] A. Kadechkar, "Development of the future generation of smart high voltage connectors and related components for substations, with energy autonomy and wireless data transmission …," *TDX (Tesis Dr. en Xarxa)*, 2020.

[4] J. Fan, K. C. Yung, and M. Pecht, "Predicting long-term lumen maintenance life of LED light sources using a particle filter-based prognostic approach," *Expert Syst. Appl.*, vol. 42, no. 5, pp. 2411–2420, 2015.

[5] L. Trevisanello *et al.*, "Accelerated life test of high brightness light emitting diodes," *IEEE Trans. Device Mater. Reliab.*, vol. 8, no. 2, pp. 304–311, 2008.

[6] J. Schmalstieg, S. Käbitz, M. Ecker, and D. U. Sauer, "From accelerated aging tests to a lifetime prediction model: Analyzing lithium-ion batteries," *2013 World Electr. Veh. Symp. Exhib. EVS 2014*, 2014.

[7] G. Yang, "Accelerated life test plans for predicting warranty cost," *IEEE Trans. Reliab.*, vol. 59, no. 4, pp. 628–634, 2010.

[8] C. Abomailek Rubio, "Development of reduced-scale tests for HTLS substation connectors," *TDX (Tesis Dr. en Xarxa)*, 2018.

[9] A. L. PETROU, M. ROULIA, and K. TAMPOURIS, "the Use of the Arrhenius Equation in the Study of Deterioration and of Cooking of Foods – Some Scientific and Pedagogic Aspects," *Chem. Educ. Res. Pr.*, vol. 3, no. 1, pp. 87–97, 2002.

[10] S. Mohajeryami, M. Nagisetty, M. Doostan, and Z. Salami, "Investigation of naturally aged timing relays' service life by employing thermally accelerated aging," *Proc. IEEE Power Eng. Soc. Transm. Distrib. Conf.*, vol. 2016-July, no. May, 2016.

[11] C. M. Liao and S. T. Tseng, "Optimal design for step-stress accelerated degradation tests," *IEEE Trans. Reliab.*, vol. 55, no. 1, pp. 59–66, 2006.

[12] "ANSI / NEMA CC 1-2009 Electric Power Connection for Substations," 2012.

[13] F. Capelli, J. R. Riba, and D. Gonzalez, "Thermal behavior of energy-efficient substation connectors," *Proc. - 2016 10th Int. Conf. Compat. Power Electron. Power Eng. CPE-POWERENG 2016*, pp. 104–109, 2016.

[14] "ANSI C119.0-2015 American National Standard for Electric Connectors," 2015.

[15] "IEC 61238-1-3:2018 Compression and mechanical connectors for power cables - Part 1-3: Test methods and requirements for compression and mechanical connectors for power cables for rated voltages above 1 kV (Um = 1,2 kV) up to 30 kV (Um = 36 kV) tested on n." Geneva, Switzerland, pp. 1–89, 2018.

[16] J. R. Riba, A. G. Mancini, C. Abomailek, and F. Capelli, "A 3D-FEM-based model

to predict the electrical constriction resistance of compressed contacts," *Meas. J. Int. Meas. Confed.*, vol. 114, no. February 2017, pp. 44–50, 2018.

[17] Y. Liu, G. Zhang, H. Qin, W. Liu, J. Wang, and J. Yang, "Study on the influence of speed in DRM of SF6 circuit breaker," *Int. J. Electr. Power Energy Syst.*, vol. 121, no. March, 2020.

[18] D. P. Rommel, D. Di Maio, and T. Tinga, "Transformer hot spot temperature prediction based on basic operator information," *Int. J. Electr. Power Energy Syst.*, vol. 124, no. June 2020, p. 106340, 2021.

[19] B. Sun *et al.*, "Remaining useful life prediction of aviation circular electrical connectors using vibration-induced physical model and particle filtering method," *Microelectron. Reliab.*, vol. 92, no. June 2018, pp. 114–122, 2019.

[20] F. Capelli, J. R. Riba, E. Ruperez, and J. Sanllehi, "A genetic-algorithm-optimized fractal model to predict the constriction resistance from surface roughness measurements," *IEEE Trans. Instrum. Meas.*, vol. 66, no. 9, pp. 2437–2447, 2017.

[21] C. Okoh, R. Roy, J. Mehnen, and L. Redding, "Overview of Remaining Useful Life prediction techniques in Through-life Engineering Services," *Procedia CIRP*, vol. 16, pp. 158–163, 2014.

[22] "RUL Estimation Using RUL Estimator Models - MATLAB & Simulink - MathWorks España." [Online]. Available: https://es.mathworks.com/help/predmaint/ug/rul-estimation-using-rul-estimator-models.html. [Accessed: 04-Feb-2020].

[23] "Three Ways to Estimate Remaining Useful Life for Predictive Maintenance - MATLAB & Simulink." [Online]. Available: https://www.mathworks.com/company/newsletters/articles/three-ways-to-estimate-remaining-useful-life-for-predictive-maintenance.html. [Accessed: 27-Mar-2019].

[24] "IS/IEC 62271-1 : 2007. HIGH-VOLTAGE SWITCHGEAR AND CONTROLGEAR," 2007.

[25] "¿Qué es el mantenimiento predictivo?" [Online]. Available: http://www.mantenimientopetroquimica.com/mantenimientopredictivo.html. [Accessed: 01-Apr-2019].

[26] N. Zhang, "Mechanical Fault Diagnosis Method Based on Machine Learning," *Proc. - 2015 7th Int. Conf. Meas. Technol. Mechatronics Autom. ICMTMA 2015*, pp. 626–629, 2015.

[27] A. Kadechkar, J. A. Martinez, and M. Moreno-eguilaz, "Experimental Study of the Effect of Aeolian Vibrations on the Contact Resistance of Substation Connectors," pp. 0–5.

[28] J. R. Riba, J. Martínez, M. Moreno-Eguilaz, and F. Capelli, "Characterizing the temperature dependence of the contact resistance in substation connectors," *Sensors Actuators, A Phys.*, vol. 327, 2021.

[29] J. Martinez, A. Gomez-Pau, J. R. Riba, and M. Moreno-Eguilaz, "On-Line Health Condition Monitoring of Power Connectors Focused on Predictive Maintenance," *IEEE Trans. Power Deliv.*, vol. 36, no. 6, pp. 3611–3618, 2021.

[30] J. Martínez, J. R. Riba, and M. Moreno-Eguilaz, "State of health prediction of

power connectors by analyzing the degradation trajectory of the electrical resistance," *Electron.*, vol. 10, no. 12, 2021.

[31] J. R. Riba, Á. Gómez-Pau, J. Martínez, and M. Moreno-Eguilaz, "On-line remaining useful life estimation of power connectors focused on predictive maintenance," *Sensors*, vol. 21, no. 11, 2021.

[32] F. De Paulis, C. Olivieri, A. Orlandi, and G. Giannuzzi, "Detectability of Degraded Joint Discontinuities in HV Power Lines Through TDR-Like Remote Monitoring," *IEEE Trans. Instrum. Meas.*, vol. 65, no. 12, pp. 2725–2733, 2016.

[33] Á. Gómez-pau, J. R. Riba, and M. Moreno-eguilaz, "Time series rul estimation of medium voltage connectors to ease predictive maintenance plans," *Appl. Sci.*, vol. 10, no. 24, pp. 1–14, 2020.

[34] M. Braunovic, "Effect of connection design on the contact resistance of high power overlapping bolted joints," *IEEE Trans. Components Packag. Technol.*, vol. 25, no. 4, pp. 642–650, 2002.

[35] S. Dutta, G. N. V. R. Vikram, M. S. Bobji, and S. Mohan, "Table top experimental setup for electrical contact resistance measurement during indentation," *Meas. J. Int. Meas. Confed.*, vol. 152, p. 107286, 2020.

[36] J. Shi, Q. He, and Z. Wang, "An LSTM-based severity evaluation method for intermittent open faults of an electrical connector under a shock test," *Meas. J. Int. Meas. Confed.*, vol. 173, no. October 2020, p. 108653, 2021.

[37] M. Khazaee, A. Rezaniakolaie, A. Moosavian, and L. Rosendahl, "A novel method for autonomous remote condition monitoring of rotating machines using piezoelectric energy harvesting approach," *Sensors Actuators, A Phys.*, vol. 295, pp. 37–50, 2019.

[38] S. E. Lee, K. S. Moon, and Y. Sohn, "Temperature dependence of contact resistance at metal/MWNT interface," *Appl. Phys. Lett.*, vol. 109, no. 2, 2016.

[39] S. S. Babu, M. L. Santella, Z. Feng, B. W. Riemer, and J. W. Cohron, "Empirical model of effects of pressure and temperature on electrical contact resistance of metals," *Sci. Technol. Weld. Join.*, vol. 6, no. 3, pp. 126–132, 2001.

[40] M. Braunovic, "Effect of Current Cycling on Contact Resistance, Force and Temperature of Bolted Aluminum-To-Aluminum Connectors of High Ampacity.," *Electr. Contacts, Proc. Annu. Holm Conf. Electr. Contacts*, vol. C, no. 1, pp. 103–116, 1980.

[41] E. Carvou, R. El Abdi, J. Razafiarivelo, N. Benjemaa, and E. M. Zindine, "Thermo-mechanical study of a power connector," *Measurement*, vol. 45, no. 5, pp. 889–896, Jun. 2012.

[42] V. Pascucci *et al.*, "A Standardized Reliability Evaluation Framework for Connections," in *SMTA International*, 2016, pp. 1–10.

[43] R. Tzeneva, "Investigation of high power bolted busbar connectors with longitudinal slots," *Prz. Elektrotechniczny*, vol. 88, no. 11 A, pp. 223–226, 2012.

[44] W. E. Wilson, S. V. Angadi, and R. L. Jackson, "Surface separation and contact resistance considering sinusoidal elastic-plastic multi-scale rough surface contact," *Wear*, vol. 268, no. 1, pp. 190–201, 2010.

[45] F. Capelli, "Development of High-Capacity Substation Connectors Compatible

with Technology," *TDX (Tesis Dr. en Xarxa)*, 2017.

[46] G. di Troia, K. Woo, and G. Zahlman, "Connector Theory and Application," *Fourh, Burndy, Londonderry*, 2007. [Online]. Available: https://www.academia.edu/9463837/BURNDY_PRODUCTS_Connector_Theory_and_Application_. [Accessed: 28-Mar-2022].

[47] P. G. Slade, *Electrical Contacts: Principles and applications*, 2nd editio. CRC Press, 2017.

[48] M. Braunovic, V. V Konchits, N. K. Myshkin, and S. Edition, *Fundamentals of Electrical Contacts*, vol. 138, no. 3479. 2006.

[49] R. Holm, *Electric Contacts*, Fourth edi. 1981.

[50] X. Wang, K. Zhou, and S. Shen, "Intelligent parameters measurement of electrical structure of medium frequency DC resistance spot welding system," *Measurement*, vol. 171, p. 108795, Feb. 2021.

[51] E. Svenman, A. K. Christiansson, and A. Runnemalm, "Experimental validation of an inductive probe for narrow gap measurement based on numerical modelling," *Meas. J. Int. Meas. Confed.*, vol. 146, pp. 396–402, Nov. 2019.

[52] N. Inomata, N. van Toan, and T. Ono, "Temperature-dependence of the electrical impedance properties of sodium hydroxide-contained polyethylene oxide as an ionic liquid," *Sensors Actuators, A Phys.*, vol. 316, p. 112369, 2020.

[53] A. Kadechkar, M. Moreno-Eguilaz, J. R. Riba, and F. Capelli, "Low-Cost Online Contact Resistance Measurement of Power Connectors to Ease Predictive Maintenance," *IEEE Trans. Instrum. Meas.*, vol. 68, no. 12, pp. 4825–4833, 2019.

[54] A. Kadechkar, J. R. Riba, M. Moreno-Eguilaz, F. Capelli, and D. Gonzalez, "On-line Resistance Measurement of Substation Connectors Focused on Predictive Maintenance," *Proc. - 2018 IEEE 18th Int. Conf. Power Electron. Motion Control. PEMC 2018*, no. 1, pp. 846–851, 2018.

[55] J. R. Jiang, J. E. Lee, and Y. M. Zeng, "Time series multiple channel convolutional neural network with attention-based long short- term memory for predicting bearing remaining useful life," *Sensors (Switzerland)*, vol. 20, no. 1, 2020.

[56] H. Guo *et al.*, "Particle Filtering Based Remaining Useful Life Prediction for Electromagnetic Coil Insulation," *Sensors*, pp. 1–14, 2021.

[57] D. Verstraete, E. Droguett, and M. Modarres, "A deep adversarial approach based on multisensor fusion for remaining useful life prognostics," *Proc. 29th Eur. Saf. Reliab. Conf. ESREL 2019*, pp. 1072–1077, 2020.

[58] A. F. Bastos and S. Santoso, "Condition monitoring of circuit switchers for shunt capacitor banks through power quality data," *IEEE Trans. Power Deliv.*, vol. 34, no. 4, pp. 1499–1507, 2019.

[59] A. Kadechkar, J. R. Riba, M. Moreno-Eguilaz, and J. Sanllehi, "Real-time wireless, contactless, and coreless monitoring of the current distribution in substation conductors for fault diagnosis," *IEEE Sens. J.*, vol. 19, no. 5, pp. 1693–1700, 2019.

[60] "IEC TS 61586:2017 Estimation of the reliability of electrical ..." [Online]. Available: https://www.une.org/encuentra-tu-norma/busca-tu-norma/iec?c=31491. [Accessed: 28-Mar-2022].

[61] L. Zeming, G. Jianmin, and J. Hongquan, “A maintenance support framework based on dynamic reliability and remaining useful life,” *Meas. J. Int. Meas. Confed.*, vol. 147, p. 106835, 2019.

[62] A. Raghavan *et al.*, “Low-cost embedded optical sensing systems for distribution transformer monitoring,” *IEEE Trans. Power Deliv.*, vol. 36, no. 2, pp. 1007–1014, 2021.

[63] H. M. Hashemian and W. C. Bean, “State-of-the-art predictive maintenance techniques,” *IEEE Trans. Instrum. Meas.*, vol. 60, no. 10, pp. 3480–3492, 2011.

[64] H. Liu, T. Claeys, D. Pissoort, and G. A. E. Vandenbosch, “Prediction of Capacitor’s Accelerated Aging Based on Advanced Measurements and Deep Neural Network Techniques,” *IEEE Trans. Instrum. Meas.*, vol. 69, no. 11, pp. 9019–9027, 2020.

[65] D. S. Richard Bardl, C. K. Steffen Großmannn, and W. Kiewitt, “Accelerated electrical and mechanical ageing test of high temperature low sag conductor.” pp. 1–4, 2017.

[66] R. El Abdi, E. Carvou, and N. Benjemaa, “Electrical resistance change of automotive connectors submitted to vibrations and temperature,” *2015 IEEE Energy Convers. Congr. Expo. ECCE 2015*, pp. 1910–1913, 2015.

[67] B. Huang, X. Li, Z. Zeng, and N. Chen, “Mechanical behavior and fatigue life estimation on fretting wear for micro-rectangular electrical connector,” *Microelectron. Reliab.*, vol. 66, pp. 106–112, 2016.

[68] L. Qingya, G. Jinchun, X. Gang, J. Qiuyan, and J. Rui, “Lifetime prediction of electrical connectors under multiple environment stresses of temperature and particulate contamination,” *J. China Univ. Posts Telecommun.*, vol. 23, no. 5, pp. 61,81-67, 2016.

[69] Y. Ren, Q. Feng, T. Ye, and B. Sun, “A Novel Model of Reliability Assessment for Circular Electrical Connectors,” *IEEE Trans. Components, Packag. Manuf. Technol.*, vol. 5, no. 6, pp. 755–761, 2015.

[70] B. Zhang, Y. Sui, Q. Bu, and X. He, “Remaining useful life estimation for micro switches of railway vehicles,” *Control Eng. Pract.*, vol. 84, no. March 2018, pp. 82–91, 2019.

[71] P. Lall, P. Sakalaukus, R. Lowe, and K. Goebel, “Leading indicators for prognostic health management of electrical connectors subjected to random vibration,” *Intersoc. Conf. Therm. Thermomechanical Phenom. Electron. Syst. ITHERM*, no. I, pp. 632–638, 2012.

[72] M. Braunovic, V. V Izmailov, and M. V Novoselova, “A Model for Life Time Evaluation of Closed Electrical Contacts,” *Proc. Fifty-First IEEE Holm Conf. Electr. Contacts, 2005.*, pp. 217–223, 2005.

[73] J. C. Lagarias, J. A. Reeds, M. H. Wright, and P. E. Wright, “Convergence properties of the Nelder-Mead simplex method in low dimensions,” *SIAM J. Optim.*, vol. 9, no. 1, pp. 112–147, 1998.

[74] M. Camp and H. Garbe, “Parameter estimation of double exponential pulses (EMP, UWB) with least squares and Nelder Mead algorithm,” *IEEE Trans. Electromagn. Compat.*, vol. 46, no. 4, pp. 675–678, 2004.

[75] Z. Chen, L. Wu, P. Lin, Y. Wu, and S. Cheng, "Parameters identification of photovoltaic models using hybrid adaptive Nelder-Mead simplex algorithm based on eagle strategy," *Appl. Energy*, vol. 182, pp. 47–57, 2016.

[76] S. Xu, Y. Wang, and Z. Wang, "Parameter estimation of proton exchange membrane fuel cells using eagle strategy based on JAYA algorithm and Nelder-Mead simplex method," *Energy*, vol. 173, pp. 457–467, 2019.

[77] British Standard, "BS EN 573-3:2019 - Aluminium and aluminium alloys. Chemical composition and form of wrought products. Chemical composition and form of products," *BSI*, 2019.

[78] AENOR, "UNE-EN 13601:2014. Copper and copper alloys - Copper rod, bar and wire for general electrical purposes," *http://www.aenor.es/*. AENOR, p. 30, 2014.

[79] C. Abomailek, J.-R. Riba, F. Capelli, and M. Moreno-Eguilaz, "Fast electro-thermal simulation of short-circuit tests," *IET Gener. Transm. Distrib.*, vol. 11, no. 8, pp. 2124–2129, Jun. 2017.

[80] A. Kadechkar, J. R. Riba, M. Moreno-Eguilaz, and J. Perez, "SmartConnector: A Self-Powered IoT Solution to Ease Predictive Maintenance in Substations," *IEEE Sens. J.*, vol. 20, no. 19, pp. 11632–11641, 2020.

[81] "Micro Ohm Meter 200Amps." [Online]. Available: http://www.raytech.ch/Products/Micro-Ohm/Micro-Centurion-II. [Accessed: 25-Jun-2020].

[82] "USB-6210 - Multifunction I/O Device Manual - National Instruments." [Online]. Available: https://www.ni.com/documentation/en/multifunction-io-device/latest/usb-6210/overview/. [Accessed: 28-Mar-2022].

[83] "Módulo de adquisición de datos USB de 8 canales de termopar." [Online]. Available: https://es.omega.com/pptst/TC-08.html. [Accessed: 28-Mar-2022].

[84] L. Chen, L. Xu, and Y. Zhou, "Novel approach for lithium-ion battery on-line remaining useful life prediction based on permutation entropy," *Energies*, vol. 11, no. 4, 2018.

[85] H. Yang, Z. Sun, G. Jiang, F. Zhao, and X. Mei, "Remaining useful life prediction for machinery by establishing scaled-corrected health indicators," *Meas. J. Int. Meas. Confed.*, vol. 163, p. 108035, 2020.

[86] H. Zhang, B. Su, H. Song, and W. Xiong, "Development and implement of an inspection robot for power substation," *IEEE Intell. Veh. Symp. Proc.*, vol. 2015-Augus, no. Iv, pp. 121–125, 2015.

[87] P. Qian, L. Hong, W. Chen, Y. Qian, Z. Wang, and H. Yao, "Optimization of the Accelerated Degradation Test Plan for Electrical Connector Contact Pairs Based on a Nonlinear Wiener Process," *Math. Probl. Eng.*, vol. 2020, 2020.

[88] M. Tadeusiewicz and S. Hałgas, "Parametric fault diagnosis of very high-frequency circuits containing distributed parameter transmission lines," *Electron.*, vol. 10, no. 5, pp. 1–14, 2021.

[89] Q. Xu, H. Huang, C. Zhou, and X. Zhang, "Research on real-time infrared image fault detection of substation high-voltage lead connectors based on improved yolov3 network," *Electron.*, vol. 10, no. 5, pp. 1–15, 2021.

[90] D. Martinez, H. Henao, and G. A. Capolino, "Overview of Condition Monitoring

Systems for Power Distribution Grids," *Proc. 2019 IEEE 12th Int. Symp. Diagnostics Electr. Mach. Power Electron. Drives, SDEMPED 2019*, pp. 160–166, 2019.

[91] A. Van Deursen, P. Wouters, and F. Steennis, "Corrosion in low-voltage distribution networks and perspectives for online condition monitoring," *IEEE Trans. Power Deliv.*, vol. 34, no. 4, pp. 1423–1431, 2019.

[92] J. Seo, H. Ma, and T. K. Saha, "On savitzky-golay filtering for online condition monitoring of transformer on-load tap changer," *IEEE Trans. Power Deliv.*, vol. 33, no. 4, pp. 1689–1698, 2018.

[93] A. A. Razi-Kazemi and M. Shariatnasab, "A New Approach on Prioritization of the Circuit Breakers for Installation of Online Monitoring Systems," *IEEE Trans. Power Deliv.*, vol. 34, no. 4, pp. 1569–1577, 2019.

[94] J. Joseph and S. T. K, "Development of Severity and Location Indices Based Condition Monitoring Scheme for Underground Cables by Impedance Spectroscopy," *IEEE Trans. Power Deliv.*, vol. 8977, pp. 1–10, 2020.

[95] Y. Wei, D. Wu, and J. Terpenny, "Robust Incipient Fault Detection of Complex Systems Using Data Fusion," *IEEE Trans. Instrum. Meas.*, vol. 69, no. 12, pp. 9526–9534, 2020.

[96] F. Yang, L. Du, H. Yu, and P. Huang, "Magnetic and electric energy harvesting technologies in power grids: A review," *Sensors (Switzerland)*, vol. 20, no. 5, pp. 1–12, 2020.

[97] G. Susinni, S. A. Rizzo, and F. Iannuzzo, "Two Decades of Condition Monitoring Methods for Power Devices," 2021.

[98] A. L. Brodersson, J. H. Jürgensen, and P. Hilber, "Towards health assessment: Failure analysis and recommendation of condition monitoring techniques for large disconnector populations," *IET Conf. Publ.*, vol. 2016, no. CP686, pp. 12–15, 2016.

[99] C. Bhargava, V. K. Banga, and Y. Singh, "Failure prediction and health prognostics of electronic components: A review," *2014 Recent Adv. Eng. Comput. Sci. RAECS 2014*, pp. 6–8, 2014.

[100] G. Hamra, R. MacLehose, and D. Richardson, "Markov chain monte carlo: An introduction for epidemiologists," *Int. J. Epidemiol.*, vol. 42, no. 2, pp. 627–634, 2013.

[101] R. L. Karandikar, "On the Markov Chain Monte Carlo ( MCMC ) method," *Sadhana - Acad. Proc. Eng. Sci.*, vol. 31, no. 2, pp. 81–104, 2006.

[102] J.-H. Lee, J.; Sung, W.; Choi, "Estimation via Markov Chain Monte Carlo," *IEEE Control Syst. Mag.*, vol. 23, no. April, pp. 34–45, 2003.

[103] J. Lee, W. Sung, and J. H. Choi, "Metamodel for efficient estimation of capacity-fade uncertainty in Li-Ion batteries for electric vehicles," *Energies*, vol. 8, no. 6, pp. 5538–5554, 2015.

[104] J. A. Vrugt, "Markov chain Monte Carlo simulation using the DREAM software package: Theory, concepts, and MATLAB implementation," *Environ. Model. Softw.*, vol. 75, pp. 273–316, 2016.

[105] "Find minimum of unconstrained multivariable function using derivative-free

method - MATLAB fminsearch - MathWorks España.” [Online]. Available: https://es.mathworks.com/help/matlab/ref/fminsearch.html. [Accessed: 23-Dec-2020].

[106] D. C. Montgomery, E. A. Peck, and G. G. Vining, *Introduction to Linear Regression Analysis*, Fith Editi. Hoboken, New Jersey, USA, 2012.

[107] C. M. Furse, M. Kafal, R. Razzaghi, and Y. J. Shin, “Fault Diagnosis for Electrical Systems and Power Networks: A Review,” *IEEE Sens. J.*, vol. 21, no. 2, pp. 888–906, 2021.

[108] J. Huang, T. Fukuda, and T. Matsuno, “Model-based intelligent fault detection and diagnosis for mating electric connectors in robotic wiring harness assembly systems,” *IEEE/ASME Trans. Mechatronics*, vol. 13, no. 1, pp. 86–94, 2008.

[109] S. Ramezani, A. Moini, and M. Riahi, “Prognostics and Health Management in Machinery : A Review of Methodologies for RUL prediction and Roadmap 1- Introduction 2- Transformation of maintenance and development of PHM,” vol. 6, no. 1, 2019.

[110] X. Hu, L. Xu, X. Lin, and M. Pecht, “Battery Lifetime Prognostics,” *Joule*, vol. 4, no. 2, pp. 310–346, 2020.

[111] K. A. Severson *et al.*, “Data-driven prediction of battery cycle life before capacity degradation,” *Nat. Energy*, vol. 4, no. 5, pp. 383–391, 2019.

[112] J. J. Zhu and Z. C. Yang, “Thermo-elasto-plastic stress and strain analysis and life prediction of gas turbine blade,” *2010 Int. Conf. Meas. Technol. Mechatronics Autom. ICMTMA 2010*, vol. 3, pp. 1019–1022, 2010.

[113] M. Tanwar and N. Raghavan, “Lubrication oil degradation trajectory prognosis with ARIMA and bayesian models,” *Proc. - 2019 Int. Conf. Sensing, Diagnostics, Progn. Control. SDPC 2019*, pp. 606–611, 2019.

[114] “GMW Associates - PEM Rogowski Coils/Current Transducers, CWT.” [Online]. Available: https://gmw.com/product/cwt/. [Accessed: 25-Jun-2020].

# APPENDIX

## A. Materials and resources

This section describes the different materials and resources considered to develop this research work. It covers the software, electronics components, hardware and test equipment used in the experimental and data processing parts.

### A.1 Software

The software used is described below:

- ✓ MATLAB®: Mathematical environment for programming and developing different models and algorithms.
- ✓ Python: Data acquisition of electrical resistance from DAQ USB-6210 and temperature data from Omega Thermocouple Data Logger.
- ✓ COMSOL Multiphysics®: Simulations for the characterization of the temperature dependence of the contact resistance.
- ✓ Notepad ++: Text and source editor.
- ✓ Microsoft Excel®: Spread sheet for data analysis.
- ✓ Microsoft Word®: Text editor.
- ✓ Microsoft Visio®: Diagram creator.

### A.2 Hardware

Several electronic components have been used in the experimental part. The CWT500LFxB Rogowski coil with sensitivity0.06 mV/A, has been used to measure the electrical current flowing through the electrical connectors. The NI USB-6210DAQ has been used to acquire the electrical current data from the Rogowski coil, the voltage drop across the terminals of the connectors and the phase shift between the voltage drop and the electrical current. The NI USB-6210 DAQ has 8 differential channels, which are enough to measure the contact resistance of 7 connectors and the electric current in real time. The Omega TC-08 USB Data Acquisition along with T Type thermocouples have

been used to collect the conductor and connector temperatures in real-time in order to correct the effect of temperature in all connectors.

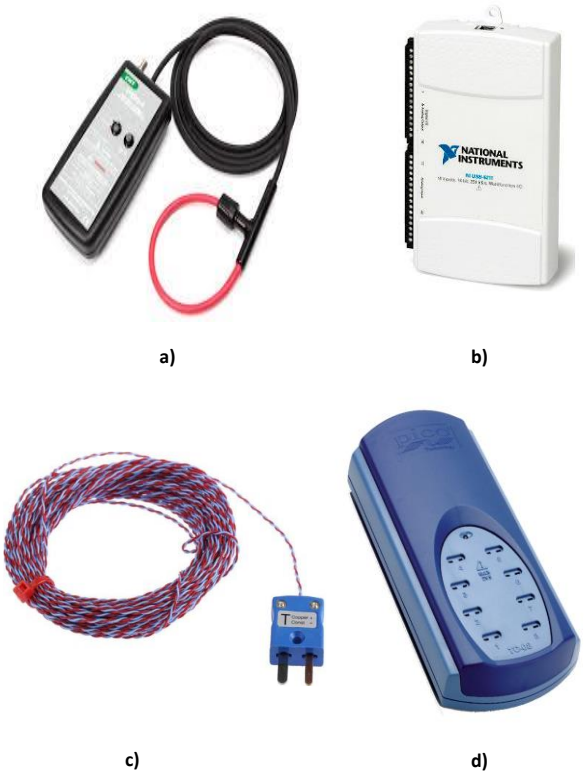


**Figure A.1.** a) Rogowski Coil CWT500LFxB[114]; b) DAQ NI USB-6210 [82]; c) Thermocouple Type T; d) Omega TC-08 USB Data Acquisition Module [83] .

## A.3 Raytech Micro-Ohmmeter 200 A Micro Centurion II

The Raytech Micro-Ohmmeter has been used for measuring the DC contact resistance. This apparatus is the basis for this research, since it allows validating the contact resistance from the AC measurements, which are collected by means of the DAQ NI USB-6210.

**Figure A2**. Raytech Micro-ohmmeter 200 A Micro Centurion II [81].

## A.4 High Current AC transformers

High current AC and DC transformers have been used to perform temperature cycle tests on electrical connectors. The variable voltage transformer shown in Figure A.3.a has an output current up to 10 kA and output voltage up to 10 V. The transformer shown in Figure A.3.b has an output current up to 2.5 kA and output voltage up to 4 V. Both are located at Amber Laboratory.

**a)** **b)**

**Figure A.3**. a) 10 kA High Current AC transformer, b) 2,5 kA High Current DC transformer.